Characterisation and Integration of Energy Flexibility through Stochastic Modelling and Control

Junker, Rune Grønborg

Publication date:
2019

Document Version
Publisher's PDF, also known as Version of record

Ph.D. Thesis
Doctor of Philosophy

DTU Compute
Department of Applied Mathematics and Computer Science

Characterisation and Integration of Energy Flexibility through Stochastic Modelling and Control

Ph.d. Thesis 2019

Rune Grønborg Junker

Kongens Lyngby 2019

DTU Compute
Department of Applied Mathematics and Computer Science
Technical University of Denmark

Matematiktorvet
Building 303B
2800 Kongens Lyngby, Denmark
Phone +45 4525 3031
compute@compute.dtu.dk
www.compute.dtu.dk

Summary

Energy grids around the world are undergoing a transformation from conventional production schemes based on carbon to renewable energy sources. This comes at a price, since most renewable energy sources can not be controlled. Considering that most problems experienced by energy grids are handled by adjusting production, this is a major challenge. To cope with this, energy flexibility from demand have been proposed, where, instead of adjusting generation, the demand is adjusted according to the needs of the energy grids.

To be able to utilise energy flexibility, first it has to be understood. Since most energy flexibility comes from systems with dynamic needs and possibilities to adjust their demand, static approaches have limited use. The main objective of this thesis, is to advance the understanding of dynamic energy flexibility. In particular, dynamic mathematical models for how to characterise energy flexibility are proposed. Contrary to previous works on energy flexibility, these models facilitate estimates of the energy flexibility *when in use*, allowing it to be understood out of steady state, where it will be found most of the time.

Models are only as useful as the applications that they facilitate, and so, this thesis includes proposals for how to integrate energy flexibility using the developed models. This ranges from component level, where appropriate control strategies have to be implemented, to the daily operation of energy grids where energy flexibility has to be utilised, all the way to the planning of future investments in the energy grids.

Resumé (Danish)

Både elnet og varmenet verden over er i gang med en transformation fra konventionelle produktionsmetoder baseret på karbon til vedvarende energikilder. Dette har sin pris, da de fleste metoder til at producere vedvarende energi ikke kan blive kontrolleret. De fleste problemer relateret til el- og varmenet er løst ved at justere energiproduktion, så dette er en stor udfordring. For at løse denne udfordring er det blevet foreslået at udnytte energifleksibilitet fra forbrug, ved at justere denne i stedet for produktion, under hensynstagen til de problemer el- og varmenettene har.

Før man kan udnytte energifleksibilitet bliver man nødt til at forstå det. Da det meste energifleksibilitet kommer fra systemer med dynamiske behov og muligheder for at ændre forbrug, er det begrænset hvor brugbare statiske metoder er. Hovedformålet med denne afhandling er at udvide forståelsen af dynamisk energifleksibilitet. I særdeleshed er der blevet udviklet matematiske og dynamiske modeller til at karakterisere energifleksibilitet. I modsætning til tidligere analyser af energifleksibilitet, så facilitere disse modeller estimater af energifleksibiliten *i brug*, hvilket gør at den kan blive brugt selvom den ikke er i sin stationære tilstand, hvilket er tilfældet det meste af tiden.

Modeller er kun så værdifulde som de applikationer de giver anledning til. Derfor inkludere dette afhandling også foreslag til hvordan energifleksibilitet kan blive udnyttet ved hjælp af disse modeller. Dette strækker sig fra komponentniveau, hvor passende kontrolstrategier skal implementeres, til den daglige operation af el- og varmenet, hvor energifleksibilitet til udnyttes, og hele vejen til fremtidige investeringer og udvidelser af el- og varmenettene.

Preface

This PhD thesis was prepared at the department of Applied Mathematics and Computer Science at the Technical University of Denmark in fulfilment of the requirements for acquiring a PhD degree in Applied Mathematics and Computer Science.

Kongens Lyngby, November 13, 2019

Rune Grønborg Junker

Acknowledgements

I would like to thank my supervisors, Henrik Madsen, Rishi Relan, Uffe Høgsbro Thygesen and John Bagterp Jørgensen. A special thanks goes to Rishi who spent a lot of time teaching me the ins and outs of academia, and was always there to share his opinions on academic writing, politics, journals and life in general. Also, I want to express my gratitude towards Henrik, whom, from the beginning have trusted me with space and time to follow my own ideas, while involving me in projects where relevant and always making me feel like a true expert. Special thanks also goes to Goran Goranović for acting like another supervisor, especially during my first time as a PhD student Goran was my main source of academic expertise.

A big thanks to NREL for hosting me during my external stay, and to Annabelle Pratt in particular for being my supervisor while staying there.

I would also like to thank all my colleagues, with whom I love to discuss big and small topics alike. Especially my office mates, Christoffer Rasmussen, Hjörleifur Bergsteinsson, Jaume Palmer Real, Dominik Franjo Dominković and Emma Margareta Viktoria Blomgren deserve special mentioning for making the countless hours spent in the office feel like a hobby rather than a job.

Finally, to my fiancée Helle Skjold Elmelund Pedersen: what would I do without you? Thank you for your unlimited support and love.

List of Publications

The results of the PhD study have been disseminated in 19 publications, including 2 articles published in and 5 submitted to peer-reviewed journals. Throughout the thesis, these publications are referenced by the letter assigned to them in the list below, while work done by other researchers is referenced according to the tags in the bibliography. Also, 16 official presentations at various conferences and workshops were conducted, listed below.

Peer-Reviewed Publications

Included in Thesis

A Rune Grønborg Junker, Armin Ghasem Azar, Rui Amaral Lopes, Karen Byskov Lindberg, Glenn Reynders, Rishi Relan, Henrik Madsen. "Characterizing the energy flexibility of buildings and districts". *Applied Energy* Volume 225, 1 September 2018, Pages 175-182.

B Rune Grønborg Junker, Rishi Relan, Henrik Madsen. "Designing Individual Penalty Signals for Improved Energy Flexibility Utilisation". *IFAC-PapersOnLine* Volume 52, Issue 4, 2019, Pages 123-128.

C Rune Grønborg Junker, Rishi Relan, Henrik Madsen. "Physical-Stochastic Continuous-Time Identification of a Forced Duffing Oscillator". Submitted to *ISA Transactions*.

D Rune Grønborg Junker, Carsten Skovmose Kallesøe, Jaume Palmer, Bianca Howard, Rui Amaral Lopes and Henrik Madsen. "Stochastic Nonlinear Modelling and Application of Price-Based Energy Flexibility". Submitted to *Applied Energy*

E Dominik Franjo Dominkovic, Rune Grønborg Junker, Karen Byskov Lindberg, Henrik Madsen. "Implementing flexibility into energy planning models: soft-linking of a high-level energy planning model and a short-term operational model". Submitted to *Applied Energy*.

Not Included in Thesis

F Nikita Zemtsov, Jaroslav Hlava, Galina Frantsuzova, Henrik Madsen, Rune Grønborg Junker, John Bagterp. "Economic MPC based on LPV model for thermostatically controlled loads". *2017 International Siberian Conference on Control and Communications (SIBCON) Proceedings*, June 2017.

G Kenneth Leerbeck, Peder Bacher, Rune Grønborg Junker, Goran Goranović, Olivier Corradi, Razgar Ebrahimy, Anna Tveit, Henrik Madsen. "Short-Term Forecasting of CO_2 Emission Intensity in Power Grids by Machine Learning". Submitted to *Applied Energy*.

Other Publications

H Søren Østergaard Jensen, Henrik Madsen, Rui Lopes, Rune Grønborg Junker, Daniel Aelenei, Rongling Li, Susanne Metzger, Karen Byskov Lindberg, Anna Joanna Marszal, Michaël Kummert, Bart Bayles, Erwin Mlecnik, Roberto Lollini, Wilmer Pasut. "Energy Flexibility as a key asset in a smart building future". *EBC Annex 67: Energy Flexible Buildings*.

I Rune Grønborg Junker, Armin Ghasem Azar, Rui Amaral Lopes, Karen Byskov Lindberg, Glenn Reynders, Rishi Relan, Henrik Madsen. "Characterizing the energy flexibility of buildings and districts". *CITIES Solutions Brochures.*

J Armin Ghasem Azar, Rune Grønborg Junker, Stig Bousgaard Mortensen, Henrik Madsen. "Dynamic CO2 Based Control". *CITIES Solutions Brochures.*

K Svend Erik Mikkelsen, Steen Hartvig Jacobsen, Henrik Madsen, Peder Bacher, Rune Grønborg Junker. "BIPVT-E: Udvikling af Styringsstrategi til Fleksibelt Energiproduktionsanlæg med Solceller, Solvvarme, Varmepumpe, Energiabsorber og Batterilager". *Elforsk projekt 349-054*

L Armin Ghasem Azar, Henrik Madsen, Rune Grønborg Junker, Razgar Ebrahimy, Zohreh Alizadeh, Giulia De Zotti, Thomas Kieldsen, Stig Holm Sørensen, Hanne Binder, Loui Algren, Miguel Marroquin, Adrian Ibañez, Claus Amtrup Andersen, Thomas Saabye, Jacob Dall, Stig Bousgaard Mortensen, Jacob Andreasen. "Results of Pilot B (Denmark)". *SmartNet.*

M Anna Joanna Marszal, Hicham Johra, Armin Knotzer, Jaume Salom, Søren Østergaard Jensen, Erwin Mlecnik, Hussain Kazmi, Roberta Pernetti, Konstantin Klein Lilli Frison, Peter Engelmann, James Parker, Laura Aelenei, Rune Grønborg Junker, Rui Amaral Lopes, Daniel Aelenei, Athila Santos, Bo Nørregaard Jørgensen, Zheng Ma. "Principles of Energy Flexible Buildings". *EBC Annex 67: Energy Flexible Buildings.*

N Anna Joanna Marszal, Tobias Weiss, Armin Knotzer, Søren Østergaard Jensen, Hussain Kazmi, Ilaria Vigna, Roberta Pernetti, Peter Engelmann, Jérôme Le Dréau, Kun Zhang, Rune Grønborg Junker, Henrik Madsen, Rui Lopes, Daniel Aelenei, Krzysztof Arendt, Glenn Reynders, Ala Hasan, Minyan Lu, Adamantios Bompoulas. "Characterization of Energy Flexibility in Buildings". *EBC Annex 67: Energy Flexible Buildings.*

O Athila Quaresma Santos, Bo Nørregaard Jørgensen, Hussain Kazmi, Reino Ruusu, Ala Hasan, Thibault Péan, Yuekuan Zhou, Sunliang Cao, Young Jae Yu, John Clauß, Rune Grønborg Junker, Christian Finck, Ali Saberi Derakhtenjani, Jose Agustin Candanedo, Andreas Athienitis, Despoina Christantoni, Anjukan Kathirgamanathan, Donal P. Finn, Kun Zhang. "Control strategies and algorithms for obtaining energy flexibility in buildings". *EBC Annex 67: Energy Flexible Buildings.*

P Hicham Johra, Tobias Weiss, Thibault Péan, Ali Saberi Derakhtenjani, José Candanedo, Andreas Athienitis, Erwin Mlecnik, Ina De Jaeger, Dirk Saelens, Hussain Kazmi, Ilaria Vigna, Marco Lovati, Roberta Pernetti, Roberto Lollini, Young-Jae Yu, Konstantin Klein, Lilli Frison, Peter Engelmann, Yuekuan Zhou, Sunliang Cao, Jérôme Le Dréau, James Parker,Laura Aelenei, Sarah O'Connell, Marcus M. Keane, Daniel Aelenei, Kun Zhang, Johann Meulemans, Marcus Brennenstuhl, Malcolm Yadack, Ursula Eicker, Kyriaki Foteinaki, Rune Grønborg Junker, Rongling Li, Christian Finck, Sahra Mohammadi, Fulin Wang, Anjukan Kathirgamanathan, Despoina Christantoni, Donal P. Finn, Francesco D'Ettorre, Killian Murphy, Mattia De Rosa, Mohammad Saffari, Eleni Mangina, Monika Hall, Athila Santos, Krzysztof Arendt, Glenn Reynders, Reino Ruusu, Ala Hasan. "Examples of Energy Flexibility in Buildings". *EBC Annex 67: Energy Flexible Buildings.*

Q Søren Østergaard Jensen, Rune Grønborg Junker. "IEA EBC Annex 67 Energy Flexible Buildings". *DYNASTEE Seminar, April 2019, Bilbao.*

R Annabelle Pratt, Mark Ruth, Fei Ding, Sivasathya Balamurugan, Emiliano Dall'Anese, Xinyang Zhou, Dheepak Krishnamurthy, Rune Junker, Prateek Munankarmi. "NIST Transactive EnergyModeling and Simulation Challenge Phase II", Section 3: "NREL Team Report: Network-Aware Transactive Energy Control Simulations" ". *National Institute of Standards and Technology.* .

S Søren Ravnsborg, Rune Grønborg Junker. "Smart Algorithm Control Power Consumption and Strengthens the Climate". *Grøn Dyst 2019.*

Presentations

1. Rune Grønborg Junker. "Smart Energiforbrug". *ATV'S Teknologiske Topmøde*. 12. November 2019, Mogens Dahl Koncertsal, Denmark.

2. Rune Grønborg Junker, Razgar Ebrahimy, Henrik Madsen. "SmartNet Pilot B: Temperature Control of Indoor Swimming Pools". *SmartNet – Fremtidsperspektiver for TSO-DSO-snittet*. 21. August 2019, Energinet, Denmark.

3. Rune Grønborg Junker, Rishi Relan, Henrik Madsen. "Continuous-time Stochastic Grey-box Model of a Duffing Oscillator based on Residual Analysis". *Oscillations, Transients and Fluctuations in Complex Networks*. 1. July 2019, University of Copenhagen, Denmark.

4. Rune Grønborg Junker, Rishi Relan, Henrik Madsen. "Designing Individual Penalty Signals for Improved Energy Flexibility Utilisation". *IFAC Workshop on Control of Smart Grid and renewable energy systems, CSGRES 2019*. 10. June 2019, Hyatt Regency Jeju, Korea.

5. Rune Grønborg Junker, Henrik Madsen. "Two-level penalty-based control of energy flexibility". *Workshop on Joint NTNU-DTU Proposals for European & Nordic Research Programmes*. 3. June 2019, Technical University of Denmark, Denmark.

6. Rune Grønborg Junker, Rishi Relan. "Continuous-time Stochastic Grey-box Model of the Nonlinear Feedback System based on Residual Analysis". *Workshop on Nonlinear System Identification Benchmarks, 2019*. 10. April 2019, Technical University Eindhoven, The Netherlands.

7. Roberta Pernetti, Rune Grønborg Junker. "Highlights of IEA Annex67 results: Principles & Characterization". *Public seminar Annex 67 - Energy Flexible Buildings*. 4. April 2019, Aalborg University, Denmark.

8. Rune Grønborg Junker. "Fleksibelt Energiforbrug". *Smartere Forbrug – Digitalisering af forsyning*, 22. January 2019 - University of Aalborg, Denmark.

9. Rune Grønborg Junker. "Characterising the Energy Flexibility of Buildings and Districts". *EBC Annex 71 5th Expert Meeting*, 17. October 2018, Palais Claudiana, Austria.

10. Rune Grønborg Junker. "Characterizing the Energy Flexibility of Buildings and Districts". *Energy Flexible Buildings - public seminar*, 12. October 2018, Polytechnique Montréal, Canada.

11. Armin Ghasem Azar, Rune Grønborg Junker. "The Danish Pilot in SmartNet". *EU H2020 SmartNet National Workshop*, 20. September 2018, Energinet, Denmark.

12. Rune Grønborg Junker, Henrik Madsen. "How to Characterise and Use the Flexibility in Integrated Energy Systems Using Control-Based Methods". *CITIES 5th General Consortium Meeting*, 20. September 2018, Energinet, Denmark.

13. Rune Grønborg Junker. "A Dynamic Characterization of Energy Flexibility". *Sustain Conference 2017*, 6. December 2017, Technical University of Denmark, Denmark.

14. Rune Grønborg Junker, Peder Bacher, Henrik Madsen. "Utilizing PV-battery systems with varying electricity prices" *Launch of DTU Solar*. 26. October 2017, Technical University of Denmark, Denmark.

15. Rune Grønborg Junker, Rui Amaral Lopes. "A Dynamic Characterization of Energy Flexibility". *EBC Annex 67 5th Expert Meeting*. 27. September 2017, Graz University of Technology, Austria.

16. Rune Grønborg Junker. "SDE modelling of cities". *PhD Bazaar 2017*. 10. May 2017, Technical University of Denmark, Denmark.

Contents

List of Figures

Nomenclature

Roman Letters

$\mathbb{E}$	Expectation operator
$\mathbb{N}$	Natural numbers
$\mathbb{R}$	Real numbers
$\mathbb{V}$	Variance operator
$\mathbb{Z}$	Integers
$\mathcal{H}$	Frequency response function
$\mathcal{X}_t$	Collection of values of X up till time t
C	Congestion
f	Frequency
H	Step function
h	Impulse response function
S	Step response function
U	Inputs
V	Voltage
W	Wiener process
X	Stochastic process
Y	Observations
i	Imaginary unit

Greek Letters

ϵ	Noise

λ Energy price

μ Mean

Σ Summation operator

σ Standard deviation

Other Symbols

$\int$ Integration operator

$\mathbf{1}$ Indicator function

$.^{\top}$ Transposition

$\|\cdot\|$ Norm

argmin The argument which minimises some function

ARMAX Auto-Regressive Moving Average with eXogeneous input

BIPVT-E Building Integrated Photo-Voltaic with Thermal Absorber

BRP Balance Responsible Party

CHP Combined Heat and Power plant

COP Coefficient of Performance

DSO Distribution System Operator

E-MPC Economical Model Predictive Control

EFS Energy Flexible System

EV Electric Vehicle

FI Flexibility Index

FIR Finite Impulse Response

MPC Model Predictive Control

ODE Ordinary Differential Equation

PDE Partial Differential Equation

PID Proportional Integral Derivative

PV Photo-Voltaic

RES Renewable Energy Source

RMS Root-Mean-Square error

ROCOF Rate of Change of Frequency

SDE Stochastic Differential Equation

TSO Transmission System Operator

Part I

Summary Report

CHAPTER 1

Introduction

1.1 Motivation

Increasing shares of Renewable Energy Sources (RESs) are transforming the way we think about energy generation [DH11; Mor+14]. While energy generation used to be, and still for the most part is, thought of as a controllable quantity, this notion is changing since most RESs are determined by weather. This makes it difficult to avoid a mismatch between production and demand, but removing conventional generators and installing RESs causes other problems as well [Por+09]. In particular, the decentralised nature of RESs requires energy grids to be operated in ways that they were never designed for [GG11]. While energy demand can be predicted quite accurately in hourly resolution [YCC03; Dot02], it is fundamentally stochastic and fluctuates constantly [WW10], meaning that energy generation has to be adjusted constantly as well [Día+14]. Especially for power systems this is important, where the almost instantaneous delivery from generation to consumption means that even short term deviations can quickly get out of hand [Flo+17]. So far, this has been done by synchronous generators, which can adjust the generation with short notice without major efficiency losses [Han+16], but the reduction in the share of synchronous generators means that this can not continue. In the future this will have to be done by RESs, but while pumped hydro is well suited for this [Man00], Photo-Voltaic (PV) and Wind Turbines are less so. The latter two are worse suited partly because they can only adjust their production by curtailing production, wasting free energy, but even more so because their production is equally stochastic [JT10]. In particular, there is nothing that a wind turbine can do if there is no wind, and similar for PVs without solar radiation.

On local scales, it is already seen how not all problems can be solved by generators, since the problem might not be related to power generation at all, but rather that some distribution grids have not been able to keep up with the continued electrification. This is especially pronounced in areas with weak distribution grids such as summer house areas, where most of the time the demand is very low and easy to handle. However, during public holidays lots of people inhabit the summer houses and consume more electricity than the local distribution grids can handle, resulting in congestion and voltage deviations.

The traditional strategy employed for overcoming these transmission and distribution challenges can be summarised with a single word: cobber. So far, whenever trans-

mission and distribution grids have faced problems, they have simply reinforced the grid. Perhaps this explains why the total cost of transmission in Denmark amounted to 653 million EUR (including PSO) in 2018 [Jak]. The total cost of electricity bought on the spot market during the same time was 630 million EUR [Ene]. It is unknown exactly how large the total costs associated with distribution grids are, but according to [Nor15] the costs related to distribution were 12.5% larger than those related to transmission (including PSO) for regular consumers. This shows that even though the power grid is functioning, it does so at an extremely high cost, and the potential savings are enormous.

To replace the role of synchronous generators, improve the quality of weak power grids and save costs of transmission and distribution, energy flexibility on the demand side will have to be utilised [OMa+16; LM06]. However, energy flexibility on the demand side is much more challenging to operate than on the supply side, since it comes in small volumes from a huge amount of consumers, rather than a few very flexible producers.

A lot of work has gone into modelling energy flexibility from the bottom up [LH16; Lop+16; RDS17; NPT14; Dhu+15], testing specific components one at a time and measuring specific characteristics [WFK18]. For example, for buildings, the building mass is typically tested thoroughly [DH13] and likewise for the heating equipment such as heat pumps [Pal+19]. While this is useful for understanding key physical capabilities and operating the hardware, it requires far too many detailed test studies before the energy flexibility can be utilised. The task is further complicated when consumers install batteries [OR16], or local energy production such as rooftop-PV [AMS13], microturbines [PRV04] or even local Combined Heat and Power plants (CHPs) [HM17]. Even with enough resources to test all components, there is currently no way to combine this knowledge to understand energy flexibility on e.g. building level.

Instead, a data-driven approach is required, where energy flexibility is assessed based on energy consumption. However, in order for the models to be useful, the connection to the physics governing the real world has to be preserved. If this is not the case, one can at best hope for models that are descriptive, while the real goal is to obtain models that accurately reflect the possibilities for *using* energy flexibility. Therefore, in this thesis, energy flexibility is characterised and analysed using a top-down approach combined with general physical considerations. This allows the developed methods to scale to large systems and work with small amounts of data.

When it comes to implementing energy flexibility there are two main approaches. The first is to directly control appliances according to grid needs, such as e.g. [Liu+17; ISM17]. In this approach it is assumed that consumers give up autonomy of their equipment to grid operators. The grid operators then have to balance discomfort imposed on consumers versus grid needs, and in this way find optimal schedules for all appliances under their control. This surely gives the largest potential for utilising energy flexibility, since all possibilities are taken into account, and thus the full space of possibilities is explored. However, prioritising the comfort of everyone is

a very complex task that, although very promising in theory [Fur35], is not feasible in practice [Kra03]. It is simply too difficult to accurately and fairly prioritise multiple individuals' comfort.

This is avoided when using indirect control revolving around economic incentives. Within this research area there are two main approaches as to how the economic incentives should be constructed. The first, transactive energy, is centered around markets at node level, in which energy flexible consumers, such as households negotiate prices in real time [Wid+14; KW16]. In this way, the demand is automatically adjusted to meet grid problems. However, the sheer amount of markets that would be required to be run in real time would require an immense amount of computational power. On top of this, the volume of traded energy in scales that small, would make for markets with almost no liquidity, which is known to result in inefficiency [CRS08].

Instead, the second economic approach is followed in this thesis, namely price-based control, where varying price-signals are designed and sent to consumers. In this approach, the owners of energy flexible systems are free to act on the price-signals as they desire, but, at least some of them, are expected to follow the economic incentives, making the price-signal act as an indirect control-signal. Thus, it is up to the consumers to make the trade-off between comfort and cost themselves, which, naturally, they are in the ideal position to do [Fri89]. It is still expected that most appliances will be operated by automatic controllers, but consumers can change the settings or go to manual control depending on their current needs.

The idea of controlling demand with price-signals was first suggested in [Sch+80]. After the idea was further examined in [Fle09] it started to get a lot of attention, In [RLJ11; H+11] local controllers designed to react to price-signals were developed, which set the stage for [Cor+13] in which it was suggested to estimate expected demand as a function of price. This inspired research on a hierarchy of controllers, where price signals were designed by a local controller, to make demand follow a reference demand profile [Hal+16] or control frequency [SEJ15]. Finally, frequency control was combined with voltage control in [De +18] and [Zot+19a].

While a lot of work has gone into most aspects of price-based control there is a major lack in the understanding and characterisation of energy flexibility. So far, the only characterisations of energy flexibility have been static or consisted of pre-specified flexibility profiles, that the grid operators can choose from and use when convenient [Zot+19b; AJ16]. If the price-based control is to be implemented in practice, then a better understanding of energy flexibility is needed, so that prices can be designed in appropriate ways. In particular different kinds of energy flexibility are well-suited for different grid problems. To assign energy flexibility to the correct problems, it will have to be understood where, when and for what problems, that it is best suited.

1.2 Research Objectives

Based on the current state of the art of energy flexibility, the following three research objectives were identified as the main topics of this PhD study.

1.2.1 Demonstration of Potential of Energy Flexibility

The first goal of this PhD study was to investigate the potential of energy flexibility and demonstrate the value, by operating the energy flexibility of systems possessing it, in a way that provides value for the owner or energy grids. This was investigated in the SmartNet project in Report L, the Annex 67 Report O and the Papers **??**. The results of this research are presented in Section 5.3.

1.2.2 Characterisation of Energy Flexibility

The second objective of the PhD study was to advance the understanding of energy flexibility. In particular, the understanding of dynamics was pursued. Finally, mathematical models should be developed, describing energy flexibility in the context of dynamic energy prices. This research objective was mainly pursued in Papers B, D, and in the Annex 67 reports N, M. Section 5.2 summarises the findings related to this objective.

1.2.3 Utilisation of Energy Flexibility

Finally, the third objective was to investigate how energy flexibility can be utilised. In particular, how different spacial scales, ranging from component level to grid level, can be tied together such that all grid problems are dealt with simultaneously. Proposals for operational implementation of the energy flexibility on grid operator level can be found in Papers C and D. The usage of energy flexibility on a strategic level is investigated and implemented in Paper E. In Section 5.4 and 5.5 the key results related to this objective are presented.

1.3 Thesis Structure

The thesis consists of 2 parts, namely a summary report and the main publications. In Part I the most essential knowledge and methods needed for the study are explained. The key components of energy grids along with the problems studied during this thesis are explained in Chapter 2. Following this is Chapter 3, in which the modelling techniques used are introduced. Next, Chapter 4 contains the control theory needed to utilise the developed models. The thesis then continues by summarising the results of the PhD study in 5 overall categories in Chapter 5. Most of the presented results

are published elsewhere, mainly in Papers A-E. However, the chapter also includes work and results not published anywhere else. The implications of the results along with perspectives for future work is presented in Chapter 6. A conclusion on the thesis is included in Section 7. In the end, Part II includes pre-prints of Papers A-E.

CHAPTER 2

Power Grids and Markets

The basis for the work done in this thesis is the problems faced by energy grids, due to increased shares of RESs. The two kinds of energy grids considered in this study are power grids and district heating grids, both of which experience varying costs of production and/or delivery. Especially power grids experience a lot of problems apt for energy flexibility, while district heating grids are well suited for providing energy flexibility. For this reason a description of power grids is included here, with emphasis on the problems that can be solved by energy flexibility. The exact market conditions for district heating grids have not been used, and thus these are omitted.

The three main actors in the operation of power grids are Transmission System Operators (TSOs), Distribution System Operators (DSOs) and Balance Responsible Parties (BRPs). Both the TSOs and DSOs are technical operators, whose only concern is that the power grid is functioning. If they fail to meet their responsibilities, the consequences are reductions in power quality ranging from dimmed lights to blackouts. Contrary to this, BRPs are economic players, that have to purchase power on behalf of their customers. They can not fail in this regard, but their expenses associated with purchasing energy depends on their ability to predict power consumption and generation.

Thus, for TSOs and DSOs energy flexibility is a means to improve the operation of energy grids, while for BRPs it is relevant to increase their profitability, helping the operation indirectly. In Section 2.1 the role of BRPs is explained, followed by the general market structure in which they act in Section 2.2. Afterwards, the responsibilities of DSOs and TSOs are explained in Section 2.3 and 2.4 respectively.

2.1 Balance Responsible Parties

Almost all power is bought through BRPs, which in turn purchased it on power exchanges. This is required to handle the enormous amounts of minor power consumptions that happen whenever an electric appliance is turned on. In principle, power generation has to be scheduled for every single instance of power consumption, and thus a direct contract between end-consumers and power generators would

necessitate exact demand predictions and purchases for all electric appliances. This is nowhere feasible, so instead, consumers are bundled together by BRPs, that then take responsibility for purchasing exactly the amount of power that the consumers need. In case of discrepancies it is the responsibility of the BRP to settle the imbalance. Consumers are then billed in simpler ways, at rates higher than on the power exchanges, so that the BRPs can make profits. Energy flexibility is interesting for BRPs, since it could be used to adjust consumption to when it is cheaper for the BRP to purchase it. Similarly, the BRP could negotiate contracts with consumers, letting the BRP bid their energy flexibility into other markets. When considering the role of BRPs it is important to keep in mind that they are profit-seeking, and thus their actions reflect this. If they are to utilise energy flexibility, then contracts have to be set up, ensuring that the best way for them to increase profits is to utilise energy flexibility in a way that helps the energy grids as much as possible. Also, consumers can not be forced to choose a particular BRP, and so utilisation of energy flexibility has to benefit them as well. This issue is discussed in detail in Section 5.4.1, where proposals on how such contracts could be defined are also analysed.

More details about BRPs can be found in [Jen16].

2.2 Power markets

The BRPs utilise different kinds of power markets to the best of their ability, in order to reduce the costs of purchasing power. The core principles are explained here, since any attempt at incorporating energy flexibility has to either function within them or propose alternative solutions to the current market conditions. The main difference between the markets is the time horizon, ranging from setting up contracts for years ahead on financial markets to requesting up or down regulation with only a few seconds of notice on the regulation market. The focus is on the Scandinavian power exchange, Nord Pool, but most of the information is valid for other areas as well.

2.2.1 Spot Market

The spot market, also known as the wholesale electricity market, is where the majority of power trading happens. Different spot markets have slightly different possibilities for trading, but the overall structure is the same. Every day, prior to noon, BRPs, representing power producers and consumers, bid available production and needed consumption into each hour for the next day. Each bid is accompanied by a price, which is the minimum price at which the producers are willing to sell and the maximum prices at which consumers are willing to buy. At noon the market is closed and cleared, as exemplified in Figure 2.1.

The figure shows how the sell offers are organised in ascending order according to price, and vice versa for buy offers. The clearing is done by finding a price, so

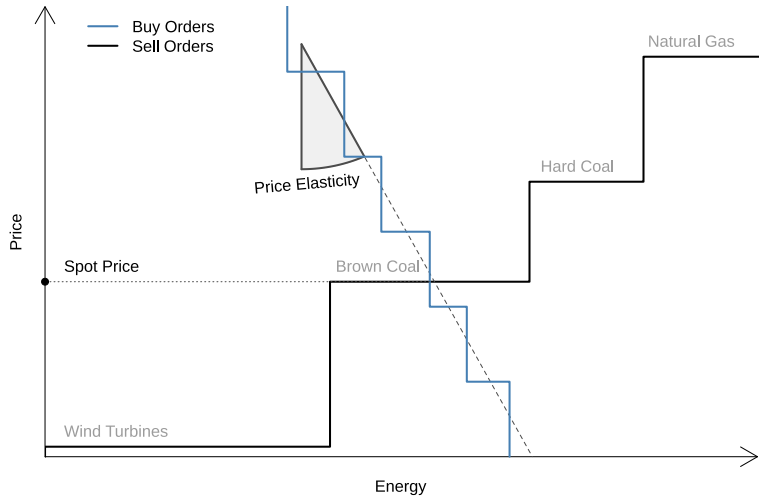

Figure 2.1: Typical example of stacked buy and sell order and the clearing mechanism used for obtaining the spot price. The angle called "Price Elasticity" is a simple measure of energy flexibility.

that the sum of all buy orders with a larger price equals the sum of all sell orders with a smaller price. This price is called the spot price, and all buy orders with price larger than the spot price are won, and have to pay the spot price. Likewise, all sell orders with prices lower than the spot price are won, and they receive the spot price in exchange for producing the specified amount of power. Having the same price for all won bids incentivises sellers to bid their power production into the market at their break-even price, and likewise for buyers.

The slope of the buy orders, indicated by the angle called "Price Elasticity" in Figure 2.1, is a simple form of energy flexibility, since the larger it is (up to 90 degrees), the more responsive the demand is to price. In reality it is almost zero, since most buy orders use a very high price, so that they are practically guaranteed to win their bids no matter what.

On Nord Pool, slightly more complicated options for using the spot market are also available. The first is "regular block orders", where a number of regular hour-bids are submitted as a bundle that can only be accepted if the whole bundle is accepted. A variation is the "linked block orders", where a hierarchy of bids are submitted. For bids in a particular layer of this hierarchy, they can only be accepted if all bids in lower layers are also accepted. Another variation is the "curtailable block orders",which are

like regular block orders, but are accompanied with a number between 0% and 100%. If this number is smaller than 100% it indicates that the bids can be accepted partially down to this number. Finally, "flexi orders" consist of an interval, $[a, b]$, a number, n, between 1 and $b - a$, and a quantity of energy, P. These bids result in P energy being bought, in the n cheapest hours of the interval $[a, b]$. In Paper D it is shown how flexi orders can be used to bid energy flexibility into the current market on Nord Pool.

See 3.1.1 in [EP07] for further details concerning the available market produts.

2.2.2 Intraday Market

The intraday market (called Elbas on Nord Pool) is a market in which energy is continuously traded as pay-by-bid. Typically, this is used to adjust the amount of energy bought and sold on the spot market. This happens when forecasts of power generation and/or demand change significantly, for example due to generation failures or changes in weather predictions. Trading is allowed up till one hour before the power is scheduled. This market is seeing only limited use with a low volume of trading.

See 3.1.2 in [EP07] for more information.

2.2.3 Regulation Market

The regulation market is different from the other markets, since here both capacity and energy is traded. When capacity is bought on this market, the buyer can, with some specified time notice, ask the seller to adjust generation or demand according to the bought capacity. This is done to balance generation and demand, when imbalances occur due to uncertainty in generation and demand. When regulation is needed, a regulation price is made as well, which is paid for the adjustment in energy to those who adjust their power production or consumption. BRPs, who did not initially sell capacity in the regulation market, can choose to participate, and be rewarded according to the regulation price, if they find this attractive.

For more information on the regulation market see section 2 in [Par17].

2.2.4 Balance Market

The balance market is an after-the-fact, purely economic mechanism, where differences in what was promised and delivered are settled. This means that, for each hour, everyone who consumed more energy than they bought, will pay for the excess consumption in the balance market. Similarly, those who consumed less than they bought are compensated accordingly. The same is true for producers who generated more or less than promised. Thus, the balance market does not include any kind of bidding or clearing, but is an automatic settling of imbalances.

The price at which this is done depends on whether the actor is producing or consuming energy. For consumers, the balance market is made quite favourable,

since the price at which imbalances are set, is in this case equal to the hourly average regulation price. For producers, the price is also equal to the average regulation price, if the imbalance caused by them was detrimental to the energy grid. Otherwise, if the imbalance was helpful to the grid, the settling price equals the spot price. This means that, on the balance market, producers are punished for causing imbalances, but not rewarded for preventing them. Meanwhile producers are also punished for causing imbalances, but on the contrary, rewarded for correcting them.

Notice that even small volumes can cause imbalances, so BRPs representing large amounts of consumption should still limit their imbalances. Otherwise their own imbalances will tend to impact the regulation price so that they pay high costs for imbalances.

For more information consult section 3 of [Par17].

2.3 Distribution System Operators

The final delivery of electricity to end-users is carried out by DSOs. Their main responsibilities are to avoid voltage problems and local congestions. Voltage problems can arise in two ways, both exemplified in Figure 2.2, where two scenarios of voltage along a feeder is shown, together with the required minimum and maximum voltage.

The Cloudy scenario is the most traditional one where there is no production on the feeder, which results in a voltage drop along it. More recently, with local power generation such as PV, consumers often have power generation surpassing their demand, and if neighbouring consumers all have PV, then this tends to happen at the same time, namely when the sun is shining. This results in a voltage increase along the feeder, as shown by the Sunshine scenario in Figure 2.2. The DSO can only control the voltage along the feeder by manipulating the voltage at the start of it. This means that only the initial voltage, V_0 in Figure 2.2, can be controlled while the slope remains outside of the DSO's control. Sometimes, the slope is too large such that no matter how V_0 is set, voltage violations (when the voltage leaves the interval between the minimum and maximum voltage) are bound to happen. In this case, the only solution is to reinforce the feeder or use energy flexibility to change the slope of the voltage change by either curtailing PV-production or increasing consumption. When the slope is smaller, such that a V_0 exists for which all voltages are within the boundaries, there are still problems, since V_0 is usually not changed automatically, but rather requires manual intervention. Before the prevalence of local production this was not a problem, since V_0 would only need to be changed rarely, but with local production different values could be needed several times a day depending on the weather.

Congestion problems arise when more power has to be transferred through a feeder than it was designed for. Currently, this does not happen frequently, since feeders have been dimensioned to handle the maximum requirements of typical consumers.

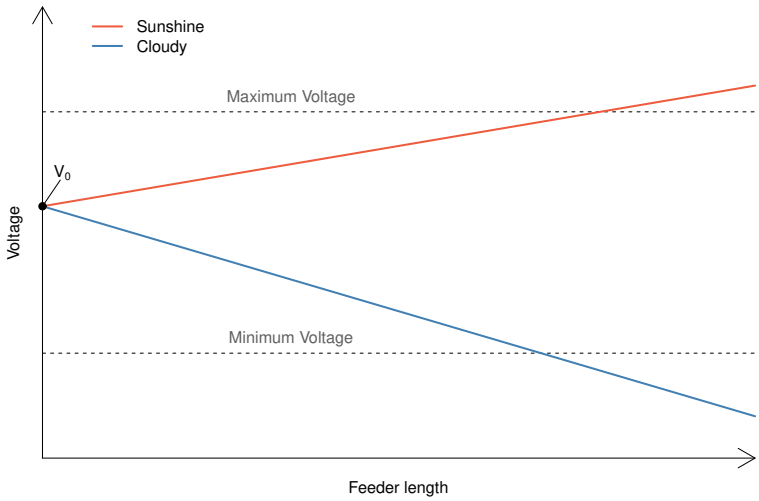

Figure 2.2: Voltage along a feeder with a lot of photo-voltaics, during sunshine when the photo-voltaics are producing and during a cloudy day when they are not.

However, with electrification of the heating and transportation sector, this is changing. Figure 2.3 shows the typical energy demand on a feeder with a lot Electric Vehicles (EVs) and electrified heating. It is clear that the demand is not evenly distributed, but rather has a peak during the morning, when people typically shower and the evening when they cook. Unfortunately, the charging of EVs is heavily concentrated at the hours just after people come home from work, park their cars and starts to cook. So, even though there is a lot of excess capacity almost all of the time, there are a few hours in which demand goes above the capacity limit.

Currently there are no markets that DSOs can use to mitigate these problems, since local production on household level is not bid into any of the current markets. In the future DSOs will have to be able to utilise the energy flexibility to some extent. In Section 5.4 methods for how DSOs could influence the price received by consumers, and thereby indirectly affect their demand, are proposed.

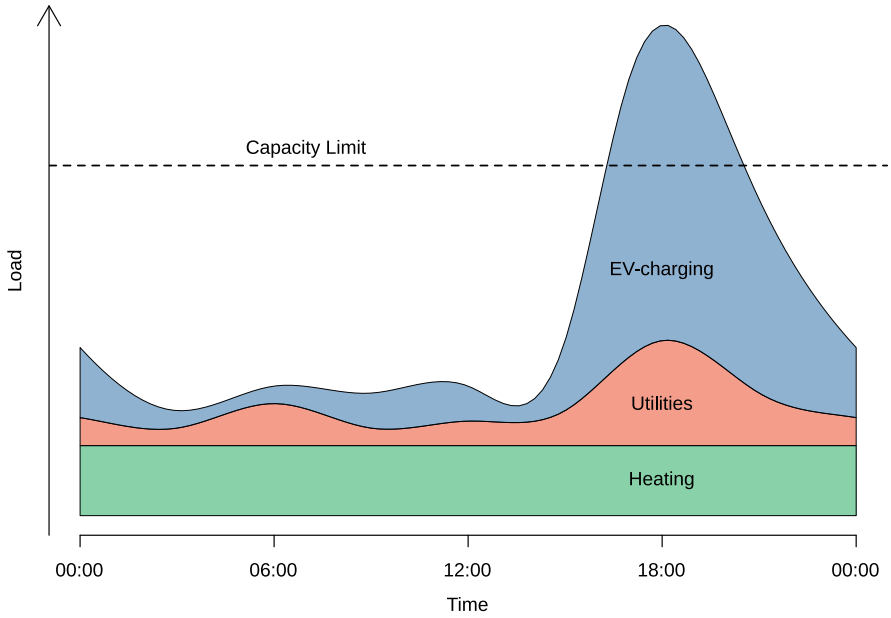

Figure 2.3: Power demand on a feeder with a lot of Electric Vehicles.

2.4 Transmission System Operators

The main responsibility of TSOs is the long-distance transmission which mainly consists of delivering power from generators to DSO-grids, and exchanging power between DSO-grids. This includes planning of power grid reinforcements to avoid congestion and connections to neighbouring power grids to enable exchange of power. TSOs are typically responsible for very large areas, on the size of smaller countries. For example, there is only a single TSO in Denmark. Thus, many DSO-areas are located within a single TSO area. The typical problems faced by TSOs are congestion and frequency problems, and more critically avoiding blackouts. The congestion is similar to that of DSO-grids, but while the cause of DSO-congestion is mostly EVs, the TSO-congestion comes from variable power generation. Especially RESs are a big problem since they vary a lot, and thus, similar to the charging of EVs there are a few hours in which the power generation is very high. The core of this issue is shown by Figure 2.4, in which the production of wind power in northern Germany is shown for 2018 (data

from [Wie+19]). It shows that the distribution is very skewed, with a few hours of very high production and many hours with only low production. Notice that the distribution would be even more skewed if the wind turbines were never turned off due to overproduction. In this case the capacity factor is 3.7 for onshore and 2.5 for offshore wind power production, meaning that, on average, the wind turbines produce $\frac{1}{3.7}$ and $\frac{1}{2.5}$ of their full capacity onshore and offshore respectively. This is a problem, since there are few hours with very high generation, so to reinforce the grid to be able to handle those few hours, would require them to, on average, be over-dimensioned between 2.5 and 3.7 times.

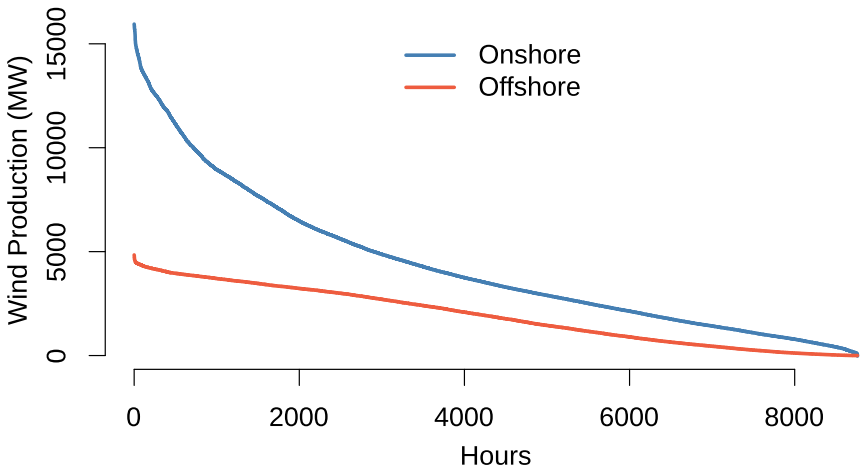

Figure 2.4: The amount of hours (x-axis) for which the wind power generation in the northern transmission system area of Germany surpassed specific amounts of generation (y-axis) in 2018, i.e. their load duration curves..

Whereas congestion problems are local in nature, frequency problems are global in the sense that the frequency can be considered constant within a TSO grid. The frequency, like the voltage, should be kept at a nominal value, since electrical appliances are designed for this. However, whenever power generation does not match power consumption, the frequency changes. When generation is larger than demand, frequency increases and vice versa when demand is larger than generation. Thus, generation and demand has to be kept in balance at all times. Traditionally, this is

done purely by adjusting generation continuously to follow the demand. The TSOs accomplish this by utilising a combination of the regulation market and the intraday market. Capacity bought on the regulation market is controlled such that it turns generation up (or demand down) when the frequency is below the nominal value and vice versa when the frequency is above the nominal value. In practice this is the dominant driver of regulation prices. When the capacity from the regulation market is insufficient to keep the frequency stable, as is the case for sustained differences in the predicted demand and/or generation, the TSO uses the intraday market. Here the TSO can make someone turn on power generation (or decrease demand) by buying energy or have someone turn off generation (or increase demand) by selling energy. It is clear that energy flexibility is well suited for this task, as it would only require minute changes in demand from the huge population of consumers within a single TSO-area,

CHAPTER 3

Stochastic Dynamic Modelling

Energy flexibility is both dynamic and stochastic in nature [Cor+13]. It is dynamic because changing demand at one point in time influences the demand at later time points. For example, a refrigerator has an interval in which the temperature of the goods inside should be kept. When the temperature is close to the lower boundary, the refrigeration can be turned off, thus reducing power consumption, but only until the temperature reaches the upper boundary. Thus, the available energy flexibility is dependent on the temperature in the refrigerator, which in turn is dependent on the usage of energy flexibility. This means that the available energy flexibility is dependent on the previous usage of the energy flexibility, and thus it is dynamic. Staying with the refrigerator analogy, the stochasticity is seen to come from multiple sources. For example, the change in temperature depends on the heat capacity of the goods in the refrigerator, which is varying and most likely unknown to whoever is utilising the energy flexibility. Moreover, interacting with the refrigerator by opening it or putting things in it, influences the temperature as well. Since it is difficult to predict exactly when someone will interact with the refrigerator, this is best described as stochastic.

In this chapter the methods used to model stochastic and dynamic systems are introduced, starting with the discrete and linear models, most often used to model time series in Section 3.1. Next, in Section 3.2 the concept of Stochastic Differential Equations (SDEs) is introduced, since these are useful for incorporating physical relationships in the modelling of dynamic systems. Building on the SDEs, Section 3.3 introduces a common method for combining stochastic processes with noisy measurements, called state-space models. Finally, the non-parametric method of spline estimation is explained in Section 3.4 since these can be combined with SDEs to form grey-box models.

3.1 Dynamic Discrete-time Models

Discrete-time models work in time steps, by directly modelling a phenomena at each time step as a function of some inputs. If previous values of the modelled phenomena are included as inputs or if inputs from different time steps are used to model the phenomena during the same time step, then the model is said to be dynamic. Thus, in general, stochastic and dynamic discrete-time models are given by

$$X_{t+1} = f(\mathcal{X}_t, \mathcal{U}_{t+1}, \epsilon_t),$$

where X_t is the value of the modelled process at time t, while $\mathcal{X}_t = \{X_s : s \leq t\}$ and $\mathcal{U}_t = \{U_s : s \leq t\}$ are collections of previous process and input values. For all $t \in \mathbb{Z}$, ϵ_t, is a random variable that accounts for unmodelled phenomenons, uncertainty in the inputs and measurement errors. For the work done in this thesis the only discrete-time models that have been used were linear, which in general form are given by

$$X_{t+1} = \sum_{k=0}^{\infty} \alpha_k X_{t-k} + \sum_{k=-1}^{\infty} \beta_k u_{t-k} + \sum_{k=0}^{\infty} \theta_k \epsilon_{t-k}, \tag{3.1}$$

where α, β and θ are parameter vectors or matrices depending on whether there are multiple inputs and/or outputs. u_t is assumed to be deterministic while ϵ_t is assumed to be independent and identically normal-distributed with some fixed variance, σ^2, that is $\epsilon_t \sim N(0, \sigma^2)$, for all time steps $t \in \mathbb{Z}$. Further simplifying the model by only including finite terms, leads to what is probably the most popular model in the field of time-series analysis, namely the Auto-Regressive Moving Average with eXogeneous input (ARMAX)-model:

$$X_{t+1} = \sum_{k=0}^{N_1} \alpha_k X_{t-k} + \sum_{k=0}^{N_2} \beta_k u_{t-k} + \sum_{k=0}^{N_3} \theta_k \epsilon_{t-k}.$$

This model structure was used to model swimming pools in Report L.

During the work carried out in this PhD study the particular subclass of ARMAX-models called Finite Impulse Response (FIR)-models was used to present the first concept of a dynamic energy flexibility representation in Paper B:

$$X_{t+1} = \sum_{k=0}^{N} \beta_k u_{t-k} + \epsilon_t. \tag{3.2}$$

The impulse and step responses are important characteristics for dynamic models, and are obtained by putting the input equal to either an impulse or a step function, and then observing the output. First, define the impulse and step functions as

$$\mathbb{1}_0(t) = \begin{cases} 1 & t = 0 \\ 0 & \text{else} \end{cases}, \quad H(t) = \begin{cases} 1 & t \geq 0 \\ 0 & t < 0 \end{cases}.$$

Then, the impulse response of an FIR model is obtained by letting $u_t = \mathbb{1}_0(t)$ in (3.2):

$$h(X)_t = \sum_{k=0}^{N} \beta_k \mathbb{1}_0(t-k) + \epsilon_t = \beta_t + \epsilon_t.$$

Likewise having $u_t = H(t)$ in (3.2) yields the step response function:

$$S(X)_t = \sum_{k=0}^{N} \beta_k H(t-k) + \epsilon_t = \sum_{k=0}^{\min(t,N)} \beta_k + \epsilon_t.$$

Linear systems are uniquely determined by both their impulse and step response. Using this fact, the step response was thoroughly interpreted for some Energy Flexible Systems (EFSs) in Paper B, to understand the nature of the energy flexibility.

Another function that can be used to represent linear systems equally well is the frequency response function. This method relies on the fact that, in frequency domain, linear systems scale the amplitude of each frequency present in the input independently. This means that by knowing the scaling factor for each frequency, the system is completely characterised. The frequency response function is easily obtained by performing the discrete Fourier transform of the impulse response function [Mad07]:

$$\mathcal{H}(X)_\omega = \sum_{k=-\infty}^{\infty} h_k \exp(-i\omega k),$$

where ω is the frequency, which for the stochastic process, X, is scaled by $\mathcal{H}(X)_\omega$, so that the amplitude of this frequency is $\mathcal{H}(X)_\omega$ times the amplitude that it had for the input. The frequency response function was used in Paper C to tailor price-signals according to what frequencies that were best suited for price-controlled systems.

Detailed information on linear time-series analysis can be found in [Mad07].

3.2 Stochastic Differential Equations

For most practical purposes time can be assumed to pass continuously [New87]. For this reason, almost all dynamic physical laws are formulated in continuous time. This is usually done with Ordinary Differential Equations (ODEs) and Partial Differential Equations (PDEs), which really means that instead of modelling the state of a process directly, as for the discrete-time models, instead the *change* of the state is modelled. This is the exact same approach for SDEs, but stochasticity is included, which necessitates some carefulness. The underlying key concept is that of the Wiener process, also known as Brownian motion. Formally, a stochastic process, W, is said to be a Wiener process if and only if

1. $W_0 = 0$.

2. W has independent increments: for every $t > 0$, the future increments $W_{t+h} - W_t,\ h \geq 0$, are independent of the past values $W_s, s < t$.

3. W has Gaussian increments: $W_{t+h} - W_t$ is gaussian with mean 0 and variance h, that is $W_{t+h} - W_t \sim N(0, h)$.

4. W has continuous paths: W_t is continuous in t.

Going through the requirements one by one, reveals why the Wiener process is well-suited for modelling process noise. It is practical to have stochastic processes that start in 0, which is the reason for condition (1) and if one wishes to have a Wiener process that does not start in zero, one can simply define it as $Z_t = W_t + a$, where a as a scalar that defines that starting value Z_0. As will be shown, it is really the increments of the Wiener process which are used to model process noise, and so conditions (2) and (3) are dealing directly with them. Condition (2) ensures that all increments are independent, i.e. their spectrum is white, which makes it easier to use them for noise representation. If one wishes to have coloured noise, then this can be obtained by filtering the Wiener process through a filter. Condition (3) is a consequence of the central limit theorem, since each increment can be expressed as a sum of infinitely more and smaller increments. The consequence is that the Wiener process is best suited for gaussian noise. This is often a good approximation for physical systems, again because the central theorem dictates that the sum of many random variables approaches the gaussian distribution (under usual regularity conditions). Finally, condition (4) ensures temporal continuity, which makes the noise approach 0 when the time step goes to 0. This is a good approximation for most noise, with the exception of event-based noise, such as a lighting strike or instantly turning a large power generator off.

With a basic understanding of the Wiener process, the general SDE can be formulated, but first consider the standard ODE:

$$\frac{\mathrm{d}x_t}{\mathrm{d}t} = f(x_t, u_t),$$

where U_t is known input and x is a function, considered to be the solution of the ODE. This is essentially the differential equation that should be expanded to a stochastic version, but since only the increments of the Wiener process are well-behaved, it has to be reformulated into integral form:

$$X_t - X_0 = \int_0^t f(X_s, U_s)\mathrm{d}s + \int_0^t g(X_s, U_s)\mathrm{d}W_s.$$

Notice that the second term is an integral w.r.t. a Wiener process. This is not the standard Riemann integral, but can be defined in a number of ways. Here the Itō-interpretation is used, in which it is the limit of of the sum approximation using the left end point of the integrand. To make the SDE look more like the ODE, the

following shorthand is usually employed, where the drift part is the deterministic part and the diffusion part explains the stochasticity:

$$\mathrm{d}X_t = \underbrace{f(X_t, U_t)\mathrm{d}t}_{\text{Drift}} + \underbrace{g(X_t, U_t)\mathrm{d}W_t}_{\text{Diffusion}}. \tag{3.3}$$

Here X is still the solution of the SDE, but it is a stochastic process, f is a function with the same interpretation as for the ODE, while g is a function modelling the process noise through the Wiener process W_t. U is input that could be either deterministic or stochastic. Using SDEs for modelling consists of choosing f according to the dynamics under consideration and g so that it represents the stochasticity.

To learn more about SDEs and their properties see [Thy16] or [Øks03].

3.3 State-Space Models

Most models do not explicitly model uncertainty, and if they do it is often assumed that only one kind of uncertainty is present. However, in reality, most systems are exposed to several kinds of uncertainty. For example, measurements of the temperature in a house with people living in it are influenced, of course, by the real temperature which is exposed to the uncertainty of the occupant behaviour. At the same time, the temperature measurements are also subject to measurement noise. These are examples of the two fundamental kinds of noise in dynamic systems, namely process noise, such as the occupant behaviour, and measurement noise. The functional difference, is that while the measurement noise is related to only one measurement, the process noise stays in the system. In (3.4), (3.5), the general continuous-time state space model based on SDEs is shown.

$$\mathrm{d}X_t = f(X_t, U_t)\mathrm{d}t + g(X_t, U_t)\mathrm{d}W_t, \tag{3.4}$$

$$Y_k = h(X_{t_k}, U_{t_k}) + \epsilon_k, \tag{3.5}$$

where $t_1 \leq t_2 \leq ... \leq t_N$, are the time points at which N observations were taken according to (3.5) with $\epsilon_k \sim \mathcal{N}(0, \sigma^2)$ being identically distributed and independent random variables, representing the measurement error. U is the collection of inputs to the system.

Figure 3.1 shows an example of a simulated time series, exposed to both process noise and measurement noise, as is typically the case for real data. The objective is to estimate the process, from which the observations come from. This can be done, simply by assuming that there is no measurement errors, in which case the measurements are assumed to be equal to the underlying process. This results in interpolation between the observations, meaning that whatever model might have been developed for the system, will be completely disregarded, shown by the green line. Another approach is to assume that a model of the system is without error, and thus any difference between the predictions of the model and the measurements have

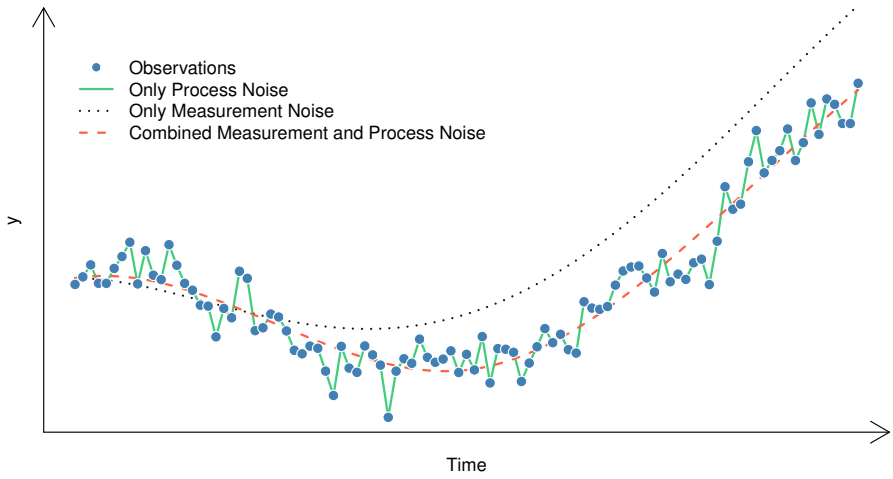

Figure 3.1: Typical time-series data and a comparison between models assuming measurement and/or process noise.

to be purely due to measurement errors. In this case the observations are completely disregarded, as shown by the black dotted line. The third and final approach is to assume that both process noise and measurement noise is present, and thus both the predictions of the model and the measurements are wrong. This results in an estimate of the underlying process that uses both the model and the observations, giving an estimate that tend to follow the observations loosely, illustrated by a red stipulated line.

The third option is exactly what is obtained for the state space models, and so this model structure was used to identify a Duffing oscillator in Paper A and the price-responsiveness of a water tower in Paper D.

Further details on state space models can be found in [Mad07].

3.4 Spline Estimation

It is preferable to use physics as the backbone of mathematical models, but sometimes it is not possible. In this case non-parametric models are useful, where input and output is given, and a relationship is then found by the non-parametric method.

A particular kind of non-parametric methods called spline estimation was used in Paper D to find the instantaneous relationship between energy prices and consumption, and thus this method is explained here.

Splines are a particular kind of basis functions, which can be used as building blocks to find non-linear relationships. For data consisting of the time series Y and X, the spline estimate of Y_t given X_t is:

$$Y_t = \sum_{k=1}^{N} \beta_k \mathrm{S}_k(X_t),$$

where for $k \in (1, 2, ...N)$, β_k are parameters that have to be identified and S_k are spline functions that are decided prior to estimation. The concept of how simple

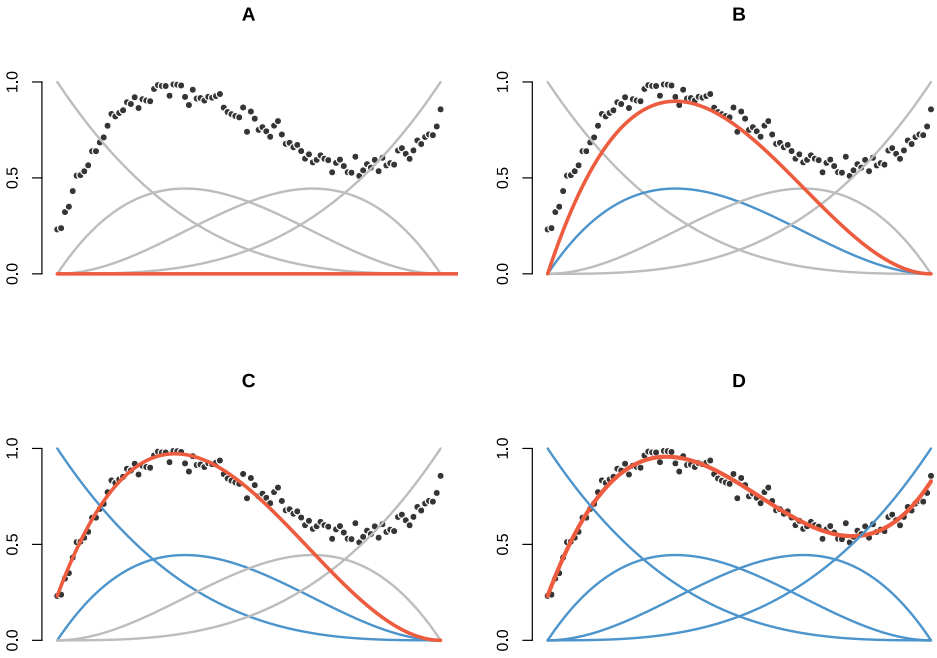

Figure 3.2: Fitting data using splines. A): 0 active splines B): 1 active spline C): 2 active splines D): 4 active splines.

spline functions can be combined to estimate non-linear relationships is illustrated in Figure 3.2. In **A** the data is shown in black and the spline functions in grey. In **B** one of the spline functions is used to fit the data, resulting in the red line. Since only one

spline is used, the fit is simply a scaled version of this one spline in this case. In **C** two of the splines are used, resulting in a fit that is quite accurate for the part of the data where these two splines are mainly used, but a poor fit for the remaining part. Finally, **D** shows the fit where all the splines have been used, and it clearly follows the data well.

One of the key advantages of spline estimation is that the splines can be computed prior to parameter estimation, in which case $\mathrm{S}_k(X)$ can simply be considered as input and the problem is reduced to linear regression. This means that computationally speaking, spline estimation can be used to reduce non-linear optimisation to linear optimisation. In particular this can be used in combination with the state space models, where the splines are treated as regular inputs. This allows parts of the state space model to be governed by physical equations and parts to be estimated purely through data, resulting in grey-box models.

Spline estimation is mostly a hands-off approach, but there is still some choices to be made by the modeller. First of all the amount of splines have to be chosen, which is the typical trade-off between bias and variance, where more splines will fit the data better, thus reducing bias, but at the same time the risk of overfitting increases, increasing variance. Also, several kinds of spline functions exist, and the modeller has to choose what kind to use. Most often the third order B-splines are chosen, as is the case in Figure 3.2. However, if particular knowledge is known about the relationship one wants to model, it might be preferable to use a different kind of splines. For the case of Paper D, where the relationship between demand and price is modelled, it is known a priori that larger prices results in lower demand. Thus, the relationship is monotonously decreasing which can be ensured by using I-splines. These are given by

$$\mathrm{I}_j(u;k,t) = \int_0^u \mathrm{M}_j(x;k,t)\mathrm{d}x,\ \mathrm{M}_j(y|k,t) = \frac{\mathrm{S}_j(y;k,t)}{\int_{-\infty}^{\infty}\mathrm{S}_j(x;k,t)\mathrm{d}x},$$

where S are S-splines, so that M are normalised S-splines. As a result I are monotonously increasing splines that starts in 0 and ends in 1. The final decision that the modeller has to make is the placement of the splines. This is done through the knot points, which are points for which the resulting fit is exact. Close to the knot points, the fit has a lot of flexibility, and thus data is fitted more accurately near the knot points. Therefore the knot points can be placed where the modeller is confident in the ability of the data to fit the phenomenon at hand. Typically these are places where the data density is high, so that a lot of data can be used to make the fit where it is accurate. Similarly, it is usually unwise to have knot points in places with a low data-density, since then the few points will tend to be overfitted.

An in depth guide to using splines in modelling can be found in [DL93].

CHAPTER 4

Control Theory

While models describe the world as it is, they do not change it. To do so, control theory is needed. In control theory the knowledge obtained from models is used to decide how to influence the world, such as to obtain some objective. In particular, the models developed in this Phd study should be used to control energy flexibility with the objective. Thus, even though this study was mostly concerned about modelling and characterising energy flexibility, control theory is needed to utilise it. Also, the developed energy flexibility characterisations assume that price-aware controllers are in charge of EFSs. This means that the controllers of EFSs are just as important for the realised energy flexibility as the physical components. Therefore, even though this PhD study did not advance the field of control theory, its results are only useful if combined with control theory. Consequently, an introduction to the parts of control theory relevant to energy flexibility are included here, and related to specific problems for which they are useful.

The chapter starts by introducing classical controllers in Section 4.1. This is extended with the class of Model Predictive Controllers in Section 4.2. In particular, the variation called Economic Model Predictive Control is of relevance to price-based control of energy flexibility, and so this is explained in Section 4.3.

4.1 Classical Control

In classical control, single input, single output systems are controlled, to make the output follow some reference. The control actions are based solely on the difference between the output and the reference. This makes for very simple and robust controllers. Usually the main point of control objectives is to minimise the squared deviation between the output and a reference:

$$\underset{U}{\operatorname{argmin}} \left(X(U) - r\right)^2,$$

where U is the input, X the output and r is the reference. Since there are no restrictions on the input in this formulation, the solution is simply to solve the equation $X_t(U_t, U_{t-1}, ...) = r_t$ for U_t, for each time step. For a few specific applications this might be satisfactory, but for dynamic systems it often results in inputs that starts to oscillate and grow in size to offset the dynamic consequences of the previous inputs.

To avoid this, numerous solutions have been proposed where it is accepted that the output will deviate slightly from the reference. These controllers can be formulated in closed loop as functions of the difference between output and reference $e_t = X_t - r_t$, as illustrated in Figure 4.1. What happens in the controller-box is defined by the particular kind of controller.

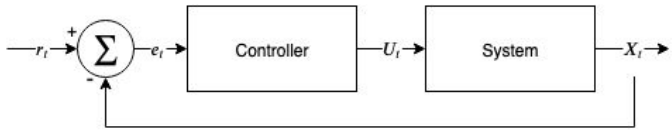

Figure 4.1: Information flow for classical controllers. The difference between reference is given to the controller which then produces a control action to the system. The output of the system is then measured and sent back, to be compared to the reference.

The majority of classical controllers falls within the framework of Proportional Integral Derivative (PID)-controllers, and so, these are briefly introduced here. The control action is in this case computed by

$$U_t = K_p e_t + K_i \int_0^t e_t \mathrm{d}s + K_d \frac{\mathrm{d}e_t}{\mathrm{d}t},$$

where still, U_t is the input and $e_t = X_t - r_t$ is the difference between the observation, X_t, and reference, r_t, at time t. K_p, K_i and K_d are tuning parameters deciding how the controller should act. It is seen that there is no explicit model in the controller, but the tuning parameters implicitly describe the dynamics of the model. For example, if $K_p < 0$, then it means that for positive values of e_t, the control action tends to be negative, which only makes sense if negative values of the input tends to decrease the output. The second term deals with the integrated errors, and thus the contribution from this term reflects a long-term bias of the errors. The last term is based the derivative of the errors, which is a simple prediction of future errors.

The tuning parameters can be estimated without having a model of the system, by simply testing different values until the system is controlled appropriately. However, prior to finding suitable values, the control could have caused fatal problems, and so, it is better to have reasonable values from the beginning. This can be obtained by first modelling the system of interest, and then estimating the tuning parameters, based on simulation of the model. Afterwards, the control-parameters can be tuned based on operation of the system, via e.g. reinforcement learning, where the performance of the control is fed back to the control parameters, which are then updated accordingly [HGB00].

The classical controllers are useful partly because they are simple, but they are also robust in the sense that their control actions are easy to anticipate, and thus one can make sure that they always provide sensible control actions. Their computational

burden is very low, and so they can be useful for highly sampled systems, where speed can leveraged.

For a general overview of the classical control theory see [Nis07].

4.2 Model Predictive Control

For more complicated systems and control objectives, it is favourable to use models explicitly for control. Model Predictive Control (MPC) works by *predicting* the consequence of particular *control* actions, using a *model*. This allows the controller to take long term consequences of its actions into account. This is particularly useful for systems with slow dynamics, since these affect the long term state of the system.

Having a model directly in the control problem is also useful when the dynamics change according to external variables, since this change can be modelled explicitly, which is much easier than having complicated relationships between the external variables and the control parameters. This is particularly important for the systems studied here, where energy flexibility has natural diurnal and seasonal patterns.

The general MPC-formulation for a model on the SDE state-space formulation of (3.4), (3.5) is

$$\begin{aligned} &\underset{U}{\operatorname{argmin}}\ \mathbb{E}\left(C(X,U)\right), \\ &\qquad \text{s.t.} \\ &\qquad X_0 \sim x_0, \\ &\qquad \mathrm{d}X_t = f(X_t,U_t,e_t)\mathrm{d}t + g(X_t,U_t,e_t)\mathrm{d}W_t, \\ &A(X,U) \geq b, \end{aligned}$$

where C is a cost function describing some cost that should be avoided and/or reward that should be maximised. x_0 is the estimated distribution of the system at time 0 and A is a function that, together with the vector b, describes conditions that should be imposed on the state and input. Overall the solution to the problem finds the sequence of control actions, that, when given as inputs to the system, yields the least cost as described by C, while still satisfying the constraints described by A and b. U and e constitute the inputs to the system, with U being controllable (such as heating in a building) and e being uncontrollable (such as outside temperature). In this formulation, the SDE constituting the model is directly included as a condition. This means that the function A will be a function of the stochastic process, X. The most meaningful ways to put constrains on a stochastic process is in terms of probabilities. For example, it is rarely possible to guarantee that a particular value should be positive i.e. that $X_t > 0$. However, it is usually possible to guarantee that it is true with some minimum probability such as 95%: $\mathbb{P}(X_t > 0) > 0.95$.

To reduce complexity it is common to instead use the expected state, for which the problem simplifies to

$$\begin{aligned} &\underset{U}{\operatorname{argmin}}\ C(\mathbb{E}(X), U), \\ &\qquad \text{s.t.} \\ &E(X_0) = x_0, \\ &\frac{\mathrm{d}\mathbb{E}(X_t)}{\mathrm{d}t} = f(\mathbb{E}(X_t), U_t, e_t), \\ &A(\mathbb{E}(X), U) \geq b. \end{aligned}$$

In this formulation x_0 is the estimated value of the system at time 0. Notice that now the conditions are only governing the expected value of the stochastic process, and so it does not ensure that the conditions are actually satisfied with some specific probabilities.

Usually it is not possible to solve the control problem for an infinite control horizon. In this case C and A are only functions of the state and input from a finite time horizon, which reduces the problem further to

$$\begin{aligned} &\underset{U_{0\dots T}}{\arg\min} \int_0^T C_s(\mathbb{E}(X_s), U_s)\mathrm{d}s, \\ &\qquad \text{s.t. } \forall t \in [0, T]\,, \\ &\mathbb{E}(X_0) = x_0, \\ &\frac{\mathrm{d}\mathbb{E}(X_s)}{\mathrm{d}s} = f(\mathbb{E}(X_s), U_s, e_s), \\ &A(\mathbb{E}(X_t), U_t) \geq b, \end{aligned}$$

where T is the control horizon. Notice that the cost function depends on how far ahead the predictions are. This reflects the fact that stochasticity will be more pronounced the further ahead in time predictions are made, and so the controller should put more emphasis on near future.

For linear models, the optimisation is computationally much lighter, and so this is preferable when possible. The general form is in this case given by the linear program [Mur83]:

$$\underset{x}{\operatorname{argmin}} \quad f^\top u \tag{4.1}$$

$$\text{s.t} \tag{4.2}$$

$$Au \geq b, \tag{4.3}$$

For MPC, u is a vector of control actions for the control horizon. f is a function expressing not only the cost of performing control, but also the cost related to the consequences of the control. A and b together gives constraints on the control.

4.3 Economic Model Predictive Control

A variant of MPC which is particularly important for the applications studied here is Economical Model Predictive Control (E-MPC). For these controllers the cost function is an economic term, describing how the cost of controlling the system varies in time. If the cost at each point in time is proportional to size of the control action, U_t, then the problem can be formulated as

$$\underset{U}{\operatorname{argmin}}\ \mathbb{E}\left(\int_t^{t+T} \lambda_t U_t \mathrm{d}t\right) + C(X),, \tag{4.4}$$

$$\text{s.t. } \forall s \in [0,T]$$

$$X_0 \sim x_0, \tag{4.5}$$

$$\mathrm{d}X_t = f(X_t, U_t, e_t)\mathrm{d}t + g(X_t, U_t, e_t)\mathrm{d}W_t, \tag{4.6}$$

$$A(X_t, U_t) \geq b, \tag{4.7}$$

where λ_t is the cost of performing control at time t. A natural example of this is when the control consists of consuming energy with a varying energy price as illustrated in Figure 4.2. This figure shows two ways of controlling the temperature of an office building. One of them is regular energy-efficient control, which is obtained by having λ_t equal to some constant value for all t. The other is an example of E-MPC, aimed at reducing the amount of emitted CO_2. For both of the controllers, the core objective is to keep the building within comfort constraints. The middle figure shows the CO_2-intensity and it is clear that the E-MPC tends to heat more in the hours with low CO_2-intensity, while the regular controller simply keeps the temperature close to the lower boundary. Notice how the temperature varies more for the E-MPC, since it takes advantage of times with low CO_2-emission. The overall energy consumption can be expected to increase for the E-MPC compared to the regular controller, but as seen in the bottom plot, the accumulated emissions are reduced.

In the general formulation given by (4.4)-(4.7), λ_t is the CO_2-intensity and U_t is the heating at time t. X is the temperature and thus if it is satisfactory to keep the expected temperature within the limits then $A(X,U) = (\mathbb{E}(X), -\mathbb{E}(X))$ and $b = (T_{\min}, -T_{\max})$, where $T_{\min}$ and $T_{\max}$ are vectors containing the minimum and maximum allowed temperatures respectively. Alternatively the constraints can be chance-based so that $A(X,U) = (\mathbb{P}(X > T_{\max}), \mathbb{P}(X < T_{\min}))$ and $b = (p_{\max}, p_{\min})$, so that the probability of being above the max temperature or below the minimum temperature are smaller than $p_{\max}$ and $p_{\min}$ respectively. If there are no preferable temperatures within the comfort interval then $C = 0$, but it could be that there were some preferable temperature, T_{opt}, in which case one could have

$$C = w\mathbb{E}\left((X_t - T_{\text{opt}})^2\right),$$

where $w > 0$ is the weight put on obtaining the optimal temperature. f and g should describe the heat dynamics of the building and the effect of the heating equipment.

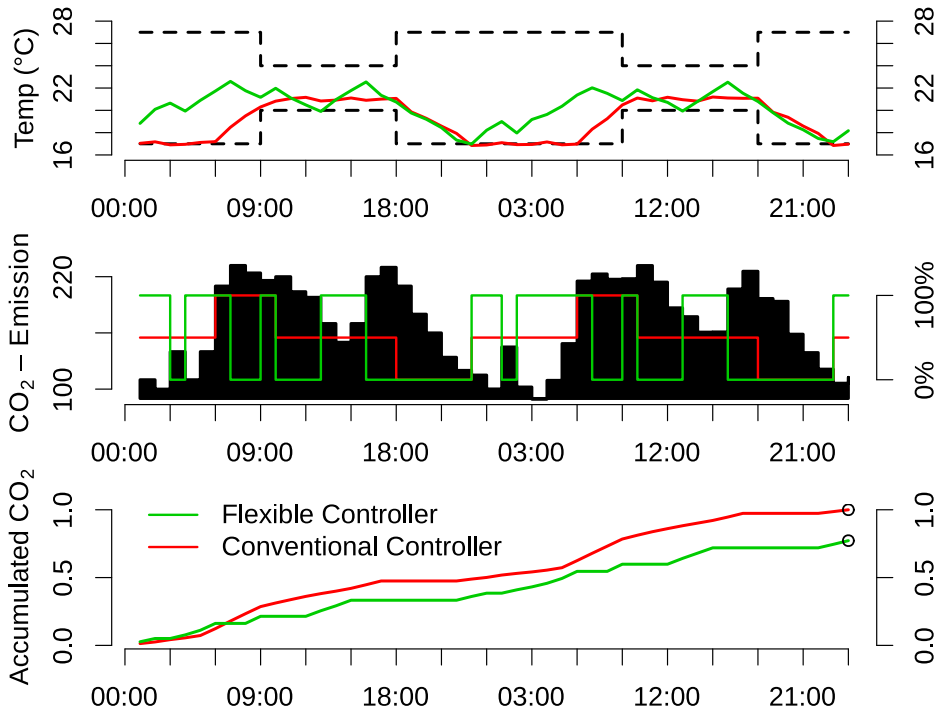

Figure 4.2: Regular (red) and Economic Model Predictive (green) control of office building with varying temperature requirements. Top: Temperature in building. Middle: CO_2-emissions of energy generation and heating profiles. Bottom: Accumulated emissions due to heating of the building.

This particular type of E-MPC is the method proposed in Paper F, and later implemented in Report L for heating of swimming pools located in Danish summer houses.

CHAPTER 5

Discussion of Contributions

The work done during this PhD study can be put into five overall categories. First, in Section 5.1 the class of models called SDEs was explored. Afterwards, in Section 5.2 the developed characterisation of energy flexibility is presented. Section 5.3 follows with a description of the methods and controllers developed to receive and act upon price signals by utilising energy flexibility. Next, Section 5.4 presents suggestions on how price signals should be designed, such that energy flexibility is utilised optimally to solve relevant problems. Lastly, in Section 5.5 the methodology for modelling energy flexibility is combined with high-level energy planing.

5.1 Continuous time modelling using stochastic differential equations

Energy flexibility is a dynamic and stochastic phenomenon, and thus should be studied using time series analysis. To support this, part of the PhD study, was spent on advancing the field of system identification of dynamic and stochastic systems using state space models based on SDEs. In particular, the purpose of the models is to be used for model *predictive* control, and so, the employed estimation and testing should reflect this.

In Paper A, it was shown how dynamic systems can be modelled using the state space formulation of (3.4), (3.5). It was demonstrated how physics can easily be incorporated in the model, enabling the modeller to utilise a priori knowledge. Subsequently a method for estimating the parameters aimed at improved long-term prediction power is presented. The same procedure was used for modelling and estimating the parameters of the flexibility function governed by (5.2)-(5.5) in Paper D.

The estimation procedure presented in Paper A is designed to deal with the fact that diffusion scales with the square root of time, while drift scales linearly with time. Formally, if e is a stochastic process governed by a drift term, μ, and a diffusion term with intensity σ:

$$de_t = \mu \mathrm{d}t + \sigma \mathrm{d}W_t,$$

where W is a Wiener process, then given $e_0 = 0$

$$\mathbb{E}(e_t^2) = \mu^2 t^2 + \sigma^2 t.$$

This means that if e_t describes the t-step errors of a model, then the result of minimising the squared errors is significantly different depending on what time step is used. Usually, it is assumed that the expected value of model errors equals zero, meaning that $\mu = 0$. In this case it does not matter what time step is used, but for real world applications it is almost never a valid assumption. Thus, the time step should be chosen to match the time steps for which the model is going to be used for.

In Paper A the performance of the model was compared to models from other researchers, based on prediction from time 0, meaning that it consisted of a 1-step prediction, a 2-step prediction and so on. Thus, the parameter estimation should reflect this, and it was chosen to minimise a cost function inspired by the negative log-likelihood function, but where the prediction and variance estimates were all made at time 0.

The downside to this approach is that the model errors can not be assumed independent. For instance, if $e_{b|a}$ $(b > a)$ is the prediction error of time b made at time a, then $e_{b|0}$ and $e_{a|0}$ are clearly dependent, since $e_{b|0}$ is a combination of $e_{b|a}$ and $e_{a|0}$. This means that it should only be used for systems where the model can predict the output accurately enough for the prediction errors to die out sufficiently fast, so that e.g $e_{b|0}$ depends mostly on $e_{b|a}$ compared to $e_{a|0}$.

In Paper D it was shown how splines can be combined with SDEs to model parts of a dynamic system non-parametrically, while other parts are modelled parametrically. This is an extremely useful feature for modelling of energy flexibility, since it is governed by both physics that are well described by parametric equations and human behaviour which is not.

5.2 Characterising Energy Flexibility

Energy flexibility is not easily quantified, since it consists of many different properties. In particular, it is dynamic, since it gets depleted when used, and thus a dynamic characterisation is required. Still, prior to this PhD study, the only characterisations of energy flexibility were static or contained only very simple descriptions of the dynamics [Zot+19b]. An example is the price elasticity defined as the slope of the demand curve in Figure 2.1. This approach has value due to its simplicity, and in particular when aggregating very large amounts of EFSs. However, the issue with the static approaches is that they are only for EFSs in a particular state. This is usually the steady state, which in many other applications is a natural assumption. However, when it comes to energy flexibility, the whole point is to exploit the flexibility of the system, in which case it is brought out of steady state! Thus, static approaches are only valid until energy flexibility is utilised, at which point they turn useless until the system is brought back to the steady state. This means that the only way to

apply energy flexibility in this case, is to use it very rarely, so that the system can be assumed to be in steady state whenever energy flexibility is activated. Seen from the perspective of applying energy flexibility, it does not matter exactly how it is exactly how it is physically obtained. What matters is the functional relationship between price and demand. By considering the price as input and demand as output, the functional relationship can be estimated as described by Figure 5.1. Here the functional relationship is termed the flexibility function, which constitutes the first dynamic characterisation of energy flexibility, as proposed in Paper B.

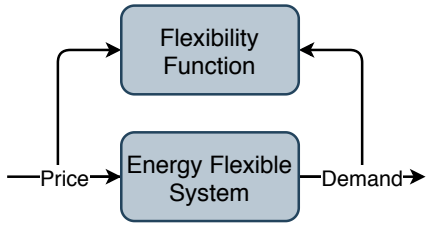

Figure 5.1: Information flow for estimation of flexibility function.

The approach was well received, especially by the building research community, where it was adopted as the primary characterisation of energy flexibility. In particular, the methodology was one of the corner stones of the EBC Annex 67 program, see Reports M,N. In the same project it was also used to characterise the energy flexibility of a number of EFSs in Report O.

Figure 5.2 portrays a flexibility function, by the change in demand of an EFS when exposed to a step-change in price. The general response, in this case, is a reduction in demand, possibly with some delay, followed by the demand gong back to normal, with the possibility of a rebound effect, in which demand is increased to bring the system back to normal. As noted in Paper B, a number of flexibility characteristics can be identified. Each of the flexibility characteristics reflect a particular aspect of the energy flexibility. τ (time) is delay before the system reacts to changes in price, which could be due to communication delays. Similarly, κ (time) is the time it takes the system to obtain the full response, which might be non-zero if appliances can not instantly shut-off or start-up. Δ (effect) gives the largest change in demand, while η (time) is the amount of time that the system can sustain the response. C (energy) is total reduction in energy, while contrary, B (energy) is the energy required for the rebound. Earlier work by other researchers have dealt with these explicitly or implicitly, one at a time. For example, implicitly, in [OCo+14], Δ and η were estimated. Similarly, C and B were estimated for thermal energy flexibility in [RDS17], while very similar quantities to τ and κ were discussed in [SNV12]. In [Rey+18] a review of the different notions of energy flexibility was conducted, but no solution for how to relate them was found. Thus, the full picture of how they interact with each other was not available prior to considering the energy flexibility as a dynamic function.

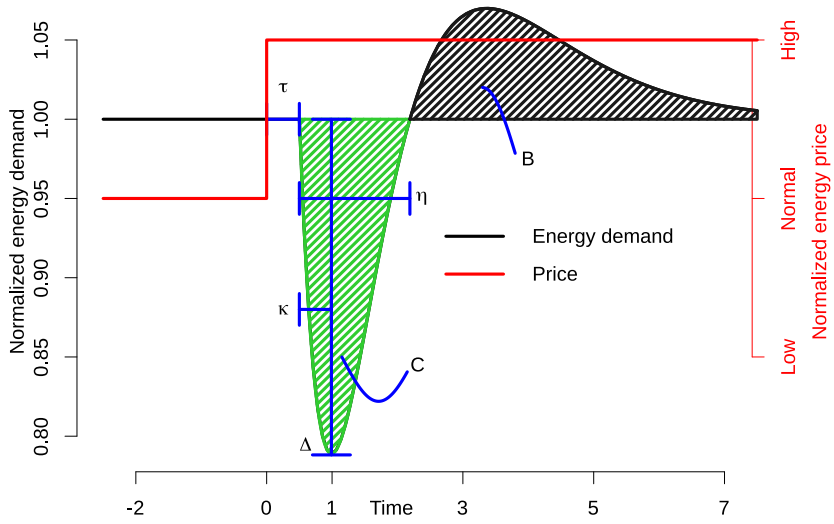

Figure 5.2: Step-response for a linear flexibility function, with the associated flexibility characteristics.

5.2.1 Flexibility Index

Because the flexibility function describes the dynamic behaviour of energy flexibility, it can be used to simulate the expected demand over a long period. In Paper B it was shown how this can be used to quantify the energy flexibility for a particular price-signal, to obtain a Flexibility Index (FI) by simply defining it as the saved cost, compared to non-flexible operation. The steps are as follows

1. Let λ_t be the energy price at time t.
2. Simulate demand using a constant price signal, and let Y_t^0 be the energy consumption at time t.
3. Simulate demand using the price signal λ, and let Y_t^1 be the energy consumption at time t.
4. The total operational cost of the price-ignorant control is given by $C^0 = \sum_{t=0}^{N} \lambda_t Y_t^0$.
5. Similarly the operational cost of the price-aware control is given by $C^1 = \sum_{t=0}^{N} \lambda_t Y_t^1$.
6. Then the quantity

$$FI = 1 - \frac{C^1}{C^0} \tag{5.1}$$

is the fractional amount of saved cost, which is the suggested FI.

By computing the FI for several price-signals, the energy flexibility is assessed for several scenarios. This can be used to obtain FIs describing the value of the energy flexibility when used for different purposes. In paper B three price-signals were designed, and the FIs were computed for three flexibility functions, yielding a total of 9 FIs. The first price-signal reflected the share of non-wind energy in the Danish power grid, the second reflected non-solar energy also in the Danish power grid and the third was proportional to the ramps experienced in the Norwegian power grid. The three flexibility functions represented three buildings with different time constants. The results are shown in Table 5.1. It is seen that for each price-signal the building with the largest FI is different. This means that the value of energy flexibility is heavily dependent on the problems that it is used to solve. Since different countries have different problems, the largest potential for energy flexibility might vary a lot between countries.

Table 5.1: Flexibility Indices for three different flexibility functions, for three different price-signals.

	Wind (%)	Solar (%)	Ramps (%)
FF_1	11.8	4.4	6.0
FF_2	3.6	14.5	10.0
FF_3	1.0	5.0	18.4

5.2.2 Non-linear Flexibility Function

While the flexibility function in Paper B was a step forward in terms of describing the dynamics of energy flexibility, it is too simple to accurately reflect the energy flexibility of most EFSs. An updated, non-linear, characterisation was proposed in Paper E, and further developed in Paper D. Here, SDEs are used to model EFSs as batteries, which are charged or discharged whenever energy flexibility is used. In Paper D it was shown how the parameters can be estimated using the approach from Paper A. While the non-linear flexibility functions lose the ability to be characterised through their step-responses, the flexibility characteristics can instead be used directly as parameters. In particular, (5.2)-(5.5) constitute the general form of the model developed in Paper D.

$$\mathrm{d}X_t = \frac{1}{C}(D_t - B_t)\mathrm{d}t + X_t(1 - X_t)\sigma_X \mathrm{d}W_t, \tag{5.2}$$

$$\mathrm{d}\delta_t = \frac{1}{\kappa}\left(l\left(f(X_t;\alpha) + g(\lambda_{t-\tau};\beta);k\right) - \delta_t\right)\mathrm{d}t, \tag{5.3}$$

$$D_t = B_t + \delta_t \Delta \left(\mathbb{1}(\delta_t > 0)(1 - B_t) \ + \mathbb{1}(\delta_t < 0)B_t\right), \tag{5.4}$$

$$Y_t = D_t + \sigma_Y \epsilon_t \tag{5.5}$$

Here, C, Δ and τ have the same interpretations in the linear case of Figure 5.2 and the nonlinear case, and while κ is measured in time in Figure 5.2 and rate in (5.3), it has the same interpretation. The flexibility characteristics, η and $\mathbf{B}$ do not make sense in the non-linear case, since neither the duration of the change in demand (η) nor the rebound effect ($\mathbf{B}$) are assumed to be independent of the amplitude of the step-change. $0 \leq Y_t \leq 1$ is the output of the model, which is the energy demand. This is given as a adjustment of some baseline demand, B_t, which has to be estimated or forecasted. $0 \leq X_t \leq 1$ is interpreted as the state of charge at time t. For example, for a water tower, as in Paper D, this is the amount of water in the water tower. More generally, it describes the system's ability to be energy flexible. If X_t is large, then the system has spare energy that it can discharge, to reduce its consumption. On the other hand it might not be able to increase its consumption a lot, if X_t is close to 1. Similarly, if X_t is small the system can increase its consumption a lot, but can only reduce it slightly. $-1 \leq \delta_t \leq 1$ is an intermediate variable that explains the desire to increase or decrease demand at time t. It is a function of X_t and the (possibly delayed) price $\lambda_{t-\tau}$, but the exact functional relation is estimated using a non-parametric function. It is used to adjust the baseline demand as described by (5.4). Notice that the change in demand compared to the baseline is proportional to either $1 - B_t$ or B_t, depending on whether the adjustment is positive or negative, reflecting how much of the potential demand that could be turned on, or how much that could be turned off.

This is a good example of how physical knowledge can be combined with statistical methods to obtain a grey-box model that combines features from white-box and black-box models. For example, having a state that describes the state of charge in the system is physically a simple idea. It is also clear that the change in demand is a function of both the state of charge and price. Similarly it is obvious that price and demand are inversely proportional and the same is true for state of charge and demand. However, the exact functional relationship is very hard to deduct. Thus, the functional relationship is estimated from data by the functions f and g, but the structure of these functions is made so that they are forced to be monotonously decreasing, by using I-splines as presented in Section 3.4. This focuses the statistical power to search for models that make physical sense. The overall effect is a reduction of computational burden, a decrease in the risk of overfitting and a model that is ensured to make sense, even for cases where data was insufficient to find good estimates.

Overall, the non-linear characterisation expands the realm of EFSs that can be characterised, while still preserving the intuitive interpretation of the linear representation. This is thanks to the simple physical knowledge put into the SDEs, which allows the flexibility characteristics to be used directly as parameters.

5.3 Bottom level - Receiving Price Signals

In the end, energy flexibility is obtained by adjusting energy consumption. In this PhD study it is has been explored how to make EFS act on price signals, such as to minimise their own costs by utilising energy flexibility. This is a topic that a lot of research has already gone into see e.g. [RAB12; VML14; Hal+12; KJB17a]. Thus, the main focus in this PhD study was to take the price-based controllers and implement them in real-world applications, to demonstrate their potential and investigate challenges.

5.3.1 Smart Control of Swimming Pools

In Report L indoor swimming pools located in Danish summer houses and equipped with electrical heating, were identified as good sources of energy flexibility due to the large heat capacity of the water, which allows the heating to be flexible without influencing the temperature a lot. In this project models were developed for the temperature of the swimming pools, according to the ARMAX model shown in (3.1). A total of 30 swimming pools were considered and all of them were located in summer houses with occasional occupants. Even though all of the swimming pools were conceptually the same, they were of different sizes, with different heating systems and manufactured in different ways. All of this meant that the parameters were different for all of them. Moreover, in order for a methodology to have a chance of becoming commercialised, the parameter estimation would have to be automatic, to reduce the expenses related to manual work. To accomplish this, the parameters of the models were estimated adaptively as described in [Pla50]. This also dealt with the fact that due to seasonality in weather conditions and occupant behaviour, the heat dynamics of the swimming pools changed significantly over time.

Furthermore, an E-MPC based on Paper F was developed to heat the swimming pools at the lowest possible cost. The controller was designed to be able to run in either 5-minute or 1-hour resolution, to reflect the simulated markets in the Smartnet project. For the 1-hour resolution the controller was first tested using the spot prices of Nord Pool, to reflect a scenario where these prices were sent directly to consumers. However, the controller works just as well when the objective is to reduce CO_2-emissions. Thus, it was also tested using CO_2-intensity $\left(\frac{\text{kg}CO_2\text{-eq}}{\text{MWh}}\right)$ of power consumption in Denmark [Tra+19], instead of a price signal, as described in Paper J. This was the first real-world implementation directly aiming at smart control for emission reduction. Finally, the controller was used with price signals in 5-minute resolution, to reflect a market in which regulation prices are updated every 5. minute and sent directly to consumers. While heat pumps are not suited for being switched off and on as often as every 5. minute, the experiments did show that computing, sending and actuating control in this resolution is possible.

5.3.2 Control of Building Integrated Photo-Voltaic with Thermal Absorber and Battery

In Report K a project aimed at developing an E-MPC for controlling a household equipped with a Building Integrated Photo-Voltaic with Thermal Absorber (BIPVT-E) is presented. The BIPVT-E produces both electricity and heat through solar radiation. The heat production is used for domestic hot water and space heating, either directly through a heat exchanger or through the cold side of a heat pump. If there is no or little solar radiation, the BIPVT-E can be used as a heat absorber by running the heat pump, making the water running through the BIPVT-E colder than the ambient temperature, so that the water absorbs heat through conduction. Finally, a battery was attached to the BIPVT-E as well, so that excess electricity production could be stored.

The purpose of the system is to satisfy heat and electricity demand as cheap as possible, under the assumption that electricity prices are varying in time. The control actions to do so are the following

1. Exchange electricity with the power grid.
2. Charge/discharge battery.
3. Run heat pump.

Notice that the heat pump is what connects heat and electricity, since it is powered by electricity and produces heat. Thus, whenever it is run, electricity is converted into heat. It is clear that whenever there is a lack of heat, the heat pump has to be run, and similarly when there is a lack of electricity it has to be bought from the grid. Apart from these two situations it is not trivial how to satisfy the heat and electricity demand.

Consider a situation with cheap electricity prices. In this case the consumer would like to take advantage by filling either the battery with cheap power and/or overheating the water used for space heating or domestic hot water usage. But the best decision is highly dependent on the forecasted consumption. If it will be a long time until hot water is needed, then excess heat in the water will have endured large losses by that time, but if a lot of hot water is needed soon, then the losses are almost negligible, and it might be preferable to store the energy as heat opposed to electricity in the battery. A third scenario is that it is expected that the household will soon receive large amounts of PV and/or solar thermal production, so that it will have more energy than is needed. Assuming that electricity can not be sold to the grid at a favourable rate, the best decision in this case is to ignore the cheap electricity from the grid, and instead rely on own-production.

Ideally, a model of the whole system would be made, from which model predictive control could be performed. However, the system is yet to be run in practice for a real household, and so there is no data to estimate a model from. It is known that the Coefficient of Performance (COP) for the heat pump is a nonlinear function of the

temperature on the cold and warm side, but the exact values are unknown. Usually, this is not a problem, since the heat pump is not operated in a flexible way, but in this case it is, and so the performance has to be known for a larger range of temperatures. Similarly, the COP of the PV is a function of its temperature, but the relationship is not known, only that lower temperatures yield a higher COP.

Thus, making a model for the full system was postponed and, instead, focus was on controlling the electricity part. In this case only two control variables are considered, namely the exchange of electricity with the power grid and charging/discharging of the battery. The electricity demand in this case consists of both regular electrical appliances and the heat pump. The state of charge of the battery can be considered a linear function with a constant efficiency, and so the linear program presented by Equations (4.1),(4.3) was suitable, to formulate the E-MPC-problem as described in Report K.

5.4 Middle level - Sending Price Signals

The price signals received by controllers of EFSs has to be computed, and should be so in a manner that makes the energy flexibility as useful as possible. In general, it can not be assumed that owners of EFSs are willing to act in ways not benefiting themselves. Thus, they will not provide information or utilise energy flexibility unless they are paid to do so. Similarly, if those who are designing the prices are profit-seeking, then contracts have to be setup so that profit-maximisation leads to optimal usage of energy flexibility as well. A method for ensuring this is presented in Section 5.4.1. Contrary, the price designers might not be profit-seeking, which reduces the complexity. In this case the price can be directly linked to grid problems, which is shown in Section 5.4.2. Finally, some proposals for how the two approaches could be merged are presented in Section 5.4.3.

5.4.1 Designed by BRPs

In Paper D it is shown how the consumption of three water towers can be manipulated to bid their energy flexibility into the Scandinavian spot market, by providing them with specific price signals. This is done by first estimating their response to price signals, i.e. the parameters of (5.2)-(5.5) and then use this to compute price signals yielding the desired consumption as shown on Figure 5.3. The figure shows how first an aggregator sends bids in the form of flexi orders (see Section 2.2.1) to the market, which then result in some amount of bought energy for each hour of the coming day. The flexibility function is then used to find a price signal that yields an expected demand equal to what was bought. In the end the real demand can be compared to what was expected and the flexibility function updated accordingly.

It was shown that, with the currently available flexi orders, the electricity bill for the water towers could be reduced by 4.1 %. The small deviations in prices on

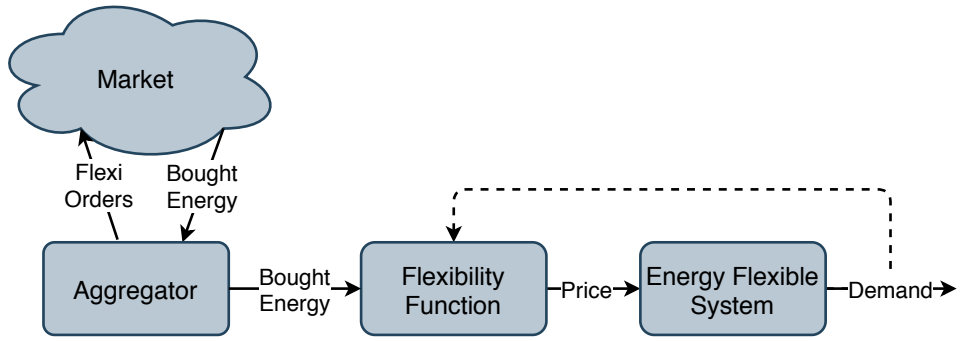

Figure 5.3: Information flow for using a flexibility function to design price signals according to energy bought on the market.

the spot market means that the current maximal potential savings are no more than 5.4%, and so the method obtained 76% of the potential.

In practice, the energy flexibility would have to be bid into the market by some aggregator, that can gather enough EFSs to satisfy the requirements of minimum capacity for entering the power markets. When considering how to design the correct incentives, the exact details about who the aggregator is are not important, what matters is that the actor is profit-seeking. Thus, it is simply assumed that BRPs are the ones utilising the energy flexibility. One of the key challenges related to having prices designed by BRPs, is to make it in their own interest to design prices that help the grid as much as possible. In particular, there needs to be contractual agreements preventing the BRP from giving too large prices. In [Zot+19b] an approach to solve this issue is proposed, where prices are forced to have time-averages equal to some constant value. However, this incentivises BRPs to make prices very high when there is little demand and high when there is a lot of demand, so that they on average receive high prices. One could even go a step further, and imagine that BRPs would bait consumers with seemingly high prices into emptying their storages, only to then increase the prices even more, when the consumers have no option but to buy at the high prices. Similarly, when storages are full BRPs could offer low prices without the possibility for consumers to take advantage of it.

Another proposal is outlined here, where the central concept is to force the average price paid across all EFSs under the control of the BRP, to remain at some constant value, $\bar{\lambda}$. This can be obtained by billing consumer n for the time interval t_1 to t_2 according to (5.6):

$$C^n(t_1, t_2) = \bar{\lambda} \int_{t_1}^{t_2} \lambda_t^n u_t^n \mathrm{d}t \sum_{i=1}^{N} \frac{\int_{t_1}^{t_2} u_t^i \mathrm{d}t}{\int_{t_1}^{t_2} \lambda_t^i u_t^i \mathrm{d}t}. \tag{5.6}$$

Here C^n is the electricity bill of consumer n for the interval from t_1 to t_2, $\bar{\lambda}$ is the average electricity price offered by the BRP. λ_t^n is proportional to the final price at time t for consumer n, but is modified to ensure that the overall average price paid by all consumers in the BRPs portfolio, during the time interval, equals $\bar{\lambda}$. This is easily verified by computing the total revenues and dividing by the total amount of consumed energy for the same period:

$$\sum_{k=1}^{N} \frac{C^k(t_1, t_2)}{\int_{t_1}^{t_2} u_t^k \mathrm{d}t} = \bar{\lambda}.$$

With the average price fixed, the BRP can not use energy flexibility to increase revenues, and thus the only use is to decrease expenses. Thus, the BRP can only use it to lower the average price at which energy is bought.

For the energy grid, low energy prices correspond to good times for using energy and vice versa, and so this will make the energy flexibility useful for the energy grid. The fact that the BRPs can utilise the energy flexibility to purchase energy cheaper also means that it can be offered cheaper to consumers, in turn making them a more competitive choice for consumers. In connection to being a competitive, alternative choice for consumers, the fixed average price is also very valuable, since it allows consumers to have an estimate of the price that they will pay. This is in contrast to regular dynamic pricing without any fixed prices, where even if the BRP is utilising energy flexibility according to grid needs, consumers can not know how expensive the solution will be for them, whereas they know the cost of fixed pricing. The main downside to this approach is that the price is not known in real time. Only λ^n is known, which, although proportional to the final price, can not be used to compare the energy price to other energy sources. Thus, this method is problematic to use for fuel-switching and energy integration in general. In practice it would be expected that the normalisation would be similar in all periods, in which case the energy price between sectors can be compared to some extend.

Notice how this approach relies on having the grid problems solved by the market. It is directly applicable to the current conditions, since the approach can easily be used to bid the energy flexibility into the regulation market as well. It is the responsibility of the BRP to estimate how much energy flexibility is available, and how to utilise it in the most profitable way. Failure to do so will hurt the BRP economically, which makes sure that they will try to prevent this. Failure also hurts the energy grid, and therefore the cost to the BRP has to match the potential cost of the grid, to ensure that they behave according to what is optimal for society.

5.4.2 Designed by Grid Operators

An alternative to bidding energy flexibility into the currently existing markets, is to have grid operators, i.e. TSOs and DSOs design price signals used to control energy flexibility. Contrary to BRPs, TSOs and DSOs are not profit-seeking and

thus they have no incentive to design prices with any other purpose than to solve grid problems. This simplifies the requirements for contractual agreements, since the grid operators can be trusted to not abuse the energy flexibility. But power grids constantly experience multiple problems, and grid operators would in this case have to decide which of the problems energy flexibility should be used to solve. This is not an obvious task, and as a result the literature only contains solutions with one or two problems considered at a time. In [SEJ15] price-based control was used to limit frequency deviations, which is probably the simplest problem to deal with since the frequency can be assumed constant throughout a power grid. Thus, it is also sufficient to have a single price that is constant for everyone. For voltage deviations, the problem is more difficult since the grid could easily experience over and under voltage at the same time, and thus individual prices are required. In Report R this is done for a small grid, which is simulated in high resolution, both spatially and temporally. Here the prices were computed based on local voltage levels, and updated very frequently, up to once a second. In [De +18], a dual objective was used, where both frequency and voltage deviation was considered simultaneously, with the power grid simplified a lot. Here, it was suggested to have a third party decide whether to give priority to TSOs or DSOs. However, this would obscure the exact requirements to gain priority, and the objectives and incentives of the third party would be unclear. This would only get worse as more than two problems are considered. Instead, clear rules for priority are needed, where there is no doubt how priority of the energy flexibility is given.

By analysing the nature of each of the problems, a strategy for what each EFS should focus on can be made. The most common problems experienced by power grids are summarised in Table 5.2. The simplified levels and severities of the problems can be used to decide what problems each EFS should focus on solving. Basically, each problem should be weighted according to the severity of it. Also, the trade-off between global and local problems should be made based on the amount of global and local problems.

Table 5.2: Typical problems experienced by power grids.

Problem	Level	Severity
Blackout	Global	Extremely high
Frequency deviation	Global	Medium
CO_2-emission	Global	Low
Congestion	Local	Medium
Voltage deviation	Local	Low

Equations (5.7)-(5.12) explain a simple approach to prioritise each of the four problems.

$$w_1 = L\left(k_1|\text{ROCOF}|\right) \quad \text{Blackouts} \quad (5.7)$$

$$w_G = (1-w_1)L(k_2|f-f_{\text{ref}}| + k_3\text{CO}_2 - k_4\left\|C\right\|_C - k_5\left\|V-V_{\text{ref}}\right\|_V) \quad \text{Global} \quad (5.8)$$

$$w_2 = w_G L\left(k_2|f-f_{\text{ref}}| - k_3\text{CO}_2\right) \quad \text{Frequency} \quad (5.9)$$

$$w_3 = w_G - w_2 \quad \text{CO}_2 \quad (5.10)$$

$$w_4 = (1-w_1-w_G)L(k_4\left\|C\right\|_C - k_5\left\|V-V_{\text{ref}}\right\|_V) \quad \text{Congestion} \quad (5.11)$$

$$w_5 = (1-w_1-w_G-w_4) \quad \text{Voltage} \quad (5.12)$$

In this formulation L is the logistic function defined by

$$L(x) = \frac{1}{1+\exp(x)},$$

which maps all inputs to the inerval $(0,1)$. w_1 is the weight put on preventing blackouts, w_2 the weight put on limiting frequency deviation, w_3 the weight on reducing CO_2 emissions, w_4 the weight on removing congestion and w_5 the weight put on reducing voltage deviation. $\left\|\cdot\right\|_C$ and $\left\|\cdot\right\|_V$ are norms describing the magnitude of all congestion and voltage deviation problems. Here, Rate of Change of Frequency (ROCOF) is used as the sole indicator for risk of blackout, but more indicators can be added without problems. $k_1, k_2, k_3, k_4, k_5 > 0$, and it is seen how the larger the value of k_1, the more weight is put on preventing blackouts and similarly for the others.

Since blackouts have much more severe consequences than any of the other problems, the initial weight put on preventing blackouts is made without consideration for the other problems in (5.7). It has to be expected that k_1 should be a large value reflecting the severe consequences of a blackout. Once w_1 has been found, the magnitude of the other global problems, frequency deviation and CO_2-emission, is compared to the local problems, congestion and voltage deviation, in (5.8), to find how much weight is put on the global problems, w_G. This weight is split between reducing frequency deviation and CO_2-emission in (5.9) and (5.10). Then, the congestion and voltage deviation problems are compared in (5.11) and weight is put on removing congestion accordingly. Finally, whatever weight is remaining, is put on reducing voltage deviation in (5.12).

The advantage of computing the weights used to prioritise each of the problems, is that now a separate price signal can be designed independently for each of the problems, and the weights can then be used to combine them. This is much simpler compared to designing price signals directly as functions of all problems. When considering only one of the problems at a time, it is obvious whether energy flexibility should be used to increase or decrease demand, and thus whether a low or high price should be sent. This could be done using a variation of the classical controllers presented in Section 4.1. Given the five price signals, $\lambda_1^n, \lambda_2^n, \lambda_3^n, \lambda_4^n, \lambda_5^n$, designed to solve each of the four problems for consumer n, the combined price signal is simply given by

$$\lambda^n = \sum_{k=1}^{5} w_k \lambda_k^n. \quad (5.13)$$

Notice that the difference in local problems is taken care of by having different price signals for each consumer, all designed to solve one particular problem at one particular location. In practice the problems require different spacial resolution. For example, prices originating from congestion on a transmission line would be constant for everyone receiving energy from this transmission line. Contrary, local voltage problems could result in different prices for streets next to each other, if one of them contained a lot of PV and the other did not. For global problems, the problems are the same within whole TSO-areas, which could reasonably be assumed to be the areas for which a single price-based controller methodology was implemented. Thus, the prices coming from the three global problems would be equal for all consumers: $\lambda_k^{n_1} = \lambda_k^{n_2}, \quad \text{for } k \in \{1, 2, 3\}, \forall n_1, n_2 \in \mathbb{N}$.

5.4.2.1 Tailoring of price signals

To further improve the utilisation of energy flexibility, a method for tailoring price signals to specific energy flexible systems was proposed in Paper C. The tailoring is done by enhancing frequencies that the energy systems can react the most to, while limiting those frequencies that they can not respond well to. For example, this makes slow reacting systems ignore fast dynamics in the price signal so that they can concentrate on the slow dynamics. Overall, this makes it so that the each system is assigned the problems that they are best suited to solve. In Paper C it was shown that the FIs for three particular examples could be increased from 8.3% to 13.9% for consumers and 8.3% to 9.3% for grid operators. Since the increase in value was present for both consumers and grid operators there is no conflict of interest, and consumers would be interested in signing up for contracts based on this approach voluntarily. If the flexibility tailoring is done for the price signal in (5.13), then the focus of each consumer depends on both their location and type of energy flexibility.

Notice that tailoring the price signals to specific kinds of energy flexibility is similar to what happens in a competitive market. For a particular problem with actors offering to solve it, the market will choose the cheapest one. Thus, problems will tend to be assigned to the actors who can solve it the most efficiently. This is what the tailoring of price signals is designed to do as well.

5.4.3 Combining grid and BRP prices

One aspect of having prices decided by grid operators which is not well understood, is how these prices are to be combined with those originating from BRPs. Regardless of whether BRPs use fixed or almost fixed prices, as is the case today, or if they utilise flexibility by varying price signals, the final price received by consumers is going to decide how they respond. Figure 5.4 shows how prices are computed by BRPs and grid operators and sent to the EFSs. The demand affects the state of the grid, and the grid state dictates the actions of the TSO and DSO. This could result in either direct price changes for the consumers or indirectly through the market where the

BRP picks up on the problems and can manipulate the price. The prices coming from the grid operators are computed based on (5.7)-(5.12), while the prices from the BRP are computed based on the flexibility function in (5.2)-(5.5), which in turn is estimated from the measured demand of the EFS. The direct link between grid operators and EFSs (in red) can be made in many ways, or simply omitted. This link will be discussed in the following.

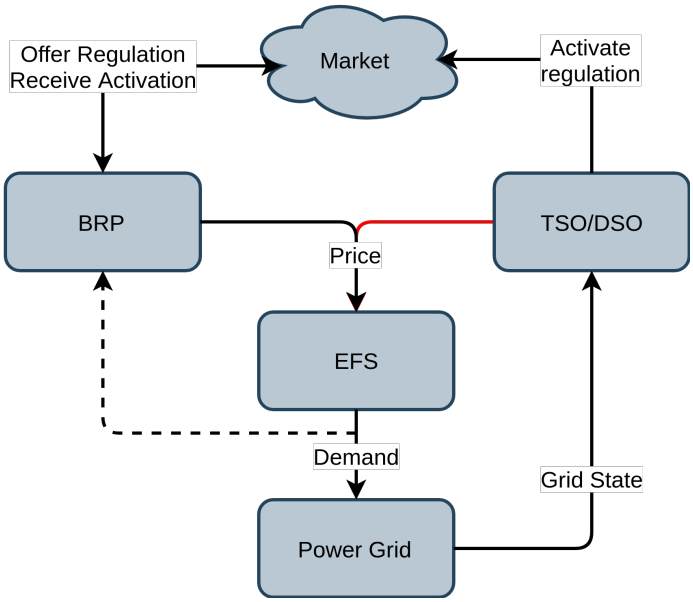

Figure 5.4: Overview of how prices are generated.

The simplest approach is to let BRPs have full control over the price sent to consumers, but let grid operators influence this indirectly by setting the regulation price, as is the case today. In this way (5.7)-(5.12) can be used to compute real time prices, but it is the job of the BRPs to relay them to consumers. It is in the interest of the BRPs to do so, since it decreases their expenses related to purchasing energy. This requires minimal change of the current infrastructure.

However, if the grid operators should have the possibility to directly change energy prices for consumers, then the setup requires careful consideration. In this case, for a particular consumer, assume that the corresponding BRP has found a price of λ^{BRP}, while the grid operators have found a price λ^{GO}. Then, the consumer is billed according to some function of these two prices

$$\lambda_t = f\left(\lambda_t^{\mathrm{BRP}}, \lambda_t^{\mathrm{GO}}\right).$$

The simplest solution is to have the final price equal the sum of the two prices. In

this case, consumers would have instantaneous energy prices of

$$\lambda_t = \lambda_t^{\mathrm{BRP}} + \lambda_t^{\mathrm{GO}},$$

meaning that if the consumption at time t is u_t, then the total cost for this consumer would be

$$\mathrm{Cost} = \underbrace{\int_0^t u_s \lambda_s^{\mathrm{BRP}} s \mathrm{d}s}_{\mathrm{BRP}} + \underbrace{\int_0^t u_s \lambda_s^{\mathrm{GO}} \mathrm{d}s}_{\mathrm{Tariffs}}.$$

A challenge for this approach is how large the grid operators should be allowed to set the prices. They would prefer to have as large prices as possible, since then they would practically dictate the demand, but this would take away power from the BRPs and vice versa. This approach would also make the effect of the prices from the grid operators vary with the size of the prices coming from the BRP, since the relative size is what matters. This could cause situations where either there are periods in which the grid operators lose control, or the grid operators have too much control most of the time.

For this reason, it might be preferable to have multiplicative prices instead, where the tariffs are a fraction of the prices, so that the instantaneous energy price would be

$$\lambda_t = \left(1 + \lambda_t^{\mathrm{GO}}\right) \lambda_t^{\mathrm{BRP}},$$

resulting in the total amount owed to BRPs remaining unchanged, but the tariffs changed such that the total costs would be

$$\mathrm{Cost} = \underbrace{\int_0^t u_s \lambda_s^{\mathrm{BRP}} \mathrm{d}s}_{\mathrm{BRP}} + \underbrace{\int_0^t u_s \lambda_s^{\mathrm{BRP}} \lambda_s^{\mathrm{GO}} \mathrm{d}s}_{\mathrm{Tariffs}}.$$

In this way the effect of λ^{GO} remains close to constant.

No matter how f is defined, it is important to consider how much weight is put on each of the two price sources. On one hand, the part of the price decided by the BRPs should be significant enough for them to utilise energy flexibility. On the other hand, the price from the grid operators should make a big enough part of the final price, to incentivise the behaviour needed for them to solve grid problems. It is also important to consider what happens to BRPs when their consumers receive prices from grid operators and consequently consume different amounts of energy than what the BRPs anticipated. One solution is to only allow grid operators to override prices in emergencies. However, this comes with a classic dilemma, where the ones deciding when there is an emergency are the same as those who benefit from declaring an emergency, namely the grid operators. This is not feasible, since there is no reason for grid operators to not overuse it as long as only BRPs suffer from it. An alternative is to have market products, where grid operators can pay BRPs for the possibility to take control of the prices for some fee. In this way the BRPs could set the price high enough for it to be profitable.

The price sent by operators reflects the regulation price, and thus the demand response followed from it will initially impact the BRPs positively, since their demand will be higher for low regulation prices and lower for high regulation prices. Thus, they will gain money on the balance market. However, this does not consider the dynamics of energy flexibility. It could be that the prices imposed by grid operators resulted in a delayed effect which was negative for the energy grid. In this case the cost associated with not foreseeing this should go to the grid operators that caused it.

In all cases the BRPs would have to anticipate the effect of the prices coming from grid operators. Even if the prices coming from grid operators would equal zero on average, the variability would be non-constant, and so the stochasticity associated with energy flexibility would be further non-constant as well. Fortunately, this can be incorporated in the model presented in (5.2)-(5.5), since it explicitly models stochasticity.

5.5 Top level - Integrating Energy Grids through Flexibility

The main motivation for utilising energy flexibility comes from the problems introduced by increasing shares of RESs in power grids. Thus, when utilising energy flexibility in district heating grids, it is only natural that the value of energy flexibility highly depends on how in can be used for assisting the power grid. In this section it is shown how energy flexibility can be used for energy system planning for integrated energy grids.

In Paper E a methodology for combining short-term energy flexibility with long-term energy system planning is presented. This was done for a district heating system, for which investments in and scheduling of heat generators were to be made. The combination of heat generators capable of delivering the required amount of heat in the cheapest possible way was found. For the study, the heat capacity of the water in the district heating system was used to provide energy flexibility by allowing the temperature to vary up to 3.5 C° from the nominal value. For newer district heating systems, there are substations between the district heating system and consumers. These are able to handle the variability caused by using the energy flexibility [GDD10], and thus comfort is not be affected with this approach. In the simulation, the energy flexibility was represented by a nonlinear flexibility function, very similar to the one described by (5.2)-(5.5). However, since there is no data for the energy flexibility on a scale appropriate for energy grid investments, the parameters of the model could not be estimated. Fortunately, the physical interpretation of the parameters allows good estimates based on general knowledge about the system. Thus, by consulting the operators of Zagreb district heating, the amount of water and flow rate was used to make a reasonable estimate of the parameters. To keep the computational complexity down, the price signal used in this paper was based directly on the marginal cost of

consuming energy. This resulted in demand being decreased in periods where demand was expensive to satisfy. Since this tends to be the hours with peak demand, most of the peaks were removed. Some of the heat production came from electric sources such as electric boilers and heat pumps, while CHPs, producing electricity in addition to heat, were also used. This meant that the costs of consuming heat were related to electricity prices, and so the use of energy flexibility was similarly linked to the electricity market. An example of the consequences of this is shown in Figure 5.5, where the heat production for two days in January is shown before and after applying energy flexibility. The figure shows how the cost of consuming heat (the shadow price) varies during the two days, and correspondingly how the heat demand was satisfied. During these days electricity prices were high and thus the electric boilers were the

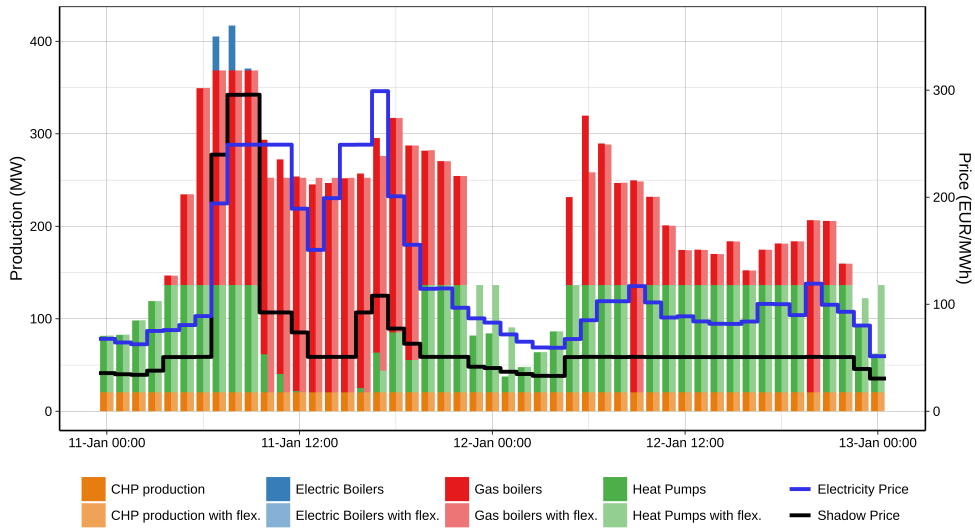

Figure 5.5: Heat production in northern district heating grid of Zagreb before and after applying energy flexibility.

most expensive generators. This caused the energy flexibility to be applied to reduce demand during hours in which the electric boilers were operated. Resulting in the electric boilers no longer being needed.

In general the cost of heat demand is proportional to the total heat demand, and thus the energy flexibility will mostly be used to flatten out demand. However, this is where sector coupling is important to consider, since the cost of heat can be low when electricity prices are high, even if the heat demand is also high. This will be be even more so as heat production is being further electrified. Thus, in some cases energy flexibility is used to reduce heat generation from electricity when electricity prices are high. In other cases, when CHPs are used as the marginal heat generators, heat

production is increased for high electricity prices, to take advantage of the possibility to sell more electricity. In Paper E it was shown that utilising energy flexibility for the heat generation increased revenues from electricity sales by 7.5%. This was mostly due to simply increasing the quantity of sold electricity by 6.5%, but the average price at which it was done was also increased, by 1.0%. In Figure 5.6 the change in electricity production of the northern district heating grid of Zagreb is shown. A clear linear relation is seen, where the amount of electricity sold increases with electricity price. The magnitude is large considering that the average amount of electricity sold per hour is 140 MWh/h, after energy flexibility had been applied. The relationship confirms that heat demand was actively adjusted in order to increase electricity sales when favourable.

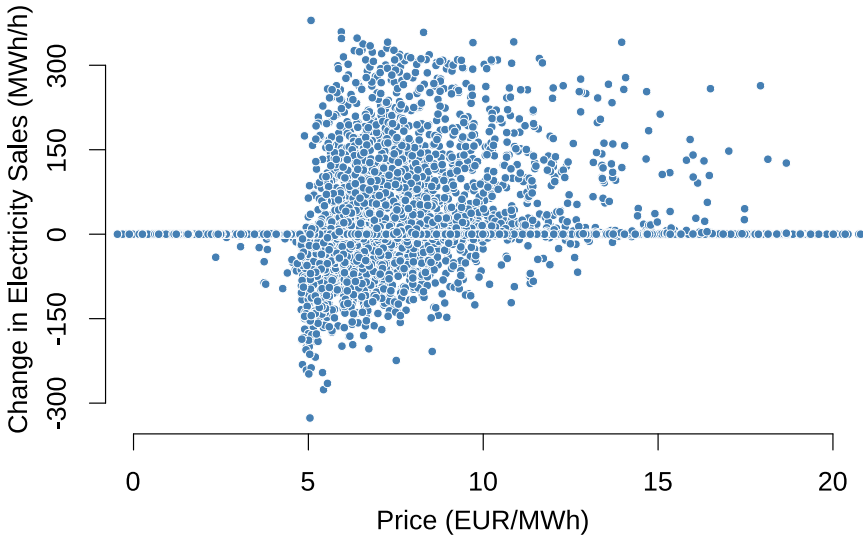

Figure 5.6: Change in electricity production of the northern district grid of Zagreb as a function of electricity price.

The increase in electricity sales induced reductions in the cost of delivering heat, but it also provided the power grid with electricity when it was needed the most. The total savings for the southern heating grid, including both investment and operational costs, was 15.5%, which is a lot for systems of this size.

Overall, district heating grids have a lot of energy flexibility, due to the inertia in the temperature of the water. This is contrary to power grids, that require almost

instantaneous consumption of the generated electricity. But since the power grids are in dire need of the energy flexibility, they benefit a lot from the energy flexibility of district heating grids. Thus there is a potential for district heating operators to save money, while at the same time supporting the power grid.

CHAPTER 6

Perspectives

The contributions presented in Chapter 5 comes with a number of limitations, assumptions and implications that should be considered. These are considered in this chapter along with perspectives for future work and required regulatory changes.

First, in Section 6.1 the method for characterising energy flexibility is evaluated. This is followed by a potential use-case for it, for whole district heating grids in Section 6.2. Next, the issue of relying on forecasted prices is discussed on Section 6.3. Finally, some problems related to how future markets should be designed to incentivise energy flexibility are discussed in Section 6.4.

6.1 Evaluation of Energy Flexibility Characterisation

The methods to characterise energy flexibility in Section 5.2 are a step forward from the static approaches previously relied upon. Especially the SDE-based formulation in (5.2)-(5.5) have shown great potential, but it still lacks further testing in more complicated settings, to evaluate how useful it really is. In particular, the notion of state of charge in the model fits very well with the water towers for which is was tested. For systems where it does not fit as well, the performance is expected to decrease. The main challenge related to further testing is to persuade owners of EFSs to have their equipment controlled in response to artificial prices, since there are no immediate economic rewards for this. Until end-consumers receive prices with sufficiently large variation to make the effort of being energy flexible worthwhile, the amount of real test cases will be small.

Another issue is to deal with the time-variation in how energy flexible systems can be. Conceptually, it is simple to let the parameters of the flexibility function vary over time or as a function of external variables, but it will have to be tested in practice, whether this can accurately represent the seasonality and variability of energy flexibility.

6.2 Large-scale Flexibility Function for District Heating Grid

It was seen in Section 5.5, that the largest potential for energy flexibility utilisation in district heating is to react to electricity prices. In particular, Figure 5.6 showed how the energy flexibility was actively used to increase electricity sales when prices were high. The energy flexibility could be characterised using this fact, by estimating a flexibility function, with the electricity price as input and electricity consumption/production of the district heating grid as output. However, this comes with some additional challenges, since heat can be from several generators with varying efficiencies and fuel sources. This means that the assumption from (5.2)-(5.5) that total demand remains constant is not even close to being valid, since the heat could be generated by e.g. bio fuel instead of electricity, and that demand can even be negative when CHPs generate electricity. Fortunately, this is mostly a function of the electricity price, so it can be incorporated in the modelling framework, simply by changing the term $(Y_t - B_t)\mathrm{d}t$ in (5.2) to $(h(Y_t, \lambda_t) - B_t)\mathrm{d}t$, where h is a function giving the expected amount of produced heat, when the electricity demand is Y_t and the electricity cost λ_t.

6.3 Control according to Forecasted Price Signals

Currently, research on price-based control of EFSs typically have control strategies that are either very simple rule-based control [Cla+17], or E-MPC, typically designed for price forecasts 24 hours as in Paper F, reports K,L, and [Hal+16; KJB17b], or at least several hours [Jin+17]. The rule-based control is only optimal in very specific scenarios, and thus should be avoided. The E-MPC is very close to optimality, but price forecasts of several hours can only be known accurately for day-ahead markets. The grid problems described in Section 5.4, are not known more than at most a few minutes ahead in time, and thus the price signals are also going to be very difficult to forecast more than a few minutes. Therefore, there is currently a lack of control methods that only depend on short-term forecasts of prices. Theoretically, the same approach can be used for short-term forecasts, but these forecasts depend on how prices are designed, which in turn depend on the expected response. Thus the design of price signals is interconnected with the forecasts of those same price-signals. The only way to deal with this is to do research where both aspects are considered simultaneously. Perhaps an iterative approach where both flexibility functions and forecasts of prices are estimated adaptively.

6.4 Decisions on Market Design

As described in Section 5.4, there are different approaches as to who will design price signals. Either it will have to be profit-seeking actors, possibly BRPs, which are commonly referred to as aggregators. Otherwise TSOs and DSOs will have to design combined price-signals themselves according to the problems that they face, or perhaps a combination is optimal. The fundamental difference between the two approaches is whether prices should be designed directly based on grid problems or an intermediate market should be used to evaluate the need for energy flexibility.

It is clear that computing prices directly from grid problems is faster than first bidding into a market and then clearing it. This might be important if energy flexibility is to be used to solve problems in real time such as frequency control, or even more importantly avoiding blackouts, where the time to respond is on the order of a few seconds [ent04]. Control based methods are also more robust in the sense that they circumvent possibilities for speculation.

Economic markets are, in general, better at finding economically optimal solutions, and there is no reason to believe that this does not apply to energy flexibility as well. For this reason a market-based solution in which aggregators bid energy flexibility into markets, in order to earn money is preferable whenever possible, since it is expected that economically optimal solutions are found in this way.

Thus, we are faced with a trade-off between timing and robustness versus economic optimality. It is clear, that, if the risk of a blackout is eminent, then it is insignificant whether the solution to prevent it is slightly more costly than the optimal solution. And so, a control-based solution is preferred in this case. Contrary, on the day-ahead market, with enough time to find optimal solutions and the ability to adjust schedules, the optimality that comes with the market based solution is preferred. The question is when to go from bidding and clearing of the markets to control. Possible factors include time until operation, geographical scale and consequences of failure.

No matter how the trade-off is made, the Danish market is ready for price-based control made by BRPs. However, the current regulatory framework disincentivises the use of energy flexibility with large and constant taxes on electricity that hides the varying costs of producing and delivering it. In 2018 the average spot-price of electricity was 44 EUR/MWh, while the taxes were 118 EUR/MWh [SKA]. The tariffs are added on top of this, but currently they do not reflect the time-varying costs of producing and delivering electricity. The market can not be expected to find the optimal investments in energy flexibility as long as the potential profits do not reflect the true value. Therefore, either taxes have to be reduced, to limit their market distortion, be multiplicative, to prevent them from affecting the relative differences in costs, or reflect the time-varying problems as described in Section 5.4.

In order to use the control based solution described in Section 5.4.2, the exact cost associated to each of the five mentioned problems has to be estimated, from which k_1, k_2, k_3, k_4 and k_5 can be deduced. Similarly, functions linking the state of the grid to the magnitude of the local problems can be constructed, i.e. the norms $\|\cdot\|_V$ and

$\|\cdot\|_C$.

Conceptually, this is all which is needed to implement the solution in practice, but in reality it would have to be tested and tuned in simulation studies first. The problem concerning this is that it is extremely complicated to simulate nationwide energy grids in their full complexity, in a time resolution high enough to accurately represent the relevant problems. For most power grid simulation tools, the spacial scale is severely limited [CSG08]. To overcome this, the time resolution can instead be reduced or only the frequency simulated [Kri+17; Wor]. However, to test multi-objective implementations of energy flexibility, the time resolution has to be at least as high as the time resolution that the problems take place in. At the same time the spatial scale has to be large enough for it to make sense to affect frequency. On top of this the simulation needs enough details to include voltage and congestion. While this is hard enough already, the energy flexibility would also need to be simulated simultaneously, to understand its effect on all parts of the simulation. In conclusion it is not computationally feasible to simulate the implementation of the solution. Instead, the effort should be to focus on particular aspects one at a time until they are understood well enough, to be confidently represented by simplified models that can be simulated with low computational burden, as was done in Paper E.

For example, the global problems can be simulated first, assuming random magnitudes of local problems, that take away weights from the global problems. Once this is done, the results can be taken as inputs to simulations focusing only on the local problems. Iterating between the global and local problems can in the end give a good estimate of the overall capabilities in a computationally feasible way.

CHAPTER 7

Conclusion

Throughout the PhD study, the nature of energy flexibility was explored, and the field was advanced, with better tools for modelling, characterising and utilising it.

It has been demonstrated that energy flexibility is present in many systems, by controlling their demand according to price-signals. This way, the energy flexibility can be used to generate profit for owners of energy flexible systems, while at the same time solving problems faced by the energy grids of today and tomorrow.

The first methods for being able to estimate and characterise the dynamics of energy flexibility from data were developed. By representing all aspects of energy flexibility in one dynamic model, the relation between previously disconnected features was revealed. Furthermore, this modelling framework have proven to represent energy flexibility accurately enough to be able to utilise it for practical purposes.

Various methods have been suggested for integrating and utilising energy flexibility for solving problems faced by energy grids and reduce operational costs. To make them realistic for practical implemention, the economic incentives of various approaches have been analysed, to come up with solutions that would incentivise desirable behaviour. It has been shown how the methods of this study can fit into these approaches.

Overall, this thesis contains the methodologies required to understand and implement energy flexibility, within energy grids operated based on economic incentives. The results provide hope for the feasibility of continued integration of more renewable energy sources, but also highlights challenges that has yet to be overcome, to unlock the potential of energy flexibility.

Bibliography

[AJ16] Armin Ghasem Azar and Rune Hylsberg Jacobsen. "Appliance scheduling optimization for demand response". In: *International Journal on Advances in Intelligent Systems* 9.1&2 (2016), pages 50–64.

[AMS13] MJE Alam, KM Muttaqi, and Darmawan Sutanto. "Mitigation of rooftop solar PV impacts and evening peak support by managing available capacity of distributed energy storage systems". In: *IEEE transactions on power systems* 28.4 (2013), pages 3874–3884.

[Cla+17] John Clauß et al. "Investigations of Different Control Strategies for Heat Pump Systems in a Residential nZEB in the Nordic Climate". In: *12th IEA Heat Pump Conference*. 2017.

[Cor+13] O. Corradi et al. "Controlling Electricity Consumption by Forecasting its Response to Varying Prices". In: *IEEE Transactions on Power Systems* 28.1 (2013), pages 421–429. ISSN: 0885-8950. DOI: 10.1109/TPWRS.2012.2197027.

[CRS08] Tarun Chordia, Richard Roll, and Avanidhar Subrahmanyam. "Liquidity and market efficiency". In: *Journal of Financial Economics* 87.2 (2008), pages 249–268.

[CSG08] D. P. Chassin, K. Schneider, and C. Gerkensmeyer. "GridLAB-D: An open-source power systems modeling and simulation environment". In: *2008 IEEE/PES Transmission and Distribution Conference and Exposition*. 2008, pages 1–5. DOI: 10.1109/TDC.2008.4517260.

[De +18] Giulia De Zotti et al. "Ancillary services 4.0: A top-to-bottom control-based approach for solving ancillary services problems in smart grids". In: *Ieee Access* 6 (2018), pages 11694–11706.

[DH11] Paul Denholm and Maureen Hand. "Grid flexibility and storage required to achieve very high penetration of variable renewable electricity". In: *Energy Policy* 39.3 (2011), pages 1817–1830.

[DH13] Roel De Coninck and L. Helsen. "Bottom-up quantification of the flexibility potential of buildings". In: 2013.

[Dhu+15] Reinhilde D'hulst et al. "Demand response flexibility and flexibility potential of residential smart appliances: Experiences from large pilot test in Belgium". In: *Applied Energy* 155 (2015), pages 79–90.

[Día+14] Francisco Díaz-González et al. "Participation of wind power plants in system frequency control: Review of grid code requirements and control methods". In: *Renewable and Sustainable Energy Reviews* 34 (2014), pages 551–564.

[DL93] Ronald A DeVore and George G Lorentz. *Constructive approximation*. Volume 303. Springer Science & Business Media, 1993.

[Dot02] Erik Dotzauer. "Simple model for prediction of loads in district-heating systems". In: *Applied Energy* 73.3-4 (2002), pages 277–284.

[Ene] Energinet. *Market Data*. `http://osp.energinet.dk/_layouts/Markedsdata/framework/integrations/markedsdatatemplate.aspx`. [Online; accessed 8-November-2019].

[ent04] entso-e. *Appendix 1: Load-Frequency Control and Performance*. Technical report. 2004.

[EP07] Lene Egeberg-Gjelstrup and Mogens R. Pedersen. *Regulation A: Principles for the electricity market*. Technical report. 2007.

[Fle09] FlexPower. *FlexPower Project*. `http://www.ea-energianalyse.dk/projects-english/1027_flexpower_market_design.html`. Accessed: 2017-12-20. 2009.

[Flo+17] Anthony R Florita et al. *Grid Frequency Extreme Event Analysis and Modeling*. Technical report. National Renewable Energy Lab.(NREL), Golden, CO (United States), 2017.

[Fri89] David D Friedman. *The machinery of freedom: guide to a radical capitalism*. Open Court Publishing Company, 1989.

[Fur35] Edgar S Furniss. "The Triumph of Soviet Planning". In: *Current History and Forum*. Volume 43. 3. CH publishing corporation, etc. 1935, page 324.

[GDD10] Jonas Gustafsson, Jerker Delsing, and Jan van Deventer. "Improved district heating substation efficiency with a new control strategy". In: *Applied Energy* 87.6 (2010), pages 1996–2004.

[GG11] Hamid Gharavi and Reza Ghafurian. "Smart grid: The electric energy system of the future". In: *Scanning the Issue* 99 (2011).

[H+11] Nidhi Hegde, Laurent Massoulié, Theodoros Salonidis, et al. "Optimal control of residential energy storage under price fluctuations". In: *Energy*. 2011.

[Hal+12] Rasmus Halvgaard et al. "Economic Model Predictive Control for Building Climate Control in a Smart Grid". In: *Innovative Smart Grid Technologies (ISGT)* 30 (2012), pages 270–278. DOI: `https://doi.org/10.1016/j.egypro.2012.11.032`.

[Hal+16] Rasmus Halvgaard et al. “Distributed model predictive control for smart energy systems”. In: *IEEE Transactions on Smart Grid* 7.3 (2016), pages 1675–1682.

[Han+16] Anca Daniela Hansen et al. “Frequency control modelling-basics”. In: (2016).

[HGB00] MN Howell, TJ Gordon, and MC Best. “The application of continuous action reinforcement learning automata to adaptive PID tuning”. In: (2000).

[HM17] Bianca Howard and V Modi. “Examination of the optimal operation of building scale combined heat and power systems under disparate climate and GHG emissions rates”. In: *Applied energy* 185 (2017), pages 280–293.

[ISM17] J. P. Iria, F. J. Soares, and M. A. Matos. “Trading small prosumers flexibility in the day-ahead energy market”. eng. In: *2017 Ieee Power and Energy Society General Meeting* (2017), 5 pp., 5 pp. DOI: 10.1109/PESGM.2017.8274488.

[Jak] Thomas Berg Jakobsen. *Sikker Forsyning bliver delt Forsyning. Årsrapport 2018*. https://energinet.dk/Om-publikationer/Publikationer/Aarsrapport-2018. [Online; accessed 8-November-2019].

[Jen16] Helle Birte Jensen. *Regulation C1: Terms of balance responsibility*. Technical report. 2016.

[Jin+17] Xin Jin et al. “Foresee: A user-centric home energy management system for energy efficiency and demand response”. In: *Applied Energy* 205 (2017), pages 1583–1595. ISSN: 0306-2619. DOI: https://doi.org/10.1016/j.apenergy.2017.08.166.

[JT10] Tongdan Jin and Zhigang Tian. “Uncertainty analysis for wind energy production with dynamic power curves”. In: *2010 IEEE 11th International Conference on Probabilistic Methods Applied to Power Systems*. IEEE. 2010, pages 745–750.

[KJB17a] Carsten Skovmose Kallesøe, Tom Nørgaard Jensen, and Jan Dimon Bendtsen. “Plug-and-Play Model Predictive Control for Water Supply Networks with Storage”. In: *IFAC 2017 World Congress, Toulouse, France* 50 (2017), pages 6582–6587.

[KJB17b] Carsten Skovmose Kallesøe, Tom Nørgaard Jensen, and Jan Dimon Bendtsen. “Plug-and-Play Model Predictive Control for Water Supply Networks with Storage”. In: *IFAC-PapersOnLine* 50.1 (2017). 20th IFAC World Congress, pages 6582–6587. ISSN: 2405-8963. DOI: https://doi.org/10.1016/j.ifacol.2017.08.616.

[Kra03] Mark Kramer. “The collapse of East European communism and the repercussions within the Soviet Union (Part 1)”. In: *Journal of Cold War Studies* 5.4 (2003), pages 178–256.

[Kri+17] Venkat K Krishnan et al. “Smart-DS: Synthetic Models for Advanced, Realistic Testing: Distribution Systems and Scenarios”. In: (2017).

[KW16] Koen Kok and Steve Widergren. “A society of devices: Integrating intelligent distributed resources with transactive energy”. In: *IEEE Power and Energy Magazine* 14.3 (2016), pages 34–45.

[LH16] Jérôme Le Dréau and Per Heiselberg. “Energy flexibility of residential buildings using short term heat storage in the thermal mass”. In: *Energy* 111 (2016), pages 991–1002.

[Liu+17] Tian Liu et al. “Market for Multi-Dimensional Flexibility with Parametric Demand Response Bidding”. eng. In: *North American Power Symposium* (2017). ISSN: 21634939.

[LM06] Henrik Lund and Ebbe Münster. “Integrated energy systems and local energy markets”. In: *Energy Policy* 34.10 (2006), pages 1152–1160.

[Lop+16] Rui Amaral Lopes et al. “A literature review of methodologies used to assess the energy flexibility of buildings”. In: *Energy Procedia* 91 (2016), pages 1053–1058.

[Mad07] Henrik Madsen. *Time series analysis*. CRC Press, 2007.

[Man00] Sa’ad Mansoor. “Behaviour and operation of pumped storage hydro plants”. PhD thesis. University of Wales, Bangor, 2000.

[Mor+14] JM Morales et al. *Integrating Renewables in Electricity Markets*. Springer, 2014.

[Mur83] Katta G Murty. *Linear programming*. Springer, 1983.

[New87] Isaac Newton. *The Principia: mathematical principles of natural philosophy*. 1687.

[Nis07] Norman S Nise. *Control system Engineering*. John Wiley & Sons, 2007.

[Nor15] NordREG. *Tariffs in Nordic countries – survey of load tariffs in DSO grids*. 2015.

[NPT14] Bijay Neupane, Torben Bach Pedersen, and Bo Thiesson. “Towards flexibility detection in device-level energy consumption”. In: *International Workshop on Data Analytics for Renewable Energy Integration*. Springer. 2014, pages 1–16.

[OCo+14] Niamh O’Connell et al. “Regulating power from supermarket refrigeration”. In: *IEEE PES Innovative Smart Grid Technologies, Europe*. IEEE. 2014, pages 1–6.

[Øks03] Bernt Øksendal. “Stochastic differential equations”. In: *Stochastic differential equations*. Springer, 2003, pages 65–84.

[OMa+16] Mark O’Malley et al. “Energy Systems Integration: Defining and Describing the Value Proposition”. In: *Contract* 303 (2016), pages 275–300.

[OR16] Sarah O'Connell and Stefano Riverso. "Flexibility analysis for smart grid demand side services incorporating 2'nd life EV batteries". In: *2016 IEEE PES Innovative Smart Grid Technologies Conference Europe (ISGT-Europe)*. IEEE. 2016, pages 1–6.

[Pal+19] Carsten Palkowski et al. "Fixing efficiency values by unfixing compressor speed: Dynamic test method for heat pumps". In: *Energies* 12.6 (2019), page 1045.

[Par17] Henning Parbo. *Regulation C2: The balancing market and balance settlement*. Technical report. 2017.

[Pla50] R. L. Plackett. "Some Theorems in Least Squares". In: *Biometrika* 37.1-2 (1950), pages 149–157. ISSN: 0006-3444. DOI: 10.1093/biomet/37.1-2.149.

[Por+09] Fernando Porrua et al. "Incorporating large-scale renewable to the transmission grid: Technical and regulatory issues". In: (2009), pages 1–7.

[PRV04] Jan Peirs, Dominiek Reynaerts, and Filip Verplaetsen. "A microturbine for electric power generation". In: *Sensors and Actuators A: Physical* 113.1 (2004), pages 86–93.

[RAB12] James B Rawlings, David Angeli, and Cuyler N Bates. "Fundamentals of economic model predictive control". In: *2012 IEEE 51st IEEE conference on decision and control (CDC)*. IEEE. 2012, pages 3851–3861.

[RDS17] Glenn Reynders, Jan Diriken, and Dirk Saelens. "Generic characterization method for energy flexibility: Applied to structural thermal storage in residential buildings". In: *Applied energy* 198 (2017), pages 192–202.

[Rey+18] Glenn Reynders et al. "Energy flexible buildings: An evaluation of definitions and quantification methodologies applied to thermal storage". In: *Energy and Buildings* 166 (2018), pages 372–390.

[RLJ11] Danping Ren, Hui Li, and Yuefeng Ji. "Home energy management system for the residential load control based on the price prediction". In: *2011 IEEE Online Conference on Green Communications*. IEEE. 2011, pages 1–6.

[Sch+80] Fred C Schweppe et al. "Homeostatic utility control". In: *IEEE Transactions on Power Apparatus and Systems* 99 (1980), pages 1151–1163.

[SEJ15] Leo Emil Sokoler, Kristian Edlund, and John Bagterp Jørgensen. "Application of economic MPC to frequency control in a single-area power system". In: *2015 54th IEEE Conference on Decision and Control (CDC)*. IEEE. 2015, pages 2635–2642.

[SKA] SKAT.dk. *E.A.4.3.6.1 Afgiftssatser og beregning*. https://skat.dk/skat.aspx?oid=2061620.

[SNV12] Igor Sartori, Assunta Napolitano, and Karsten Voss. "Net zero energy buildings: A consistent definition framework". In: *Energy and buildings* 48 (2012), pages 220–232.

[Thy16] Uffe Thygesen. *Lecture notes on Diffusion and Stochastic Differential Equations*. 2016.

[Tra+19] Bo Tranberg et al. "Real-time carbon accounting method for the European electricity markets". In: *Energy Strategy Reviews* 26 (2019), page 100367.

[VML14] Cynthujah Vivekananthan, Yateendra Mishra, and Fangxing Li. "Real-time price based home energy management scheduler". In: *IEEE Transactions on Power Systems* 30.4 (2014), pages 2149–2159.

[WFK18] Tobias Weiß, Anna Maria Fulterer, and Armin Knotzer. "Energy flexibility of domestic thermal loads – a building typology approach of the residential building stock in Austria". In: *Advances in Building Energy Research* 13.1 (2018), pages 122–137. DOI: 10.1080/17512549.2017.1420606.

[Wid+14] S Widergren et al. "Residential transactive control demonstration". In: *ISGT 2014*. IEEE. 2014, pages 1–5.

[Wie+19] Frauke Wiese et al. "Open Power System Data – Frictionless data for electricity system modelling". In: *Applied Energy* 236 (2019), pages 401–409. ISSN: 0306-2619. DOI: 10.1016/j.apenergy.2018.11.097. URL: http://dx.doi.org/10.1016/j.apenergy.2018.11.097.

[Wor] Power World. *PowerWorld Simulator*. https://www.powerworld.com/products/simulator/overview/. [Online; accessed 1-November-2019].

[WW10] Joakim Widén and Ewa Wäckelgård. "A high-resolution stochastic model of domestic activity patterns and electricity demand". In: *Applied energy* 87.6 (2010), pages 1880–1892.

[YCC03] Albert WL Yao, SC Chi, and JH Chen. "An improved grey-based approach for electricity demand forecasting". In: *Electric Power Systems Research* 67.3 (2003), pages 217–224.

[Zot+19a] Giulia De Zotti et al. "A Control-based Method to Meet TSO and DSO Ancillary Services Needs by Flexible End-Users". English. In: *I E E E Transactions on Power Systems* (2019). ISSN: 0885-8950.

[Zot+19b] Giulia De Zotti et al. "Analysis of rebound effect modelling for flexible electrical consumers". In: *IFAC-PapersOnLine* 52.4 (2019). IFAC Workshop on Control of Smart Grid and Renewable Energy Systems CSGRES 2019, pages 6–11. ISSN: 2405-8963. DOI: https://doi.org/10.1016/j.ifacol.2019.08.146.

Part II

Publications

PAPER A

Physical-Stochastic Continuous-Time Identification of a Forced Duffing Oscillator

Authors: Rune Grønborg Junker, Rishi Relan and Henrik Madsen.
Submitted to:
ISA Transactions.

Physical-Stochastic Continuous-Time Identification of a Forced Duffing Oscillator

Rune Grønborg Junker[a], Rishi Relan[a,b], Henrik Madsen[a]

[a]*Technical University of Denmark, Kongens Lyngby, 2800, Denmark (e-mail: rung@dtu.dk, risre@dtu.dk, hmad@dtu.dk).*
[b]*Siemens Limited, Generator R&D, Gurgaon 122015, India (e-mail: rishi.relan@siemens.com).*

Abstract

The richness of the available model structures and estimation approaches makes nonlinear system identification a significant challenge. The dynamics of many physical nonlinear systems can be described using the widely studied Duffing equations. Although the Duffing equations can not accurately describe the dynamics of all physical systems for a wide range of frequency bands and amplitude of excitation, it is still possible to use the Duffing equations to describe their behaviour qualitatively for many real-world engineering systems. Therefore, the main objective of this paper is to study if the prior (or the lack of) knowledge of the system structure approximated by the Duffing oscillator can be utilised in combination with the measured input-output data in efficiently identifying a model of the Duffing oscillator. Stochastic differential equations (SDEs) allow us to combine the physics of the considered system with the data-driven statistical estimation framework to develop a grey-box model of the system. Hence, in this paper, we utilise the SDEs based modelling framework for estimating a continuous-time physical-stochastic (grey-box) simulation model for the Duffing oscillator. The model structure and its performance is then improved based on an iterative residual analysis. The benchmark data from the so-called Brussels "SilverBox system", which is an electrical circuit mimicking the forced Duffing oscillator dynamics is used for the identification purpose. Finally, the identified model performance (the simulation errors) is compared with the existing results available in the literature.

Keywords: Stochastic differential equations, Physical-stochastic models, Grey-box models, Duffing oscillator, Benchmark identification, Residual analysis

1. Introduction

Mathematical models are ubiquitous in every branch of science and engineering. In engineering practice, mathematical models of dynamic systems are used to analyse, simulate and predict the behaviour of systems to various input excitation during the design phase or to design and implement controllers. There are three main modelling philosophies which are prevalent in engineering sciences namely the white-box modelling (Isermann and Münchhof, 2010; Ljung and Glad, 1994); the data-driven statistical black-box modelling (system identification, machine learning) (Ljung, 1999; Pintelon and Schoukens, 2012) and the grey-box modelling (Kristensen et al., 2004a,b; Møller et al., 2018). White-box models (both micro and macro scales) are derived from system's underlying physics whereas the data-driven statistical black-box models assume no prior knowledge of the underlying physics of the system and can be estimated accurately based on input-output measurements. Grey-box models start with the underlying physical (generally partial but robust) prior knowledge of the system, and use data-driven statistical modelling and estimation techniques to fine-tune the model. This approach provides a good trade-off between robustness and accuracy.

A quasi linear or weakly nonlinear behaviour is exhibited by many real world systems during their normal operation (e.g. at low amplitude of the input excitation signal), and a strong nonlinear effect may be exhibited by the same system (e.g. at larger amplitude of the input excitation signal). A typical example of such systems is the *forced Duffing oscillator*, which arises in a vast number of real-world applications in various fields of engineering and physics. Specific applications of the Duffing equations are seen in secure communication (Liu et al., 2015), feature extraction from weak mechanical fault signals (Han et al., 2016), weak-signal detection (Lai and Leng, 2016) and for the design of nonlinear vibration absorbers (Das and Santhosh, 2016; Rice and McCraith, 1987).

Several results have been reported in the literature where the authors approached the modelling of the forced Duffing system as a pure parameter-estimation problem. These approaches implicitly assume that the physical structure of the real system under consideration is governed exactly by Duffing equations. This kind of parameter-based modelling approach is known as white-box modelling. For example, a nonlinear subspace identification method combined with different excitation inputs was used to identify the Duffing equation by (Gandino et al., 2013). (Tang et al., 2016) identified the parameters of an experimental beam shaker described as the Duffing-type system by measuring the jump-down frequencies. A comprehensive review of parameter identification of Duffing oscillators especially in the field of structural dynamics can be found in (Kerschen et al., 2009; Noël and Kerschen, 2017).

On the other end of the spectrum several black-box identification approaches have also been applied to model the Duffing oscillator system. One of the earliest instances of identifying a nonparametric model of the Duffing oscillator using artificial

neural networks is reported in (Masri and Caughey, 1979). The same authors revisited the problem for the identification of a parametric model based on a set of basis functions in (Masri et al., 2004). The authors in (Goharoodi et al., 2018) applied a recently developed method of sparse identification of nonlinear dynamics (Brunton et al., 2016) in combination with the alternating direction method of multipliers (ADMM) optimisation approach to identify the model of a forced duffing oscillator.

Both white-box and black-box identification methodologies have their own advantages and disadvantages in modelling the Duffing system. For example, white-box models, though continuous in nature have the disadvantage that the true structure of the dynamic system under consideration may not always be fully describable by the considered deterministic physical equations. Whereas, the black-box models are generally discrete-time in nature, which makes it problematic to describe data with irregular sampling times, while also making the parameters difficult to interpret in terms of physics that tend to need continuous time parameters. This is a major drawback for real-world applications involving physical analysis, irregular sampling times or control of physical quantities not explicitly modelled by the black box models. Grey-box models uses the data-driven approach of black-box models, but are based on physical considerations, thus preserving the intuitive interpretation of white-box models while also providing the accuracy of black-box models. Therefore, this paper shows how to combine white-box and black-box methodologies to estimate the stochastic grey-box continuous-time models for the Duffing oscillator.

The paper is structured as follows: Section 2 very briefly describes the forced Duffing oscillator. The concept of continuous-time state-space models is presented in Section 3, with a particular focus on stochastic differential equations and an alternative to the usual 1-step ahead-based maximum likelihood estimate. An introduction to the Brussels SilverBox benchmark system and experimental data is given in Section 4.1 followed by a walk-through of the modelling of this system in Section 4.2. In Section 5, the results of the identification methodology are discussed and compared with the results reported in the literature, and finally the conclusions are given in Section 6.

2. The Forced Duffing Oscillator

The Duffing equation in its various forms has been reported in the literature for the analysis of many nonlinear systems. Although for the description of most real-world physical systems the Duffing equation is not sufficiently accurate especially over a wide range of operating conditions, such as frequency and amplitude of excitation, but in many cases it is still possible to use the Duffing equation to qualitatively study their behaviour. In some very specific situations e.g. for small amplitudes of the input excitation signals, even a quantitative analysis can be performed.

In fact, in many cases, the Duffing equation is the fundamental first step while extending the analysis from a linear to a nonlinear system. For example, the jump phenomenon, limit cycles, bifurcations and other nonlinear behaviour can be illustrated easily by analysing the simple Duffing oscillator (Nayfeh and Mook; Stoker, 1966). A good understanding of the low-order structure of the Duffing oscillator system model has helped in the development of reduced-order models of complex nonlinear mechanical systems ranging from microscales to macroscales (Lifshitz and Cross, 2008). The basic Duffing oscillator with viscous damping and external forcing can be described using the differential equation as shown below (Kovacic and Brennan, 2011):

$$\ddot{x}_t = \dot{x}_t + a_1\dot{x}_t + k_1 x_t + k_3 x_t^3 = u(t), \tag{1}$$

where $x_t, t, a_1, u(t), k_1$ and k_3 are the displacement, time, damping ratio, excitation signal, linear and cubic stiffness parameter, respectively.

3. Continuous-Time State-Space Models

Most models implicitly assume that the only form of uncertainty is through measurement errors. However, in practice it is often seen that uncertainties in inputs and model deficiencies are significant as well. To accommodate this kind of stochasticity, state-space models offer a way to split noise into measurement noise and process noise. This is done by having one or more state equations that govern the evolution of the states with stochasticity included, and a measurement equation explicitly including the measurement noise as well. In continuous time the state equations are most naturally governed by Stochastic Differential Equations (SDEs), which will be explained in 3.1, while the observation equation is briefly described in 3.2.

3.1. Stochastic Differential Equations

SDEs are the natural stochastic extension of Ordinary Differential Equations (ODEs). In general any SDE can be formulated in integral form as

$$X_t - X_{t_0} = \int_0^t f(X_s, U_s, s; \theta)\mathrm{d}s + \int_0^t \sigma(X_s, U_s, s; \theta)\mathrm{d}W_s, \tag{2}$$

which is usually expressed by the shorthand notation as:

$$\mathrm{d}X_t = \underbrace{f(X_t, U_t, t; \theta)\mathrm{d}t}_{\text{Drift}} + \underbrace{\sigma(X_t, U_t, t; \theta)\mathrm{d}W_t}_{\text{Diffusion}}, \quad t_0 \le t \le T. \tag{3}$$

The stochastic state variables of the system are given by $X_t \in \mathcal{X} \subset \mathbb{R}^n$, X_{t_0} represents the stochastic initial condition satisfying $\mathbb{E}\left[\, \left\|(X_{t_0})\right\|^2 \,\right] < \infty$, and the vector of the deterministic inputs known $\forall t$ is given by $U_t \in \mathbb{R}^d$. The vector $\theta \in \Theta \subset \mathbb{R}^p$ contains the system's parameters. The existence of a strong solution is guaranteed by assuming sufficient regularity conditions for the drift $f : \mathbb{R}^n \times \mathbb{R}^d \times [t_0, T] \longmapsto \mathbb{R}^n$ and the diffusion terms $\sigma : \mathbb{R}^n \times \mathbb{R}^d \times [t_0, T] \longmapsto \mathbb{R}^{n\times m}$ in (3). The standard Wiener process $W_t = (W_t^1, W_t^2, \cdots, W_t^m)^T \in \mathbb{R}^m$ represents the process noise. For a detailed introduction to the SDEs and its applications, the readers are referred to (Øksendal, 2010; Thygesen, 2016).

The evolution of the states of a dynamical system w.r.t. time is separated into two distinct terms namely the drift f and the

diffusion σ respectively as shown in (3). Both the drift and the diffusion terms can be modelled either by parametric or non-parametric, linear or nonlinear functions. This distinct separation results in an accurate description of the system dynamics as it allows to explicit separation of the modelling error into the error due to the unmodelled dynamics (i.e. model approximations and noise originating from unknown disturbances to the system) using the diffusion term and the uncorrelated error due to noisy measurements (Øksendal, 2010). Notice that even though the inputs are assumed to be known and deterministic, the diffusion term can implicitly account for uncertainties in the inputs, if the input distribution is sufficiently close to the Gaussian distribution.

As mentioned before, the solution to (3) is a stochastic process and the transition probabilities of the stochastic process are given by the Fokker-Plank equation (Klebaner, 2005). In the context of this paper, the following assumptions have been made to formulate the problem:

Assumption 1. *The diffusion term in* (3) *is independent of the stochastic state variables i.e.*

$$dX_t = \underbrace{f(X_{t_k}, U_{t_k}, t_k; \theta)dt}_{\textit{Drift}} + \underbrace{\sigma(U_{t_k}, t_k, \theta)dW_t}_{\textit{Diffusion}}; \quad t_0 \leq t \leq T, \tag{4}$$

Remark 3.1. *Under this assumption the parameter estimation becomes more feasible. For example, to make the filter approximations sufficiently accurate, the Extended Kalman Filter (EKF) based estimation algorithms for SDEs require transformations that can transform the state dependent diffusion term into a state independent diffusion term or can move the state dependence to the drift term (Baadsgaard et al., 1997). To allow the application of the EKF based estimation framework for a restricted class of nonlinear dynamic systems with state dependent diffusion terms or level effects, a Lamperti transformation may be applied as shown by (Møller and Madsen, 2010; Nielsen and Madsen, 2001).*

Remark 3.2. *The SDEs formulated in* (3) *can either be interpreted in the sense of Stratonovich in which the integrands are evaluated in the center point or Itô where they are evaluated in the left-most point. The Itô interpretation is more suitable for parameter estimation due to its martingale property w.r.t. the Brownian motion and the absence of spurious drift-term (Kloeden et al., 2012), therefore in this paper, the Itô interpretation is adapted.*

3.2. Observation equation

To obtain a state-space model, the state equations are connected with the observation equation which in its general form is given by

$$Y_k = g(X_{t_k}, U_{t_k}, t_k; \theta) + \underbrace{e_{t_k}}_{\text{Measurement noise}}, \tag{5}$$

where $Y_{t_k} \in \mathcal{Y} \subset \mathbb{R}^L$ represents the discrete-time observations (outputs) of a function of the observable stochastic states which are linked with the continuous-time state equation through the continuously differentiable (w.r.t. the states X_t) nonlinear function $g_{t_k}(X_k, U_k, t_k, \theta) \in \mathbb{R}^{\mathcal{L}}$. $t_k, k = 0, \cdots, N$ represents the sampling instants and $e_{t_k} \sim \mathcal{N}(0, \sigma)$ represents the zero mean Gaussian white noise process. Generally, $\forall t$ and t_k, mutual independence is assumed amongst the stochastic entities X_{t_0}, W_t and e_{t_k}.

3.3. Estimation

The literature contains various methods for parameter estimation in SDEs, the reader is referred to the following texts for good comparative reviews of the various methods (Nielsen et al., 2000; Shoji and Ozaki, 1997; Singer, 2004) .

3.3.1. One-step Ahead Prediction Model:

The problem of the parameter estimation in one-step ahead prediction model can be formulated as a maximum likelihood estimation (MLE) problem (Kristensen et al., 2004a). Given the sequence of measurements $\mathcal{Y}_N$, the likelihood function is based on the conditional one-step ahead prediction residuals. Due to the Markov property of (2) and the independence of the measurement errors, the joint probability density can be written as the product of the marginal densities:

$$\mathcal{L}(\theta|\mathcal{Y}_N, \mathcal{U}_N) = \prod_{k=1}^{N} p(Y_k|\theta, \mathcal{Y}_{k-1}, \mathcal{U}_k) p(X_0|\theta), \tag{6}$$

where $p(x|y)$ is the conditional probability density of $X = x$ given $Y = y$. Using the one-step prediction errors, $\epsilon_{k|k-1} = y_k - \hat{y}_{k-1}$, and the associated variances, $R_{k|k-1} = \mathrm{Var}(y_k|\mathcal{Y}_{k-1}, \theta)$ the likelihood function can be formulated as below (Kristensen et al., 2004a).

$$\begin{aligned} \mathcal{L}(\theta; \mathcal{Y}_N, \mathcal{U}_N) &= p(\mathcal{Y}_N, \mathcal{U}_N|\theta) \\ &= \left(\prod_{k=1}^{N} \frac{\exp\left(-\frac{1}{2} \epsilon_k^\top R_{k|k-1}^{-1} \epsilon_k \right)}{\sqrt{\det(R_{k|k-1})(\sqrt{2\pi})^{\mathrm{L}}}} \right) p(y_0|\theta) \\ &= -\frac{1}{2} \sum_{k=1}^{N} \left(\epsilon_k^\top R_{k|k-1}^{-1} \epsilon_k + \log \det R_{k|k-1}^{-1} + \mathrm{L} \log 2\pi \right), \end{aligned} \tag{7}$$

where θ is a set of parameters, $\mathcal{Y}_N$ is the set of observations, L is the dimension of the observation space, and y_0 is initial measurement. The parameter estimates are found by minimising the negative log-likelihood:

$$\hat{\theta} = \underset{\theta \in \Theta}{\operatorname{argmin}} \{ (\mathcal{L}(\theta; \mathcal{Y}_N, \mathcal{U}_N)|z_0) \}. \tag{8}$$

The corresponding value of the negative log-likelihood is the observed maximum likelihood value for that data set and model. Maximising the likelihood, part of the objective is a weighted least squares problem where the squared standardised residuals, given by $\epsilon_{k|k-1}^\top R_{k|k-1}^{-1} \epsilon_{k|k-1}$ in (7) are minimized. For clarity, consider this in the one dimensional case for the h-step residuals:

$$\mathbb{E}(\epsilon_{k+h|k}^2) = \mathbb{E}(\epsilon_{k+h|k})^2 + \mathbb{V}(\epsilon_{k+h|k}). \tag{9}$$

As long as h is not too large, the following relationships hold (Thygesen, 2016):

$$\mathbb{E}(\epsilon_{k+h|k})^2 \propto h^2\mathbb{E}(\epsilon_{k+1|k})^2, \tag{10}$$

$$\mathbb{V}(\epsilon_{k+h|k}) \propto h\mathbb{V}(\epsilon_{k+1|k}), \tag{11}$$

where $\mathbb{E}[\cdot]$ is the expectation operator, $\mathbb{V}(\cdot) = \text{Var}[\cdot]$ is the variance operator and $\propto$ is the proportionality operator. From these equation we see that as h increases the first term of (9) increases much faster than the second, which means that is more important to minimise the first term than the second. However, if the one-step ahead residuals are minimised, the two terms in (9) have equal weights, thus, parameter estimation based on the one-step ahead residuals can be expected to focus too little on minimising the expected value of the residuals, if the model is going to be used for long-term predictions (larger h). To remedy this, an alternative cost function is formulated, which is more focused on the long-term predictions.

3.3.2. Simulation Model:

In this paper we seek a model that can provide us with accurate predictions without using any residuals. To reduce the bias associated with predicting further ahead than the time-step used for estimation, the following cost function is minimised instead of the likelihood function:

$$F(\theta|\boldsymbol{\mathcal{Y}}_N, \boldsymbol{\mathcal{U}}_N) = -\log\left(\prod_{k=1}^{N} p(Y_k|\theta, \boldsymbol{\mathcal{Y}}_0, \boldsymbol{\mathcal{U}}_k)p(X_0|\theta)\right). \tag{12}$$

That is, the logarithm of the likelihood of each observation based on predictions from time 0, multiplied together. This is equal to the negative log-likelihood if the prediction errors are independent. We have that

$$p\left(Y_k|\theta, \boldsymbol{\mathcal{Y}}_N, \boldsymbol{\mathcal{U}}_k\right) = \frac{1}{\sqrt{2\pi\sigma^2_{k|0}}}\exp\left(-\frac{(Y_k - \hat{y}_{k|0})^2}{2\sigma^2_{k|0}}\right).$$

where $\hat{y}_{k|s} = \mathbb{E}(Y_k|\boldsymbol{\mathcal{Y}}_s)$ and $\sigma^2_{r|s} = \mathbb{V}(X_k - \hat{y}_{k|s})$. Inserting this in Equation (12) yields

$$\begin{aligned}
&F(\theta|\boldsymbol{\mathcal{Y}}_N, \boldsymbol{\mathcal{U}}_N) \qquad (13)\\
&= -\left(\sum_{k=1}^{N} \log\left(p(Y_k|\theta\boldsymbol{\mathcal{Y}}_0, \boldsymbol{\mathcal{U}}_k)\right) + \log(p(Y_0|\theta))\right)\\
&= -\left(\sum_{k=1}^{N} \log\left(\frac{1}{\sqrt{2\pi\sigma^2_{k|0}}}\exp\left(-\frac{(Y_k - \hat{y}_{k|0})^2}{2\sigma^2_{k|0}}\right)\right) + \log(p(Y_0|\theta))\right)\\
&= \sum_{k=1}^{N}\left(\underbrace{\frac{(Y_k - \hat{y}_{k|0})^2}{2\sigma^2_{k|0}}}_{\text{Weighted least squares}} + \underbrace{\log\left(\sqrt{2\pi\sigma^2_{k|0}}\right)}_{\text{uncertainty penalty}}\right) - \underbrace{\log(p(Y_0|\theta))}_{\text{Initialisation}}.
\end{aligned}$$

Notice how the cost consists of three terms with distinct interpretation. The first expresses the ability of the model to correctly predict the observations, weighted by estimated uncertainty $\sigma^2_{k|0}$. The weighting makes particular residuals less influential when the estimated uncertainty for the corresponding time step is large and vice versa when it is small. The second term penalises large estimates of the uncertainty, so that the final estimate of $\sigma^2_{k|0}$ is a compromise between reducing the cost the residual $(Y_k - \hat{y}_{k|0})$ and the cost of $\log\left(\sqrt{2\pi\sigma^2_{k|0}}\right)$. The third term deals with the prediction of the first time step, which need not be normally distributed. For long time series this term is almost irrelevant. Finally, the expected value and variance used in the cost function are computed by

$$\frac{\mathrm{d}\mathbb{E}(X_t)}{\mathrm{d}t} = f(\mathbb{E}(X_t), u_t), \tag{14}$$

$$\begin{aligned}
\frac{\mathrm{d}\mathbb{V}(X_t)}{\mathrm{d}t} =& A(\mathbb{E}(X_t), u_t)\mathbb{V}(X_t) \qquad (15)\\
&+\mathbb{V}(X_t)A(\mathbb{E}(X_t), u_t)^\top + \sigma(u_t)\sigma(u_t)^\top,
\end{aligned}$$

where

$$A(\mathbb{E}(X_t), u_t) = \left.\frac{\mathrm{d}f(x, u_t)}{\mathrm{d}x}\right|_{x=\mathbb{E}(X_t)}.$$

These equations are obtained by linearising f at each time step, so that they correspond to the propagation of the mean and variance in the linear setting (Juhl et al., 2013).

3.4. Optimisation

To estimate the parameters of the models proposed in this paper, the cost function described by Equation (13) was minimised using a combination of the global optimiser named Multi-Level Single-Linkage (MLSL) described in (Rinnooy Kan and Timmer, 1987a,b) and the local optimiser called Bound Optimization By Quadratic Approximation (BOBYQA) described in (J. D. Powell, 2009). The MLSL optimiser initiates local minimisations using the BOBYQA optmiser, and compares the resulting objective values obtained this way. Based on the results from the local minimisations it initiates new local minimisations at locations that the local minimisers did not search, so that it covers more of the total search space and does not get stuck in local minimas.

The BOBYQA is a trust-region based optimiser (Conn et al., 2000), which, as the name suggests, uses a quadratic approximation in the trust region. BOBYQA was chosen as the local optimiser since it performs well for twice differentiable objective functions, as we have here. On top of this it works well for parameters on different scales (i.e. some are much larger than others), which is the case for the models in this paper. The global optimiser MLSL was chosen because it works well with a low accuracy, which is useful to obtain the approximate parameter values. The estimate can then be improved afterwards by a high accuracy local optimisation, without having the computational burden explode.

The identification aprocedure was implemented using the free statistical software, R (version 3.3.2), and the "*CTSM-R-package*" (Continuous Time Stochastic Modelling in R version 0.6.8-5, Juhl (2015)) and the optimisation procedure was implemented using the freely available optimisation *NLopt-R* package (Ypma et al., 2018).

4. Model Identification and Validation

The identification procedure described in Section 3.1 is utilised here to identify a grey-box model of the forced Duffing oscillator. The experimental measurements for the identification are acquired on the SilverBox benchmark (Pintelon and Schoukens, 2012). In the section below, a very brief description of the benchmark and experimental details are provided.

4.1. The SilverBox Benchmark

The Silverbox benchmark is an electronic circuit mimicking the behaviour of the Duffing Oscillator. The electronic circuit

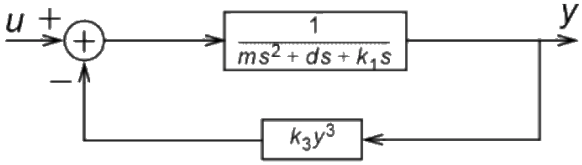

Figure 1: The dynamics of the SilverBox electronic circuit represented as a nonlinear feedback circuit.

mimics the behaviour of a second-order nonlinear mechanical resonating system with a moving mass m, a viscous damping d, a linear spring constant k_1 and a nonlinear spring constant k_3 as shown in Figure 1. The dynamics of the ideal electronic circuit can described by the following differential equation:

$$m\ddot{y}(t) + a_1\dot{y}(t) + k_1 y(t) + k_3 y^3(t) = u(t). \tag{16}$$

The SilverBox electronic circuit mimicking the Duffing oscillator is very close to but not equal to the idealised representation of the Duffing Oscillator with a cubic nonlinearity.

A general waveform generator (HPE1445A) was used to excite the SilverBox electronic system. A discrete-time input reference signal $r(k)$ was converted into an analogue signal $r_c(t)$ using a zero-order-hold reconstruction circuit. The final input excitation signal $u(t)$ was then obtained by passing $r_c(t)$ through an analogue low-pass filter $G(p)$, where p is the differentiation operator. This operation eliminates the high frequency contents around the multiples of the sampling frequency. The final input is given by

$$u(t) = G(p)r_c(t). \tag{17}$$

The HP1430A data acquisition cards were used to measure the input and the output signals. During the data acquisition it was made that the clocks synchronisation of the acquisition and generator cards was ensured. The sampling frequency f_s was kept at 610.35 Hz.

Figure 2 shows the acquired input in blue and output in green, black and red. The reference signal $r(k)$ consists of two parts: The first part (40000 samples shown in green) is a white Gaussian noise sequence filtered by a 9^{th}-order discrete-time Butterworth filter with a cut-off frequency of 200 Hz. The amplitude is varied linearly over the interval from zero to its maximum

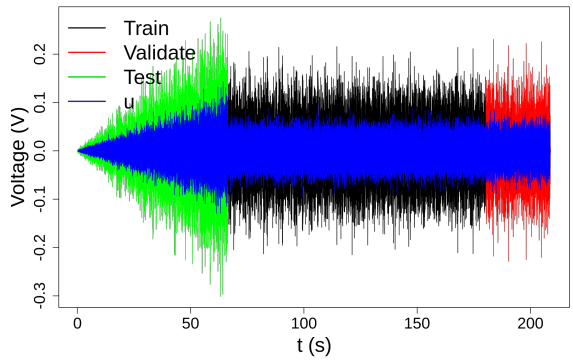

Figure 2: The data from the Silverbox benchmark and how it has been distributed for the work done in this paper.

value. The second part of the signal consists of 10 successive realisations of a random odd multisine signal given by:

$$r(k) = \sum_{k=1}^{K_{max}} A\cos(2\pi f_o k + \phi_k). \tag{18}$$

In the benchmark data experiments only the odd harmonics were excited. To fit the signal within the range of the generator the amplitude A was scaled. $1/f_0$ represents the period of the multisine such that $f_0 = f_s/8192\ \text{s}^{-1}$. The maximum excited frequency was $\approx$ 200Hz and the total number of excited odd harmonics were 1342. The phases ϕ_k were independent and uniformly distributed in $[2\pi, 0[$. Ten realisations of the random odd multisine were merged, each of them separated by 100 zeros to indicate the tart of a new realisation. These periods were split in two parts, consisting of 8 periods for training shown in black and two periods for testing shown in red.

4.2. Model Structure Identification

In this section a number of grey-box model structures will be identified using the estimation framework presented in Section 3.3.2. To start with, the initial model structure is obtained directly by transforming the duffing equations given by (1) into a state-space form as formulated below:

$$\frac{\mathrm{d}X_t}{\mathrm{d}t} = V_t, \tag{19}$$

$$\frac{\mathrm{d}V_t}{\mathrm{d}t} = -a_1 V_t - k_1 X_t - k_3 X_t^3 + b_1 u_t, \tag{20}$$

where X_t and V_t are the position and velocity respectively and u_t is the input to the system. To account for any uncertainty (process noise) in the system states, the duffing equations are extended to the SDE form as explained in Section 3.1:

$$\begin{aligned} \mathrm{d}X_t &= V_t\mathrm{d}t + \sigma_X \mathrm{d}W_t^X, \\ \mathrm{d}V_t &= (-a_1 V_t - k_1 X_t - k_3 X_t^3 + b_1 u_t)\mathrm{d}t + \sigma_V \mathrm{d}W_t^V, \end{aligned} \tag{21}$$

where σ_X and σ_V determines the magnitude of the process noise entering in the position and velocity state respectively. Similarly, any measurement noise in the observed state (position) is accounted directly in the measurement equation:

$$Y_k = X_{t_k} + e_k, \tag{22}$$
$$e_k \sim \mathcal{N}(0, \sigma^2). \tag{23}$$

The model structure described by (21) is considered a white-box model and hereinafter termed as Model 1, since the structure is obtained directly from the underlying physics.

The residuals obtained after the identification procedure for both the one-step prediction model and/or simulation model contain a lot of information about the performance of the model structure in explaining the data. That is, unexplained dynamics can be discovered by carefully analysing the residual of particular model structures. For example a white-box model structure can be extended to explain the data better by adding the residual terms into the initial white-box model structure.

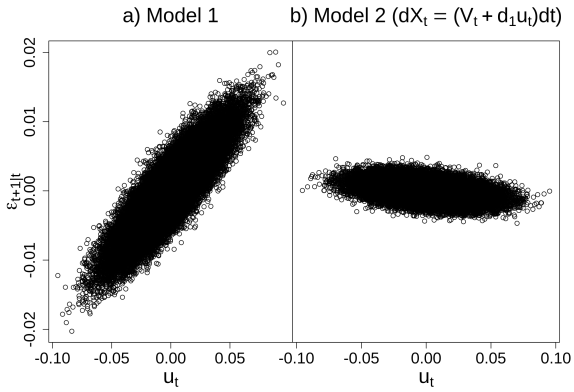

Figure 3: One-step ahead prediction residuals versus input lagged by one time step. The improvement from Model 1 to Model 2 is due to an added term in the position state equation.

To start with, (13) is used to estimate the parameters of the model structure described by (21) and the residuals are subsequently obtained. In Figure 3a the one-step ahead prediction residuals of Model 1 are plotted against the lagged input signal. It can be clearly seen that how Model 1 residuals are linearly dependent on the input signal. This linear relationship between the Model 1 residual and the input signal suggests that it affects the output faster than the model can explain.

To overcome this deficiency in the structure of Model 1, the SDE governing the position is modified to include a direct contribution from the input. The new model structure described below is termed as Model 2:

$$\mathrm{d}X_t = (V_t + d_1 u_t)\mathrm{d}t + \sigma_X \mathrm{d}W_t^X.$$

The one-step prediction residuals of Model 2 are shown in Figure 3b, where it can be clearly observed that the linear relation between $\epsilon_{t+1|t}$ and u_t has been almost removed.

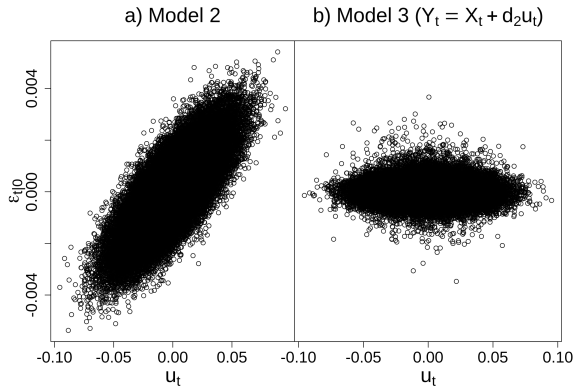

Figure 4: Simulation residuals versus input. Model 2 is improved by adding a term directly linking the input to the output.

For Model 2, the residuals for the simulation are also plotted against input in Figure 4a) where a linear trend can be clearly seen. The result plotted display the input and the output for the same time step. Therefore, the only way to account for the dependence is by adding the input directly to the observation equation, resulting in Model 3:

$$Y_k = X_{t_k} + d_2 u_t + e_k. \tag{24}$$

It is evident that the Model 3 structure makes the residuals independent of the input, as clearly seen in Figure 4b).

Furthermore, for several lags a nonlinear dependence was also observed between the estimated velocity and the residuals of the simulation model. Especially for lag 2 a strong cubic relationship can be seen in Figure 5a). For discrete-time models, this issue can easily be resolved by inserting a term with the lagged velocity directly in the model. However, for continuous-time models this can be resolved only by increasing the state

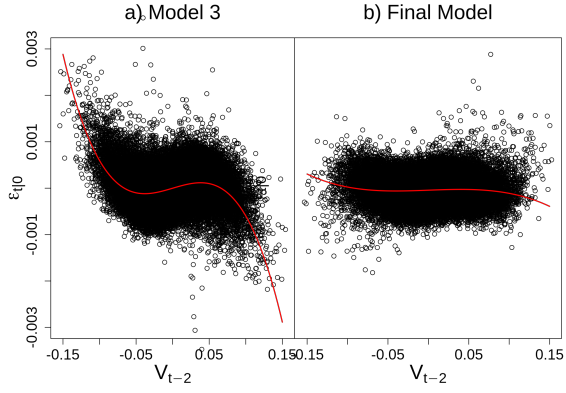

Figure 5: Simulation residuals versus estimated velocity lagged by two time steps. The improvement is due to adding a nonlinear function of a lagged velocity estimate.

dimension by incorporating an auxiliary state into the model as shown below:

$$\mathrm{d}P = a_2(V_t - P_t)\mathrm{d}t + \mathrm{d}w_t^P. \tag{25}$$

For positive values of a_2 the drift term is positive whenever P_t is smaller than V_t and vice-versa when it is larger. This makes P_t follow V_t, hence it can be considered as equivalent to the delayed velocity term. The contribution of the new state P_t is added both in the position state equation and the observation equation. This modification then yields the most generic model structure considered in this paper as described below:

$$\mathrm{d}X_t = (V_t + d_1u_t + g_1P_t + g_2P_t^2 + g_3P_t^3)\mathrm{d}t + \sigma_X\mathrm{d}w_t^X, \tag{26}$$

$$\mathrm{d}V_t = (-a_1V_t - k_1X_t - k_2X_t^2 - k_3X_t^3 + b_1u_t)\mathrm{d}t + \sigma_V\mathrm{d}w_t^V, \tag{27}$$

$$\mathrm{d}P_t = a_2(V_t - P_t)\mathrm{d}t + \sigma_p\mathrm{d}w_t^P, \tag{28}$$

$$Y_k = X_{t_k} + d_2u_{t_k} + f_1P_{t_k} + f_2P_{t_k}^2 + f_3P_{t_k}^3 + e_k. \tag{29}$$

Notice how the term $k_2X_t^2$ was added to the model as well. This is common practice for statistical models, to avoid artificial limitations on higher order terms, which in this case is $k_3X_t^3$ (Crawley, 2016). Furthermore, the authors in (Nöel et al., 2015; Schoukens et al., 2003) established that there is an asymmetry in its nonlinear spring characteristic. This asymmetry is well modelled by the additional quadratic stiffness term.

To decide which parameters should be kept and which should be removed in the final model structure, several combinations of parameters were considered. The final choice of different parameters in a particular model structure was based on the statistical significance of various parameters fitted on the training data. In the next step, the simulation error i.e. the Root-Mean-Square error (RMS) value (in mV), for various model structures is computed for the validation data, and the test data which gave a measure of the performance of a particular model.

Table 1: RMSE (mV) based on simulation for the train, validation and test data.

Excluded terms	Train	Validation	Test
None	**0.262**	**0.273**	**0.419**
f_1, f_2, f_3	0.266	0.276	0.426
$\boldsymbol{g_2, g_3}$	**0.285**	**0.292**	**0.396**
f_1, f_2, f_3, g_2, g_3	0.338	0.340	0.481
k_2	0.275	0.288	0.461
f_1, f_2, f_3, k_2	0.275	0.288	0.461
g_2, g_3, k_2	0.302	0.313	0.420
$f_1, f_2, f_3, g_2, g_3, k_2$	0.355	0.362	0.497

Table 1 shows the computed simulation error in (RMS in mV) for each of the data subsets for different model structure. It can be seen that the lowest simulation error (RMS in mV) for the validation data is obtained by the full model (26) in which no terms were excluded. Hence, it can be chosen as the candidate model structure. This further suggests that even addition of more terms may improve it further, but this was not pursued, since the objective of the proposed methodology was to keep the model structure simple enough. The performance of the full model on the test data was 0.419 as shown in Table 1. The other tested models performed similarly on the test data, with one of them even outperforming the chosen model. Having similar performance of alternative models is a good sign, since it indicates that the performance is not over-optimistic.

5. Results and Discussion

Table 2 shows the performance of other methods applied to the SilverBox benchmark system. It can be seen that the model structure proposed in (Ljung et al., 2004) and (Paduart et al., 2010) performed very good but the model structure has a large number of parameters. Furthermore, it is not clear whether the final model was obtained on the validation or the test data. Hence, a fair comparison can not be made. Nevertheless, we include the results for completeness. Similarly, the model structure described in (Espinoza et al., 2004) performed very well due to 500 parameters.

Both (Verdult, 2004) and (Hjalmarsson and Schoukens, 2004) performed significantly worse than our method, although the number of parameters in (Hjalmarsson and Schoukens, 2004) is also lower than the proposed method in this paper. When it comes to (Marconato et al., 2012) and (Mulders et al., 2013), they both outperform our method, in the case of (Marconato et al., 2012) this comes at the price of 9 more parameters, but (Mulders et al., 2013) is able to perform better even with 2 parameters less. But its should be noted that the both are discrete-time black-box models and require multistage identification procedure as well as good initialisation. In many applications, the discrete-time black-box model structure is of limited usefulness for control, whereas the continuous-time grey-box model presented here allows easy access to model-based control strategies.

Also, while the SilverBox benchmark system data is very high resolution data with no missing values, this is often not the case in real-world applications. It is not straight-forward to handle the issue of missing values during the identification of the discrete-time models. On the contrary the continuous time model structure presented here is almost unaffected by missing values in the input-output data.

Finally, the authors would like to point out a limitation in using the RMS as evaluation criteria and an advantage of the statistical models developed here. The RMS solely evaluates models based on their ability to make predictions close to the observations, and while this surely is the most important property, it is not the only one. Another, often overlooked, property of good statistical models is to estimate their own accuracy. This is especially important when the model accuracy is not constant, as is the case for non-linear models. This is easily obtained for the models developed here by the use of (15), and is incorporated in the likelihood function when one-step ahead predictions are of interest and the cost function defined in (13) when the simulation performance is of interest. For the final model produced in this paper:

$$F(\theta^{\text{optimal}}|\mathcal{Y}_{100:40500}, \mathcal{U}_{100:40500}) = -249240.5V^2.$$

We invite future research on this and other benchmarks to include this performance criteria as well.

Table 2: Performance of various methods from the literature applied to the Silverbox benchmark.

Authors	#parameters	RMSE (mV)
Ljung et al. 2004	>700	0.30
Espinoza et al. 2004	500	0.32
Paduart et al. 2010	37	0.26
Marconato et al. 2012	23	0.34
Verdult 2004	16	1.3
Mulders et al. 2013	12	0.35
Hjalmarsson et al. 2004	5	0.96
This paper 2019	14/12	0.42/0.4

6. Conclusion

The forced Duffing oscillator equations are used in various forms for description as well as analysis of many real-world nonlinear systems. Though limited in application over a wide range of operational conditions, such as frequency and amplitude of excitation, the Duffing equations still offer a good start to qualitatively understand the behaviour of many nonlinear system and discovering many nonlinear characteristics. Identification of such models described by the forced Duffing oscillator equations still remains a challenge. In this paper, SDEs based modelling framework was extended to identify the grey-box models for the forced Duffing oscillator.

Although the SDEs find more applications in the time-series modelling work and minimisation of the one-step ahead prediction error remains the main objective for such application, in this paper we extended the SDE based modelling framework to identify a simulation model for the forced Duffing oscillator. It was shown how the correct physical model structure for the deterministic part was inferior to extended models. The residual based identification methodology used for structure identification combined with the novel cost function can directly be applied to other applications, in which the resulting models should provide predictions on longer time scales than the sampling time. Finally the performance of the proposed methodology was tested on the SilverBox benchmark system. It has been clearly demonstrated that the performance of the proposed grey-box models is either better or on par with previous models found in the literature, with an added value of being continuous-time and having physically sensible states useful for control applications.

Acknowledgment

The authors would like to thank the Centre for IT–Intelligent Energy Systems (CITIES) project supported by Innovation Fund Denmark for the financial support needed to conduct the research reported in this paper.

References

Mikkel Baadsgaard, Jan Nygaard Nielsen, Henrik Spliid, Henrik Madsen, and Michael Preisel. Estimation in stochastic differential equations with a state dependent diffusion term. *IFAC Proceedings Volumes*, 30(11):1369 – 1374, 1997. ISSN 1474-6670. IFAC Symposium on System Identification (SYSID'97), Kitakyushu, Fukuoka, Japan, 8-11 July 1997.

Steven L Brunton, Joshua L Proctor, and J Nathan Kutz. Sparse identification of nonlinear dynamics with control (sindyc). *IFAC-PapersOnLine*, 49(18): 710–715, 2016.

A. Conn, N. Gould, and P. Toint. *Trust Region Methods*. Society for Industrial and Applied Mathematics, 2000. doi: 10.1137/1.9780898719857.

Michael J. Crawley. *Statistics: An introduction using R – Second edition*. 2016. ISBN 978-1-118-94109-6.

A Subin Das and B Santhosh. Energy harvesting from nonlinear vibration absorbers. *Procedia engineering*, 144:653–659, 2016.

Marcelo Espinoza, Kristiaan Pelckmans, Luc Hoegaerts, Johan A.K. Suykens, and Bart De Moor. A comparative study of ls-svm's applied to the silver box identification problem. *IFAC Proceedings Volumes*, 37(13):369 – 374, 2004. ISSN 1474-6670.

E Gandino, L Garibaldi, and S Marchesiello. Covariance-driven subspace identification: A complete input–output approach. *Journal of Sound and Vibration*, 332(26):7000–7017, 2013.

S Khatiry Goharoodi, Kevin Dekemele, Luc Dupre, Mia Loccufier, and Guillaume Crevecoeur. Sparse identification of nonlinear duffing oscillator from measurement data. *IFAC-PapersOnLine*, 51(33):162–167, 2018.

Dongying Han, Yanlong Sun, Xiao Su, and Peiming Shi. Feature extraction method for weak mechanical fault signal based on double coupled duffing oscillator and emd. In *2016 IEEE 13th International Conference on Signal Processing (ICSP)*, pages 1863–1866. IEEE, 2016.

Håkan Hjalmarsson and Johan Schoukens. On direct identification of physical parameters in non-linear models. *IFAC Proceedings Volumes*, 37(13):375 – 380, 2004. ISSN 1474-6670.

R. Isermann and M. Münchhof. *Identification of Dynamic Systems: An Introduction with Applications*. Springer Berlin Heidelberg, 2010. ISBN 9783540788799.

M J. D. Powell. The bobyqa algorithm for bound constrained optimization without derivatives. *Technical Report, Department of Applied Mathematics and Theoretical Physics*, 01 2009.

Rune Juhl. *CTSM-R: Continuous Time Stochastic Modelling in R: User's Guide and Reference Manual*, 2015. R package version 0.6.8-5.

Rune Juhl, Niels Rode Kristensen, Peder Bacher, Jan Kloppenborg, and Henrik Madsen. Ctsm-r user guide. 2013.

Gaëtan Kerschen, Maxime Peeters, Jean-Claude Golinval, and Alexander F Vakakis. Nonlinear normal modes, part i: A useful framework for the structural dynamicist. *Mechanical Systems and Signal Processing*, 23(1):170–194, 2009.

F.C. Klebaner. *Introduction to Stochastic Calculus with Applications*. Imperial College Press, 2005. ISBN 9781860945663.

P.E. Kloeden, E. Platen, and H. Schurz. *Numerical Solution of SDE Through Computer Experiments*. Universitext. Springer Berlin Heidelberg, 2012. ISBN 9783642579134.

I. Kovacic and M.J. Brennan. *The Duffing Equation: Nonlinear Oscillators and their Behaviour*. Wiley, 2011. ISBN 9780470977835.

Niels Rode Kristensen, Henrik Madsen, and Sten Bay Jørgensen. Parameter estimation in stochastic grey-box models. *Automatica*, 40(2):225 – 237, 2004a. ISSN 0005-1098.

Niels Rode Kristensen, Henrik Madsen, and Sten Bay Jørgensen. A method for systematic improvement of stochastic grey-box models. *Computers Chemical Engineering*, 28(8):1431 – 1449, 2004b. ISSN 0098-1354. doi: https://doi.org/10.1016/j.compchemeng.2003.10.003.

Zhi-hui Lai and Yong-gang Leng. Weak-signal detection based on the stochastic resonance of bistable duffing oscillator and its application in incipient fault diagnosis. *Mechanical Systems and Signal Processing*, 81:60–74, 2016.

Ron Lifshitz and MC Cross. Nonlinear dynamics of nanomechanical and micromechanical resonators. *Review of nonlinear dynamics and complexity*, 1: 1–52, 2008.

Ping Liu, Hongjun Song, and Xiang Li. Observe-based projective synchronization of chaotic complex modified van der pol-duffing oscillator with application to secure communication. *Journal of Computational and Nonlinear Dynamics*, 10(5):051015, 2015.

L. Ljung and T. Glad. *Modeling of Dynamic Systems*. PTR Prentice Hall, 1994. ISBN 9780135970973.

Lennart Ljung. System identification. *Wiley Encyclopedia of Electrical and Electronics Engineering*, pages 1–19, 1999.

Lennart Ljung, Qinghua Zhang, Peter Lindskog, and Anatoli Juditski. Esti-

mation of grey box and black box models for non-linear circuit data. *IFAC Proceedings Volumes*, 37(13):399 – 404, 2004. ISSN 1474-6670.

Anna Marconato, Jonas Sjöberg, Johan Suykens, and Johan Schoukens. Identification of the silverbox benchmark using nonlinear state-space models. *IFAC Proceedings Volumes*, 45(16):632 – 637, 2012. ISSN 1474-6670.

SF Masri and ToK Caughey. A nonparametric identification technique for nonlinear dynamic problems. *Journal of Applied Mechanics*, 46(2):433–447, 1979.

SF Masri, JP Caffrey, TK Caughey, AW Smyth, and AG Chassiakos. Identification of the state equation in complex non-linear systems. *International Journal of Non-Linear Mechanics*, 39(7):1111–1127, 2004.

Jan Kloppenborg Møller and Henrik Madsen. *From state dependent diffusion to constant diffusion in stochastic differential equations by the Lamperti transform*. DTU Informatics, 2010.

Anne Van Mulders, Johan Schoukens, and Laurent Vanbeylen. Identification of systems with localised nonlinearity: From state-space to block-structured models. *Automatica*, 49(5):1392 – 1396, 2013. ISSN 0005-1098.

Jan Kloppenborg Møller, Goran Goranović, Niels Kjølstad Poulsen, and Henrik Madsen. Physical-stochastic (greybox) modeling of slugging. *IFAC-PapersOnLine*, 51(8):197 – 202, 2018. ISSN 2405-8963. doi: https://doi.org/10.1016/j.ifacol.2018.06.377. 3rd IFAC Workshop on Automatic Control in Offshore Oil and Gas Production OOGP 2018.

A.H. Nayfeh and D.T. Mook. *Nonlinear Oscillations. Pure and Applied Mathematics*. John Wiley and Sons.

Jan Nygaard Nielsen and Henrik Madsen. Applying the EKF to stochastic differential equations with level effects. *Automatica*, 37(1):107–112, 2001.

Jan Nygaard Nielsen, Henrik Madsen, and P. C. Young. Parameter estimation in stochastic differential equations; an overview. *Annual Reviews in Control*, 24:83–94, 2000. ISSN 1367-5788.

Jean-Philippe Noël and Gaëtan Kerschen. Nonlinear system identification in structural dynamics: 10 more years of progress. *Mechanical Systems and Signal Processing*, 83:2–35, 2017.

JP Nöel, Johan Schoukens, and Gaetan Kerschen. Grey-box nonlinear state-space modelling for mechanical vibrations identification. *IFAC-PapersOnLine*, 48(28):817–822, 2015.

B. Øksendal. *Stochastic Differential Equations: An Introduction with Applications*. Springer, 2010. ISBN 9783642143946.

Johan Paduart, Lieve Lauwers, Jan Swevers, Kris Smolders, Johan Schoukens, and Rik Pintelon. Identification of nonlinear systems using polynomial nonlinear state space models. *Automatica*, 46(4):647 – 656, 2010. ISSN 0005-1098.

Rik Pintelon and Johan Schoukens. *System identification: a frequency domain approach*. John Wiley & Sons, 2012.

HJ Rice and JR McCraith. Practical non-linear vibration absorber design. *Journal of Sound Vibration*, 116:545–559, 1987.

A. H. G. Rinnooy Kan and G. T. Timmer. Stochastic global optimization methods part i: Clustering methods. *Mathematical Programming*, 39(1):27–56, Sep 1987a. ISSN 1436-4646. doi: 10.1007/BF02592070.

A. H. G. Rinnooy Kan and G. T. Timmer. Stochastic global optimization methods part ii: Multi level methods. *Mathematical Programming*, 39(1): 57–78, Sep 1987b. ISSN 1436-4646. doi: 10.1007/BF02592071. URL `https://doi.org/10.1007/BF02592071`.

Johan Schoukens, József G Nemeth, Philippe Crama, Yves Rolain, and Rik Pintelon. Fast approximate identification of nonlinear systems. *Automatica*, 39(7):1267–1274, 2003.

Isao Shoji and Tohru Ozaki. Comparative study of estimation methods for continuous time stochastic processes. *Journal of Time Series Analysis*, 18 (5):485–506, 1997.

Hermann Singer. A survey of estimation methods for stochastic differential equations. Technical report, Fern University, 2004.

J.J. Stoker. *Nonlinear Vibrations*. 1966.

Bin Tang, MJ Brennan, G Gatti, and NS Ferguson. Experimental characterization of a nonlinear vibration absorber using free vibration. *Journal of Sound and Vibration*, 367:159–169, 2016.

Uffe Thygesen. *Lecture notes on Diffusion and Stochastic Differential Equations*. Polyteknisk boghandel, 08 2016.

Vincent Verdult. Identification of local linear state-space models: The silverbox case study. *IFAC Proceedings Volumes*, 37(13):393 – 398, 2004. ISSN 1474-6670.

Jelmer Ypma, Hans W Borchers, Dirk Eddelbuettel, and Maintainer Jelmer Ypma. Package 'nloptr'. 2018.

PAPER B

Characterizing the energy flexibility of buildings and districts

Authors:
Rune Grønborg Junker, Armin Ghasem Azar, Rui Amaral Lopes, Karen Byskov Lindberg, Glenn Reynders, Rishi Relan and Henrik Madsen.

Published in:
Applied Energy.

Characterizing the Energy Flexibility of Buildings and Districts

Rune Grønborg Junker[a,*], Armin Ghasem Azar[a], Rui Amaral Lopes[c,d], Karen Byskov Lindberg[b], Glenn Reynders[e], Rishi Relan[a], Henrik Madsen[a,b]

[a] *Technical University of Denmark*
[b] *Norwegian University of Science and Technology (ZEN-project)*
[c] *Department of Electrical Engineering, Faculty of Science and Technology, Universidade NOVA de Lisboa*
[d] *Centre of Technology and Systems/UNINOVA*
[e] *EnergyVille - KU Leuven*

Abstract

The large penetration rate of renewable energy sources leads to challenges in planning and controlling the energy production, transmission, and distribution in power systems. A potential solution is found in a paradigm shift from traditional supply control to demand control. To address such changes, a first step lays in a formal and robust characterization of the energy flexibility on the demand side. The most common way to characterize the energy flexibility is by considering it as a static function at every time instant. The validity of this approach is questionable because energy-based systems are never at steady-state. Therefore, in this paper, a novel methodology to characterize the energy flexibility as a dynamic function is proposed, which is titled as the *Flexibility Function*. The Flexibility Function brings new possibilities for enabling the grid operators or other operators to control the demand through the use of penalty signals (e.g., price, CO_2, etc.). For instance, CO_2-based controllers can be used to accelerate the transition to a fossil-free society. Contrary to previous static approaches to quantify Energy Flexibility, the dynamic nature of the Flexibility Function enables a Flexibility Index, which describes to which extent a building is able to respond to the grid's need for flexibility. In order to validate the proposed methodologies, a case study is presented, demonstrating how different Flexibility Functions enable the utilization of the flexibility in different types of buildings, which are integrated with renewable energies.

Keywords:
Energy Flexibility, Demand Response, Flexibility Function, Smart Building, Flexibility Index, Smartness

1. Introduction

The sustainable transition to a fossil-free energy system with a high penetration of energy conversion technologies based on fluctuating renewable energy resources, like wind and solar, calls for a paradigm shift in power systems [1, 2]. Traditionally, power systems have been designed with centrally-situated large power generation units that are operated to meet the demand. However, to support the transition to a renewable energy system with intermittent and fluctuating power generation, a change is commonly suggested, where demand is adjusted to the available generated power [3, 4]. Moreover, renewable energy generation is often locally situated, changing the present system from a unidirectional centralized system towards a bidirectional decentralized system with smaller units and multiple prosumers [5]. Such disruptive changes imply increased utilization of advanced control systems to enable flexible demand through demand response technologies and proper system integration [6]. The flexibility potential is already present (e.g., through heat storage [7]), and is further enhanced by advances and increased utilization of batteries [8]. Today, the use of model predictive control in buildings is seen as a strong opportunity to minimize costs, while still meeting the comfort requirements [9]. This control can be done either centralized by e.g., a grid operator (direct control), or decentralized by each building owner [10]. In this paper, the focus is on the latter type. The strategies used for defining the optimal controller can take a variety of parameters into account. For buildings the focus can be on energy efficiency, CO_2 efficiency, or minimizing the total cost [11], where trade-offs arise as a part of selecting the strategy. For example, a controller that is energy-efficient is typically not price-optimal given the energy markets and the energy-related taxes that exist today [12].

The building sector plays a key role in the future smart energy system as buildings account for approximately 40% of the global energy consumption [13]. Flexible buildings can provide grid services and thereby accelerate the transition to a low carbon energy system. The potential for using a building for demand response is defined as its energy flexibility [14]. The buildings' ability to provide energy flexibility is influenced by several factors [15]: 1) its physical characteristics such as thermal mass, insulation, and architectural layout, 2) its technologies such as ventilation, heating, and storage equipment, 3) its control system that enables user interactions; the possibility to respond and react to external signals such as electricity price or CO_2 factors, and 4) the occupants' behaviour and comfort

* Corresponding Author
Email address: rung@dtu.dk
Postal Address: Anker Engelunds vej 1, Building 101A, 2800 Kongens Lyngby, Denmark

requirements.

The energy flexibility potential can be found either by building *simulation* tools, i.e., deductively, or by use of experimental data, i.e., inductively by statistical *time series analysis*. Similar to a prediction of the energy consumption of a building, predicting the energy flexibility requires detailed dynamic modeling of a building's energy systems, including technical constraints, occupancy behaviour, and boundary conditions; see e.g., [16–18]. Using experimental data for estimating the energy flexibility of households with a price-responsive load was first suggested as a part of the FlexPower project [19]. However, the concept of controlling the energy balance in power systems using prices is not new, since it was first presented in [20]. In [21], the authors suggested the use of time series analysis tools to quantify the flexibility of buildings as a response to time-varying prices for the electricity using data from the Olympic Peninsula Project [22]. Similarly, in [23], a method based on inverse optimization was used to estimate the flexibility using real data. It was shown by [21] how the variations in penalties could be used to shift the load from peak hours to off-peak hours. The authors in [6, 12] went a step further and demonstrated that the frequency and voltage in power grids could also be controlled by this method. However, they failed to specify which systems (e.g., buildings, districts, pools, etc.) are suitable for this approach.

Characterizing energy flexibility in a structural way is challenging as it involves many aspects [24]. A characterization of the energy flexibility and structural thermal energy storage is made in [25]. Here, the authors propose three characteristics: 1) available storage capacity, 2) storage efficiency, and 3) power shifting capability that reflects the relation between the aspects of power, duration and comfort constraints. Authors in [26], on the other hand, investigate the flexibility of a heat pump pool, and propose some characteristics; one example being the time until the electricity has returned to the baseline load. The drawback of the characterization methods in [25, 26] is that they focus on specific characteristic numbers independently of each other. Furthermore, communicating the values of all these characteristics is complicated, and thus, there is a need for a simplified characterization that can take the dynamics of the system into account. The fact that these methods refer to a baseline load also makes them difficult to use in practice, where there is no baseline.

In this paper we propose a method to characterize the energy flexibility as a dynamic function, titled the Flexibility Function (FF). Unlike the bidding-based approaches that assume constant flexibility as described in [27, 28], the dynamic nature of the FF enables the description of energy flexibility transients. Thus, it is useful even when the system is not in steady state, which is the case whenever energy flexibility has recently been utilized. The suggested method does not need any calculation of a baseline load. The FF can be determined either by simulation or by analyzing time series data. In situations where the FF is based on experimental data, it indirectly considers other factors such as heating equipment, usage, comfort and controllability. This generic energy flexibility characterization enables a comparison between systems with vastly different characteristics (e.g., an office building and a sewer system). It also enables the computation of the total flexibility when combining several systems. The suggested methodology for a dynamic characterization of the flexibility of e.g., a building, is designed such that it can be used for providing the energy system and the grid with ancillary services. Such services are given a high priority in the EU Winter Package [29]. In the linear case, the flexibility can be characterized using impulse response functions, step response functions, frequency response, and transfer functions - see also [30, 31]. Consequently, the flexibility can easily be described using different approaches and characterized either in time or frequency domain. Since the intermittent energy sources may only partly be predictable, methodologies for energy demand management for dynamic systems under uncertainty must be established. It will be argued that the suggested dynamic description of the energy flexibility is designed such that it facilitates methods for providing grid services such as voltage control, load balancing, and other ancillary services. In this paper, we will focus on buildings, but the technology can be used for other types of flexible responses like waste water treatment plants [32] and supermarket cooling [33, 34].

Based on the FF, a method for calculating a Flexibility Index (FI), which measures the reaction of a building or cluster of buildings to penalty signals like CO_2 intensity or control signals imposed by the grid, is also proposed. For instance, a FI of zero indicates that the building does not react at all, whereas a FI equal to 0.2 denotes that 20% of the penalty-related cost can be saved due to the smartness and flexibility of the building. This generic characterization of energy flexibility assumes that the system under consideration either contains a penalty-aware controller [6, 11, 35] or a manual response to variations in penalty signals like electricity price or CO_2 intensity (hereinafter referred as penalties) as described in [36]. The FI holds the essential information for particular applications of flexibility, and can be understood and communicated without technical insight in energy flexibility.

The paper is structured as follows: In Section 2 the novel idea of a FF is introduced along with the requirements for using it. Then, in Section 3 three applications of the FF is presented: 1) Quantitative description of energy flexibility, 2) Computing FIs, 3) Performing ancillary services. Next, Section 4 illustrates the concepts in a case study. Finally, Section 5 is a short summary and outlines plans for the future work.

2. Characterizing Flexibility of Penalty-Aware Buildings

This section introduces the novel idea of characterizing energy flexibility through a dynamic function, the FF, and the prerequisites for applying it. In this paper, we consider the building level. However, the methodologies can be applied to any energy-consuming system, e.g., a sewing system, a group of buildings, or a district. In many cases, it would actually be more optimal to consider a group of buildings, a smart district or a smart city, since the large scale offers solutions for energy production and storage, which may not be economically or practically suitable in the case of a single building. In fact, the district heating network in Denmark is a key element for

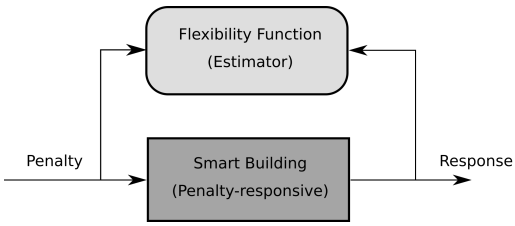

Figure 1: A smart building is able to respond to a penalty or external control signal.

the operation of the Danish power system that consists of more than 40% fluctuating wind energy [37].

2.1. Penalty-Aware Control and Smart Buildings

The methodology for characterizing energy flexibility presented in this paper are based on the general assumption that the system providing the flexibility is *smart* in a manner that it is able to respond to an external *penalty* signal. Penalty signals express the importance of a local and temporal adaption of the power consumption. Therefore, in this context, a smart building is an energy-flexible building, which is equipped with penalty-aware controllers responding to external penalty or control signals, as illustrated in Figure 1. The choice of control methodology for reacting to penalty signals is independent of the characterization of the energy flexibility. However, in this paper, we utilize an economic model predictive control methodology [6, 11, 35].

As a typical example, consider a building that needs to be heated and let the penalty be the energy-price. In this case, the penalty-aware controller will try to keep the building within thermal comfort boundaries at the lowest possible cost. This is illustrated in Figure 2, where the top plot shows temperature in a building using both a penalty-aware controller that minimizes costs (green, dashed), and a regular one that minimizes energy usage (red, solid). The middle plot shows the penalties (black columns) and the heating operation of the controllers. It is seen that in general the regular controller keeps the temperature just above the minimum required value. On the other hand, the penalty-aware controller tends to heat when the penalty is low, which results in the temperature varying more. The lower plot shows the accumulated penalty, and as expected, the regular controller accumulates more penalty than the penalty-aware controller. This principle of penalty-aware control for diverse flexible systems and for a variety of penalty signals has been applied in many studies [12, 32, 35, 38].

Depending on the context of application, e.g., local energy mix, energy system constraints, or even societal ambitions, different penalty signals can be constructed to tailor the optimal energy demand. Let us consider three different penalty signals:

- **Real time CO_2**. If the real time (marginal) CO_2 emission related to the actual electricity production is used as penalty, then, a smart building will minimize the total carbon emission related to the power consumption. Hence, the building will be *emission efficient*.
- **Real time price**. If a real time price is used as penalty, the objective is to minimize the total cost. Hence, the building is *cost efficient*.
- **Constant**. If a constant penalty is used, then, the controllers will simply minimize the total energy consumption. The smart building is, then, *energy efficient*.

It is clear that smart buildings with controllers with the objective of minimizing the total emission will in general use more energy, but this happens at periods with, for instance, a large wind power production. Thus, the alternative might be to stop some wind turbines.

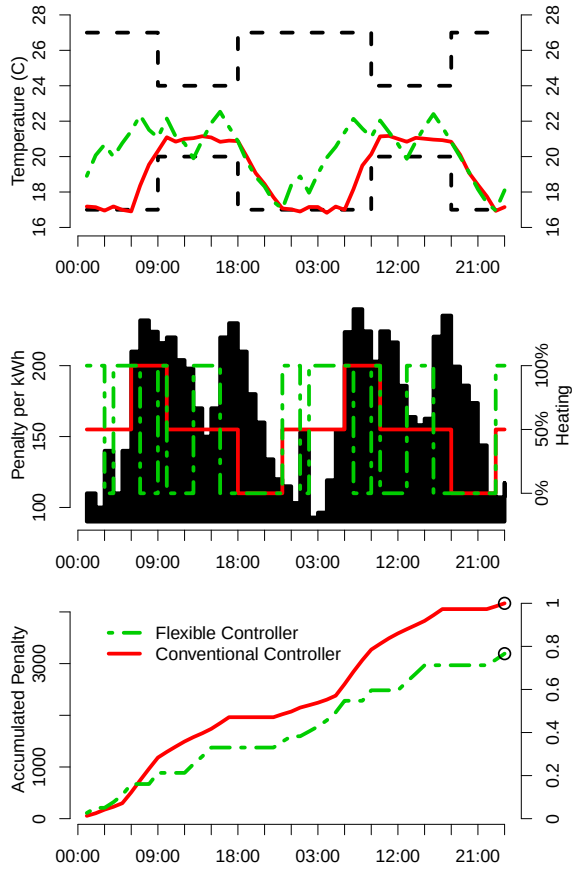

Figure 2: Top plot: An example of the temperature in a building controlled by a penalty-aware controller (green, dashed) and a conventional controller (red, solid). Both controllers are restricted to stay within the dashed lines. Middle plot: The black shading gives the penalties, while the green and red lines show when the two controllers heat, respectively. Bottom plot: These graphs illustrate the accumulated penalty for each of the controllers.

2.2. The Flexibility Function

The principles described in this paper can be used for any power-related flexibility. However, we will consider heating as

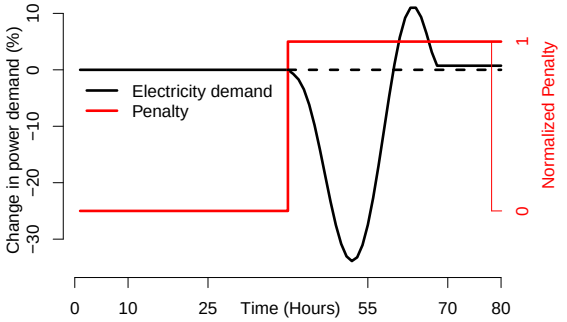

Figure 3: The expected change in energy consumption due to an increase in penalty for an indoor swimming pool. The red line shows the penalty while the black line shows the expected change in energy consumption.

an important example of a flexible power load. It is clear that a heating system can be turned off for some periods (minutes to hours) without any remarkable consequences on the thermal comfort. As flexibility is a dynamic phenomenon, the relationship between the penalty signal and the response must be described using a dynamic function. For simplicity, we assume that the building and the response to the penalty signal can be considered *linear and time-invariant*. Furthermore, we assume that the resulting load when exposed to a penalty signal can be separated into two parts; the load that responds to the penalty, and the non-responsive load R_t. In this case, the load (i.e., the response) Y_t at time t can be described as

$$Y_t = \sum_{k=0}^{\infty} h_k \lambda_{t-k} + R_t, \tag{1}$$

where $\{\lambda_t\}$ is the penalty signal, and R_t is the non-responsive consumption. Here, it is assumed that the penalty is constant between time steps. The length of the time steps can vary between a second and whole days, depending on the problem being solved. In the example illustrated by Figure 2, the penalty changes once every hour, and thus, in this case, it makes sense to let the time steps be equal to one hour. In continuous time, the convolution sum in Equation (1) is simply the convolution integral. In linear systems theory, see e.g., [31], the function $\{h_k\}$ is called the impulse response function. It reflects the effect of penalty on demand response after k time-steps. However, it is more appropriate to find the step response function, since it contains information about important characteristics of the system related to flexibility, as will be explained in Section 3.1. Thus, we define the FF as the step response function, i.e., by finding the expectation at time t when $\lambda_k = 0$ for $k < 0$ and $\lambda_k = 1$ for $k \geq 0$:

$$FF(t) = \sum_{k=0}^{t} h_k. \tag{2}$$

Figure 3 shows the estimated FF of a summer house with an indoor swimming pool located in Denmark. The swimming pool is being controlled using CO_2 intensity in the Danish power grid as penalty signal. The set-up is described in [39]. It is seen how the energy demand drops shortly after the penalty increases, since heating of the swimming pool, in this case, will usually be turned off. After a while, the energy demand starts increasing, since as time continues, to avoid the temperature dropping too low, the heating has to be resumed. At some point in time, the energy demand exceeds the initial level prior to the increase in penalty to bring the temperature back to the initial state. Later, the energy demand comes to rest at the energy demand prior to the increase in penalty. Notice that the response is extremely slow due to occasional technical issues in the control setup resulting in occasional unresponsiveness of the heating system.

In this example the FF is estimated based on time series data consisting of penalties and the penalty responsive load. A similar result was obtained in [21] for residential buildings. Alternatively, the FF can be found from first principles by setting up a detailed model of the systems, its constraints, occupancy behaviour, controllers and boundary conditions. Such a simulation-based approach has been used in e.g., [16–18]. In general, we might need to consider varying coefficient models where the flexibility depends on external variables like the ambient air temperature. Varying coefficient models can be written as

$$Y_t = \sum_{k=0}^{\infty} h_k(\theta) \lambda_{t-k} + R_t, \tag{3}$$

where θ is given by the external variables. As an example the ambient temperature has a large impact on the flexibility, since the heating/cooling system can only provide flexibility when the respective need is verified. The relationship can be estimated through e.g., non-parametric kernel estimation [40, 41]. Using Equation (2), it is straightforward to define the FF in the nonlinear and time-varying cases as well. It is also to be expected that the FF, due to physical changes in e.g., buildings and electrical grid, changes over time. Thus, the models should also be adaptive as described in [31, 42].

3. Applications of the Flexibility Function

In this section it is shown how characterizing the FF can be used to differentiate between different kinds of flexibility. It is, then, described how the FIs, that quantify usefulness of flexible systems in different settings, can be computed based on the FF. Lastly, a brief description of how the FF can be used to perform ancillary services is presented.

3.1. Characterizing the Energy Flexibility

Most commonly, the time constants constitute the main part of characterizing the energy flexibility [34, 43, 44]. Indeed, this is an important parameter. For instance, the illumination of a room has a very small time constant, since the full effect of illumination from turning light-bulbs on or off happens almost immediately. On the contrary, the heating of a swimming pool, due to its thermal dynamics, has a large time constant. However, only the information about the time constants of a system is not sufficient to fully characterize and quantify its energy flexibility. Again, referring back to the swimming pool, it is not

particularly flexible if the heating equipment is sized in such a way that it needs to run all the time, since in this case it can never be switched off to provide flexibility. However, as heating systems are usually sized to cover the maximum load on the coldest day, the swimming pool has excess heating power throughout most of the year. This excess heat pump capacity, then, is able to provide all the heat the swimming pool needs in a short time span. Thus, the heating time can, to some degree, be chosen to match when it is most beneficial to do so.

Six characteristics for the FF, termed hereinafter as the Flexibility Characteristics (FC) as shown in Figure 4, are identified as follows:

- τ (Time): The delay from adjusting the energy price and seeing an effect on the energy demand. 0.5 in the example.
- Δ (Power): The maximum change in demand following the penalty change. 0.2 in the example.
- α (Time): The time it takes from the start in change in demand until it reaches the lowest level. 0.6 in the example.
- β (Time): The total time of decreased energy demand. 2 in the example.
- A (Energy): The total amount of decreased energy demand.
- B (Energy): The total amount of increased energy demand.

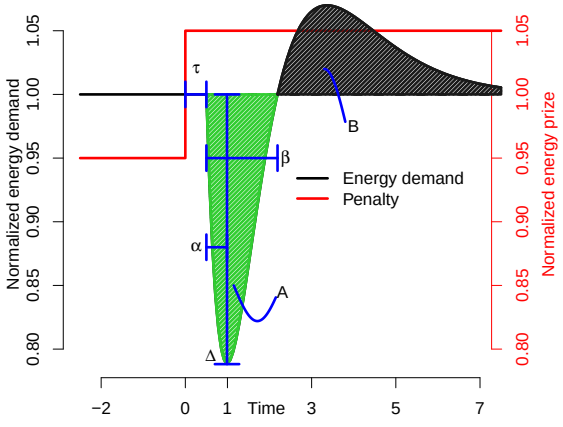

Figure 4: Flexibility Characteristics.

These FC describe how feasible control strategies can be constructed. For example, Δ has to be larger than the adjustment that one wants to make, while β has to be greater than the amount of time that one wants to adjust the demand. If the effect of the control needs to happen quickly, then, it is important to have a small τ and α. Similarly, it is of great interest to consider **A** since it gives how much demand one can move in total. The size of **B** is related to the loss in efficiency that one can expect when utilizing flexibility. These characteristics are useful for determining what kind of renewable energy sources can be used to integrate, as shown through a case study in Section 4. The FC also gives the feasibility of participating in different energy markets. For example small values of τ and α enable participating in balancing markets while **A** is more important for participating in day ahead markets. However, currently participation in these markets requires much more than one building. A proposed solution to this problem is to aggregate buildings in a district or buildings connected to a district heating network [45]. One of the advantages of this characterization is that the aggregated flexibility of several buildings is given by estimating the FF from their combined energy usage. Alternatively the additivity of the FF, allows the aggregated FF to be found by summing the individual FFs. The FC are readily obtained from the aggregated FF. This means that the exact same methodology can be used for the individual buildings and districts of buildings alike. Notice that the time constants of the individual buildings are not assumed to be equal. Indeed, a district of buildings can consist of a mix of well-insulated buildings with large time constants and poorly-insulated buildings with smaller time constants. If a district of buildings is provided with the same penalty signal, then the aggregated FF is of interest. In general, the grid operator requires FFs in the same or higher spatial resolution as that of the penalty signals. If penalty signals are constant within districts of buildings, then, it is the accumulated energy demand and flexibility that is of interest, and thus it makes sense to estimate the aggregated FF.

3.2. Flexibility Indexes for Buildings

This section introduces the concept of a FI, which combines the penalty signals from Section 2.1 and the building's FF from Section 2.2. The motivation for introducing a FI is that it communicates the *value* of utilizing the flexibility dependent on its purpose, e.g., cost minimization or CO_2 minimization. Moreover, while the FC defined in Section 2.2 have clear value for engineers and researchers in a design and control context, this FI is expected to be easier to interpret for a wider audience, such as end-users and legislative bodies.

Seen from the building owners' perspective, their benefit of utilizing buildings' flexibility is determined by the cost savings that is achieved by utilizing it. This leads to the Expected Flexibility Savings Index (EFSI). On the other hand, from the grid operators' point of view, their benefit of utilizing buildings' flexible resources is to know how much of their request/need for demand response can be activated. In this case, the penalty signal could be linked to wind availability, peak load reduction, or balancing of the electrical grid, etc., yielding the FI.

The most accurate way to identify a FI is to have two identical buildings with identical usage behavior; for one performing the control based on penalties while letting the other be penalty-ignorant. The ratio between the accumulated penalties would then tell us how large the relative savings would be. This is, however, not feasible in practice. Instead, we propose that the FI for buildings can be assessed by simulating its operation by using the FF with both penalty-aware and penalty-ignorant controllers, and comparing the accumulated penalty of the two. If, for instance, the penalty is the real time electricity cost, then the

index will show how large savings one would be able to achieve. What the test really shows is how much the smart building (thermal mass, controllers, etc.) is able to react to the penalty signal.

In summary, two different FIs are suggested. The first index is related to the actual penalty, and hence to the actual costs. The second index is based on a reference penalty designed to test certain characteristics. The FIs are:

- *Expected Flexibility Savings Index*: This index is related to actual costs, meaning that an EFSI equal to 0.10 implies that the expected savings for the actual smart building is 10%. A drawback of this definition is that it depends on the actual level of the penalties, and it might be difficult to get an EFSI larger than, say, 0.25.
- *Flexibility Index*: This index is related to reference penalties and these reference penalties will be designed such that the FI will be able to take values between zero and one. If, for instance, we are focusing on a flexibility for peak shaving, then this alternative definition could lead to a FI equal to 1 if power consumption in the peak periods is avoided completely.

Both indexes are calculated using the same procedure which is described in the following, exemplified by the FI. The FI uses the reference penalty signal, λ, and consists of the following steps:

1. Let λ_t be the penalty on the energy consumption at time t.
2. Simulate the control of the building *without considering* the penalty, and let u_t^0 be the energy consumption at time t.
3. Simulate the control of the building *considering* the penalty, and let u_t^1 be the energy consumption at time t.
4. The total operational cost of the penalty-ignorant control is given by $C^0 = \sum_{t=0}^{N} \lambda_t u_t^0$.
5. Similarly the operational cost of the penalty-aware control is given by $C^1 = \sum_{t=0}^{N} \lambda_t u_t^1$.
6. Then the quantity

$$FI = 1 - \frac{C^1}{C^0} \tag{4}$$

gives us the fractional amount of saved weighted cost, and this is the suggested FI.

If the penalty signal, λ, is the actual cost (like real-time price or CO_2), the calculation procedure leads to the EFSI instead of the FI. The controller in a smart building must be able to respond to the external penalty signal. If the controller is unable to do so, then $FI = 0$. An example of the procedure can be seen at the bottom of Figure 2, where the accumulated cost is shown. The flexible controller accumulates around 80% of the regular controller cost, and thus for this particular building and penalty signal $EFSI = 0.2$. Indeed, it is seen that the ability to estimate the long-term expected savings is due to the transient behavior being included in the FF. Static flexibility representations lack this quality, which means that the same approach is not applicable for them.

The penalty signal for calculating the FI should be long enough to include relevant seasonal effects. Most renewable energy resources includes yearly variations, and to capture this, the time period chosen for the case study is one year. The penalty signals can be designed as typical scenarios for e.g., the CO_2 variability for the considered area, as done in Section 4. In Denmark, a typical scenario should be related to the variability of wind power, and wind might be present or missing for 1-3 days, as shown by Figure 6. For countries with a lot of solar power, the scenario should be linked to the truncated harmonic variation of solar power, and hence the low penalty should be around say 8 hours. For countries like Norway, with a lot of hydro power, but where the typical morning and afternoon peak load is covered by fossil sources, the penalty should be around say 2-3 hours. In fact this illustrates that the suggested concept could be used to create a FI for buildings optimized for wind power, solar power or optimized for peak shaving for a couple of hours.

3.3. Ancillary services

Problems related to frequency, voltage, and congestion have historically been solved by the supply side. However, according to [46] recent increases of e.g., PV integration mean that local demand side flexibility is required. In this scenario, traditional transactional solutions are ill-suited for the fast activation of flexibility required for proper grid management and therefore other approaches should be introduced. For instance, it is suggested by [46] to perform ancillary services by adjusting the electricity price for the loads causing the problems. This corresponds to penalty-based control of the load, where the penalty is chosen as the solution to specific problems. For example in case of voltage magnitude regulation, a problem formulation could be

$$\arg\min_{\lambda_t} \left\| f\left(\sum_{k=0}^{\infty} h_k \lambda_{t-k}\right) - v_{ref} \right\| + \alpha \|\lambda_t - \lambda_{ref}\|,$$

where λ_t is the penalty at time t, v_{ref} is the nominal voltage and f is a function mapping the load to voltage. The first term describes the cost of violating the nominal voltage level, while the second term ensures that the penalties do not deviate too much from the nominal level, λ_{ref}. α determines how much weight is put on each of the objectives. The coefficients h_k, used to determine the load as a function of penalty, are given by the FF. Thus, the penalty provided for each area is determined by its FF. Similarly, frequency and congestion problems can be solved the same way. Another major advantage of this method over the transactive energy approaches, is that it only needs one-way communication to send the penalty signals, compared to the two-way communication needed to negotiate prices.

4. Case Study

This section demonstrates how different FFs enable the utilization of flexibility toward integrating various types of renewable energies. Three theoretical FFs are shown in Figure 5. For the sake of simplicity assume that these represent three buildings, having vastly different FC. Building 1 is able to move the largest amount of energy, while Building 3 is able to move the

least. On the other hand, Building 3 is able to respond faster than the other two. Building 2 is somewhat in the middle. We can also consider a combination of the buildings, which is easily as the average of the FFs.

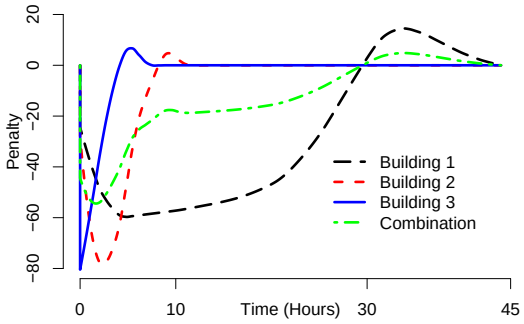

Figure 5: The Flexibility Function for three different buildings.

Let us consider, how well each building performs in environments dominated by different kinds of renewable energy, namely wind, solar, and hydro power. For wind and solar power, we have used the production of 2017 in Denmark to make penalty signals inversely proportional to the amount of produced wind or solar power. Hydro power can be controlled and thus, it does not experience the same kind of problems as wind and solar. The problems still experienced are mainly due to large ramps in demand during the morning and afternoon hours. Therefore, a penalty signal based on these ramps has been constructed from the 2017 data obtained from the Norwegian power grid [47].

A period of the penalty signals can be seen in Figure 6. The daily variation is seen for the solar penalty, and since the period is during the winter where the solar power production is large only for short periods of the day. The wind penalty starts at zero due to the period starting with windy weather. Then, it changes for a couple of days where apparently the wind power production is small. However, after this period, we see almost three days of zero penalty, which means that there were lots of wind. The ramp penalty remains close to zero with only a few peeks when the ramp in demand was large. This snapshot of the data is representative of the penalty signals in general, where in short: wind is dominated by low frequency variation, solar by 24-hour variation, and ramp by few sudden spikes.

Computing the EFSI as described in Section 3.2, Table 1 quantifies how well each of the buildings' flexibility is utilized in the integration of wind power, solar power, and dealing with ramping problems, respectively. It is seen that the EFSI is heavily dependent on the penalty signal, to the extent that for each penalty signal a different building is the most flexible. Building 1 is able to make the most of the wind penalty, since it is the only building that is able to sustain a demand response on a time scale similar to that which the wind penalty changes on. For the solar and ramp penalties it does not matter that Building 1 is able to sustain the demand change for such a long time, since these two penalties change much more frequently. In fact,

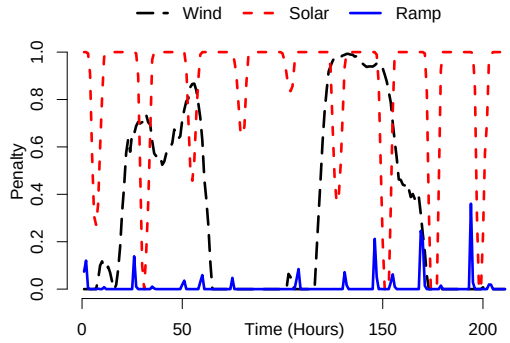

Figure 6: Penalty signals based on wind and solar power production in Denmark during 2017. Ramp penalty based on Consumption in Norway during the same period.

the response of Building 1 is so slow that usually it is not able to react to the changes in penalty when based on solar or ramp. For these two penalty signals the faster speed at which Building 2 and 3 can react with is critical. In the end, the solar penalty is slower than the ramp penalty making it better suited for building 2 that can sustain its response for a while, while the very fast variations in the ramp penalty can only be captured by the fast response of Building 3. Due to the linearity of the FF, the combination of each of the buildings simply obtains FIs equal to the average of the buildings. The swimming pool obtains low scores due to the technical issues in the control setup, but is still able to provide some flexibility for the wind-based penalty scenario.

Table 1: Expected Flexibility Savings Index (EFSI) for each of the buildings and the swimming pool based on wind, solar and ramp penalty signals.

	Wind (%)	Solar (%)	Ramp (%)
Building 1	11.8	4.4	6.0
Building 2	3.6	14.5	10.0
Building 3	1.0	5.0	18.4
Combination	5.4	8.0	11.5
Swimming Pool	3.5	2.7	0.6

To get the FI we use simple deterministic reference scenarios that represent the issues related to ramps and integration of wind and solar power. Examples of this can be seen in Figure 7. The wind penalty is constant for 36 hours, alternating between 0 and 1. The sun penalty is equal to 0 for 8 consequent hours each day and 1 otherwise, while the ramp penalty is equal to 0 all the time except for two periods of two hours each, every day, where it is equal to 1. These signals are simple, and more sophisticated signals can be developed to better represent reality. However, by repeating these signals and simulating each of the buildings' response, we compute the FI based on these scenarios and obtain Table 2. Comparing with Table 1, the trend is similar except that the numbers are approximately 3 to 4 times larger. This means that even these very simple reference penalty signals are sufficient for testing the energy flexibility. Furthermore, the reference scenarios indicate how close the building is

to reaching the limit of what is possible for the given reference scenario. For example, we see that Building 3 achieves a FI of 71% of the maximum amount of possible energy flexibility when it comes to the ramp-based penalty.

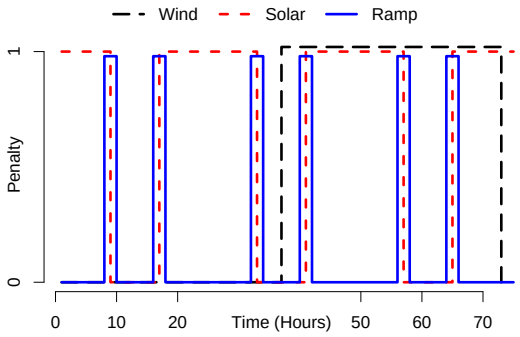

Figure 7: Reference scenarios of penalty signals related to ramping or peak issues as well as the integration of wind and solar power.

Table 2: FI for each of the buildings and the swimming pool based on reference penalty signals representing wind, solar and ramp problems.

	Wind (%)	Solar (%)	Ramp (%)
Building 1	35.1	7.2	18.9
Building 2	10.3	24.0	37.5
Building 3	4.9	11.1	71.0
Combination	16.8	14.1	42.5
Swimming Pool	8.1	4.0	2.8

5. Summary and Future Work

Planning and control problems experienced in power systems, when integrating considerable amounts of fluctuating renewable energy resources, call for a paradigm shift to a demand control approach. With buildings accounting for a considerable amount of global energy consumption, the energy flexibility offered by this sector can be used to implement required demand response measures. Taking this into consideration, this paper proposes an energy flexibility characterization methodology based on the presented flexibility function, which describes the reaction of a specific smart building, or cluster of smart buildings, to a penalty signal. The dynamic nature of the flexibility function enables it to be useful even when the system is not in steady state. Assuming linearity and time-invariance, the flexibility function contains all information about the relationship between the penalty signal and the resulting energy demand profile. Several important features of the flexibility function determine what kind of grid problems can be solved by the available energy flexibility, as demonstrated by the presented case study. In particular the flexibility index quantifies the overall effectiveness of utilizing the referred energy flexibility, in different scenarios.

In addition to the technical and operational applicability of the methodology, the flexibility characteristics and flexibility index are also used for labelling of energy flexible systems, such as buildings. This is an important step forward compared to previous static approaches. Flexibility labels can be obtained by defining standardized penalty signals and comfort intervals (for temperature, humidity, etc.). Under those standardized boundary conditions, results can be used for an inter-comparison of technologies, buildings or even districts in their potential energy flexibility. As such, the presented methodology can, for example, contribute to the development of the smart readiness indicator, which is currently being investigated as an amendment to the European Energy Performance of Buildings Directive [48] to assess the level of smartness of buildings.

Within the framework of the International Energy Agencies' Energy in Buildings and Communities Annex 67, the proposed energy flexibility characterization methodology will be further developed and evaluated. Specifically, more data will be collected to assess the described time invariance and linearity assumptions. Nevertheless, as shown in Section 2.2, time varying models are a natural extension. The nature of possible nonlinearities will have to be investigated, to decide on appropriate methods to deal with them.

Acknowledgment

The work has been carried out as a part of IEA EBC Annex 67 'Energy Flexible Buildings', CITIES, SmartNet, and the FME ZEN Centre. The authors are thankful to The Danish Energy Agency (EUDP), Innovation Fund Denmark, EU-H2020, and the Norwegian Research Council for the support. Furthermore, the presented work partially receives the support of the European Union, the European Regional Development Fund ERDF, Flanders Innovation & Entrepreneurship and the Province of Limburg. Finally, we acknowledge the members of IEA EBC Annex 67 for a lot of fruitful comments and suggestions.

References

[1] Paul Denholm and Maureen Hand. Grid flexibility and storage required to achieve very high penetration of variable renewable electricity. *Energy Policy*, 39(3):1817–1830, 2011.

[2] JM Morales, AJ Conejo, H Madsen, P Pinson, and Marco Zugno. *Integrating Renewables in Electricity Markets*. Springer, 2014.

[3] Henrik Lund and Ebbe Münster. Integrated energy systems and local energy markets. *Energy Policy*, 34(10):1152–1160, 2006.

[4] Mark O'Malley, Benjamin Kroposki, Bryan Hannegan, Henrik Madsen, Mattias Andersson, William D'haeseleer, Mark F McGranaghan, Chris Dent, Goran Strbac, Suresh Baskaran, et al. Energy systems integration: Defining and describing the value proposition. *Contract*, 303:275–300, 2016.

[5] Hamid Gharavi and Reza Ghafurian. Smart grid: The electric energy system of the future. *Scanning the Issue*, 99, 2011.

[6] Rasmus Halvgaard, Niels Kjølstad Poulsen, Henrik Madsen, and John Bagterp Jørgensen. Economic model predictive control for building climate control in a smart grid. *Innovative Smart Grid Technologies (ISGT)*, 30:270–278, 2012.

[7] J. Le Dréau and P. Heiselberg. Energy flexibility of residential buildings using short term heat storage in the thermal mass. *Energy*, 111:991 – 1002, 2016.

[8] Xiaosong Hu, Changfu Zou, Caiping Zhang, and Yang Li. Technological developments in batteries. *Ieee Power and Energy Magazine*, 15(5):20–31, 2017.

[9] Abdul Afram and Farrokh Janabi-Sharifi. Theory and applications of hvac control systems–a review of model predictive control (mpc). *Building and Environment*, 72:343–355, 2014.

[10] F. Tahersima, P. P. Madsen, and P. Andersen. An intuitive definition of demand flexibility in direct load control. In *2013 IEEE International Conference on Control Applications (CCA)*, pages 521–526, Aug 2013.

[11] Xiaohua Wu, Xiaosong Hu, Scott Moura, Xiaofeng Yin, and Volker Pickert. Stochastic control of smart home energy management with plug-in electric vehicle battery energy storage and photovoltaic array. *Journal of Power Sources*, 333:203 – 212, 2016.

[12] Henrik Madsen, Jacopo Parvizi, Rasmus Halvgaard, Leo E Sokoler, John B Jørgensen, Lars H Hansen, and Klaus B Hilger. Control of electricity loads in future electric energy systems. *Handbook of Clean Energy Systems*, 2014.

[13] Karen Byskov Lindberg. *Impact of Zero Energy Buildings on the Power System*. NTNU, 2017. Doctoral Thesis, 2017-35.

[14] Søren Østergaard Jensen, Anna Marszal-Pomianowska, Roberto Lollini, Wilmer Pasut, Armin Knotzer, Peter Engelmann, Anne Stafford, and Glenn Reynders. Iea ebc annex 67 energy flexible buildings. *Energy and Buildings*, 155:25 – 34, 2017.

[15] Glenn Reynders. Quantifying the impact of building design on the potential of structural storage for active demand response in residential buildings, 2015.

[16] Sebastian Stinner, Kristian Huchtemann, and Dirk Müller. Quantifying the operational flexibility of building energy systems with thermal energy storages. *Applied Energy*, 181:140–154, 2016.

[17] Frauke Oldewurtel, David Sturzenegger, Goran Andersson, Manfred Morari, and Roy S Smith. Towards a standardized building assessment for demand response. In *Decision and Control (CDC), 2013 IEEE 52nd Annual Conference on*, pages 7083–7088. IEEE, 2013.

[18] Roel De Coninck and Lieve Helsen. Quantification of flexibility in buildings by cost curves–methodology and application. *Applied Energy*, 162:653–665, 2016.

[19] Flexpower project. `http://www.ea-energianalyse.dk/projects-english/1027\_flexpower\_market\_design.html`, 2009. Accessed: 2017-12-20.

[20] Fred C Schweppe, Richard D Tabors, James L Kirtley, Hugh R Outhred, Frederick H Pickel, and Alan J Cox. Homeostatic utility control. *IEEE Transactions on Power Apparatus and Systems*, 99:1151–1163, 1980.

[21] O. Corradi, H. Ochsenfeld, H. Madsen, and P. Pinson. Controlling electricity consumption by forecasting its response to varying prices. *IEEE Transactions on Power Systems*, 28(1):421–429, Feb 2013.

[22] DJ Hammerstrom, R Ambrosio, J Brous, TA Carlon, DP Chassin, JG DeSteese, RT Guttromson, GR Horst, OM Järvegren, R Kajfasz, et al. Pacific northwest gridwise testbed demonstration projects. *Part I. Olympic Peninsula Project*, 210, 2007.

[23] Gianluca Fabio Dorini, Pierre Pinson, and Henrik Madsen. Chance-constrained optimization of demand response to price signals. *Ieee Transactions on Smart Grid*, 4(4):2072–2080, 2013.

[24] Glenn Reynders, Rui Amaral Lopes, Anna Marszal-Pomianowska, Daniel Aelenei, João Martins, and Dirk Saelens. Energy flexible buildings: An evaluation of definitions and quantification methodologies applied to thermal storage. *Energy and Buildings*, 166:372 – 390, 2018.

[25] Dirk Saelens Glenn Reynders, Jan Diriken. Generic characterization method for energy flexibility: Applied to structural thermal storage in belgian residential buildings. *Applied Energy*, 198:192–202, 2017.

[26] David Fischer, Tobias Wolf, Jeannette Wapler, Raphael Hollinger, and Hatef Madani. Model-based flexibility assessment of a residential heat pump pool. *Energy*, 118:853–864, 2017.

[27] Tian Liu, Bo Sun, Xiaoqi Tan, and Danny H. K. Tsang. Market for multi-dimensional flexibility with parametric demand response bidding. *North American Power Symposium*, 2017.

[28] J. P. Iria, F. J. Soares, and M. A. Matos. Trading small prosumers flexibility in the day-ahead energy market. *2017 Ieee Power and Energy Society General Meeting*, pages 5 pp., 5 pp., 2017.

[29] Winter package. `http://eur-lex.europa.eu`. Accessed: 2017-02-26.

[30] Henrik Madsen, Peder Bacher, Geert Bauwens, An-Heleen Deconinck, Glenn Reynders, Staf Roels, Eline Himpe, and Guillaume Lethé. Thermal performance characterization using time series data-iea ebc annex 58 guidelines. Technical report, Technical University of Denmark (DTU), 2015.

[31] Henrik Madsen. *Time series analysis*. CRC Press, 2007.

[32] Rasmus Fogtmann Halvgaard, Luca Vezzaro, M. Grum, Thomas Munk-Nielsen, Peter Tychsen, and Henrik Madsen. *Stochastic Greybox Modeling for Control of an Alternating Activated Sludge Process*, volume 8. DTU Compute, 2017.

[33] Niamh O'Connell, Pierre Pinson, Henrik Madsen, and Mark O'Malley. Economic dispatch of demand response balancing through asymmetric block offers. *IEEE Transactions on Power Systems*, 31(4):2999–3007, 2015.

[34] Niamh O'Connell, Henrik Madsen, Pierre Pinson, Mark O'Malley, and Torben Green. Regulating power from supermarket refrigeration. In *Innovative Smart Grid Technologies Conference Europe (ISGT-Europe), 2014 IEEE PES*, pages 1–6. IEEE, 2014.

[35] Nikita Zemtsov, Jaroslav Hlava, Galina Frantsuzova, Henrik Madsen, Rune Grønborg Junker, and John Bagterp Jørgensen. Economic mpc based on an lpv model for thermostatically controlled loads. *International Siberian Conference on Control and Communications (SIBCON)*, 2017.

[36] Majken Kirkegård Rasmussen, Mia Kruse Rasmussen, Nervo Verdezoto, Robert Brewer, Laura L. Nielsen, and Niels Olof Bouvin. Exploring the flexibility of everyday practices for shifting energy consumption through clockcast. *Australian Conference on Human-Computer Interaction (OzCHI)*, 29, 2017.

[37] New record-breaking year for danish wind power. `https://web.archive.org/web/20160125083857/http://energinet.dk/EN/El/Nyheder/Sider/Dansk-vindstroem-slaar-igen-rekord-42-procent.aspx`, 2015. Accessed: 2018-02-06.

[38] John Clauß, Christian Finck, Pierre Vogler-Finck, and Paul Beagon. Control strategies for building energy systems to unlock demand side flexibility – a review. *IBPSA Building Simulation*, 2017. `http://hdl.handle.net/10197/9016`.

[39] Dynamic co2-based control of summerhouse swimming pool heating. `http://smart-cities-centre.org/wp-content/uploads/CITIES-CO2-based-control-Demo-Project-Description.pdf`. Accessed: 2018-04-04.

[40] Vladimir Katkovnik and Ilya Shmulevich. Kernel density estimation with adaptive varying window size. *Pattern Recognition Letters*, 23:1641–1648, 2002.

[41] Henrik Madsen and Jan Holst. *Modelling Non-Linear and Non-Stationary Time Series*. 2006.

[42] Alfred Karsten Joensen, Henrik Aalborg Nielsen, Torben Skov Nielsen, and Henrik Madsen. Tracking time-varying parameters with local regression. *Automatica*, 36(8):1199–1204, 2000.

[43] Henrik Madsen and Jan Holst. Estimation of continuous-time models for the heat dynamics of a building. *Energy and Buildings*, 22(1):67–79, 1995.

[44] Glenn Reynders, Jan Diriken, and Dirk Saelens. Quality of grey-box models and identified parameters as function of the accuracy of input and observation signals. *Energy and buildings*, 82:263–274, 2014.

[45] Henrik Aalborg Nielsen and Henrik Madsen. Modelling the heat consumption in district heating systems using a grey-box approach. *Energy and Buildings*, 38(1):63–71, 2006.

[46] G. De Zotti, S. A. Pourmousavi, H. Madsen, and N. Kjølstad Poulsen. Ancillary services 4.0: A top-to-bottom control-based approach for solving ancillary services problems in smart grids. *IEEE Access*, 6:11694–11706, 2018.

[47] Statnett. `http://www.statnett.no/en/Market-and-operations/Data-from-the-power-system/Hydrological-data/`. accessed: 2018-02-08.

[48] EnergyVille-VITO, ECOFYS, Waide Strategic Efficiency, and OFFIS. Support for setting up a smart readiness indicator for buildings and related impact assessment. https://smartreadinessindicator.eu/, 2017-2018.

PAPER C

Designing Individual Penalty Signals for Improved Energy Flexibility Utilisation

Authors:
Rune Grønborg Junker, Rishi Relan and Henrik Madsen.

Published in:
IFAC Proceedings.

Designing Individual Penalty Signals for Improved Energy Flexibility Utilisation ⋆

Rune Grønborg Junker * **Rishi Relan** * **Henrik Madsen** *

* *Technical University of Denmark, Kgs. Lyngby, 2800 Denmark (e-mail: rung@dtu.dk, risre@dtu.dk, hmad@dtu.dk).*

Abstract: The energy flexibility associated with energy consumption must be exploited to accommodate more fluctuating renewable energy. The only solution that enables this without violating privacy concerns is penalty-based control, where penalty signals are designed to give incentives for the consumers to adjust their demand according to the needs of the grid. Designing the penalty signals is a challenging task due to different flexibility potential offered by various energy consuming systems. In this paper, it is shown that the best utilisation of energy flexibility requires individual penalty signals tuned towards the energy flexibility of each consumer. Here, we present a very simple yet novel approach for designing such individual penalty signals for each consumer, such that the value of the energy flexibility is increased, for both the grid operators and the consumers.

Keywords: Renewable Energy, Energy Flexibility, Flexibility Function, Step Response, Discrete Fourier Transformation.

1. INTRODUCTION

The ever-increasing share of renewable energy is helping to reduce the share of the electricity produced by fossil fuel based plants in electrical grids, but at the same time it is giving rise to new challenges related to operation of the grids. According to a recent study, approximately 40% of the global energy consumption is due to energy consumed by buildings (Lindberg (2017)). There are many sources which offer a great potential to provide demand response, defined as their energy flexibility. Perhaps the most obvious source for energy flexibility is batteries (Kneiske and Braun (2017)), that are explicitly designed to store energy. Batteries can act in a fast and efficient manner but they are very expensive (Lund et al. (2016)).

It is economically and environmentally much more viable to use already existing sources of energy flexibility (Dominković et al. (2018)), such as thermal mass of buildings (Dréau and Heiselberg (2016)); bodies of water such as domestic hot water tanks (Halvgaard et al. (2012)), district heating networks (Madsen et al. (1996)), or swimming pools (Zemtsov et al. (2017)). It is very attractive to use the energy flexibility offered by buildings in the design of future smart energy systems (Østergaard Jensen et al. (2017)). The main challenge in the design of the future smart energy systems is the proper utilisation of the energy flexibility. This is due to the varying nature of the energy flexibility offered by different types of buildings (Reynders et al. (2018)). For example, buildings differ in their thermal properties such as insulation and location of thermal mass; the energy consuming processes like ventilation and heating; the behaviour of occupants and their willingness to be flexible; and most importantly the installation of the automatic controllers which enable the activation of the demand response (Oldewurtel et al. (2013); Stinner et al. (2016); Coninck and Helsen (2016)). Moreover, the energy flexibility offered by different sources in buildings is available for different time-scales.

Additionally, some other challenges associated with the integration of renewable energy resources include frequency, ramping and grid balancing problems due to the fact that the availability of the electricity from renewable energy sources is dictated by weather conditions. Similarly, voltage problems are caused by prosumers injecting power into the grid and increased utilisation of the electricity is also causing problems, such as congestion, when many Electrical Vehicles (EVs) have to be charged at the same time in Distribution System Operator (DSO) grids.

To solve these problems and ultimately enable higher shares of renewable energy, energy demand response has been suggested in the literature. Within the field of energy demand response two main approaches exist; the direct control (Tahersima et al. (2013)) and indirect control (Corradi et al. (2013); Zhou et al. (2017)). The direct control approach consists of controlling electric appliances directly, while the indirect approach utilises incentives. The incentives can be formulated in terms of penalty signals, where the consumers should minimise their accumulated penalty. The most obvious kind of penalty is price, so that consumers minimise their total cost. Furthermore, in the indirect approach the demand response depends on grid location, if one wants to solve voltage problems and do congestion management.

For the current market structure usually the Balance Responsible Party (BRP) controls the prices received by

⋆ The authors would like to thank the Centre for IT–Intelligent Energy Systems (CITIES) project supported by Innovation Fund Denmark for the financial support needed to conduct the research reported in this paper.

the consumers, and thus they should design the penalty signals. However, the grid-problems are the responsibility of the Transmission System Operators (TSOs) and the DSOs. Therefore the communication would either have to be fast between the BRPs and these two parties, or the market structure would have to be changed such as to allow the TSOs and the DSOs to directly modify the penalty signals. In any case, the approach presented in this paper can help tailor the penalty signals regardless of the entities designing them.

As mentioned before, batteries provide short-term energy flexibility, while the thermal mass of swimming pools and district heating systems provide long-term flexibility. Some work has already gone into utilising this, by having several control loops, operating in different time resolutions, where the low resolutions are utilised for the balancing market and high resolutions for the regulation market (Fabietti et al. (2018)). However, while this approach does improve the utilisation of energy flexibility, it requires, for each device, a decision, in which market it should participate. Moreover, it only deals with differences in time scales, while ignoring other, potentially important Flexibility Characteristics (FC) such as the maximum effect and size of the rebound effect (Junker et al. (2018)). Therefore, in this paper, it is shown with a simple yet novel approach, how the penalty signals can be individually designed for different sources to improve utilisation of their energy flexibility while taking into account all the FCs.

The paper continues by introducing the methodology and evaluation criteria in Section 2. Then, Section 3 explains the novel algorithm to tailor penalty signals towards a specific kind of energy flexibility. An online version of this algorithm is introduced in Section 4. In Section 5 the designed penalty signals are evaluated, and conclusions are summarised in Section 6.

2. METHODOLOGY

In this section, we first explain briefly the methodology followed to design the individual penalty signals. Before proceeding towards the explanation of the methodology all the assumptions are stated explicitly below.

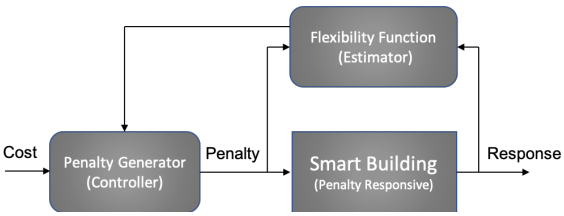

Fig. 1. A smart building is able to respond to a penalty or external control signal.

Assumption 1. *The systems under consideration (buildings) are assumed to be penalty-responsive energy systems as shown in Figure 1.*

Remark 1. *This implies that all consumers receive penalty signals that vary in time, that they respond to, such as to move their consumption away from periods with large penalties.*

Assumption 2. *The output response of the system to penalty signals is linear.*

Remark 2. *This implies that such systems can be characterised using their step-response function and that only the frequencies present in the input will be present in the output.*

Assumption 3. *All grid problems such as demand ramps, frequency/voltage deviations, demand-supply balance, etc. for each point in time, can be collected in a total cost, that quantifies all costs associated with consumed electricity.*

Remark 3. *One cost makes univariate control of the energy flexibility possible, which is much simpler and faster to implement in real-time than multivariate control for all grid problems.*

Remark 4. *Throughout the paper, signals will be referred to without subscripts, while the value at a specific point in time, is referred to using subscripts, i.e if u is a signal then u_n is the value at time n.*

The objective of the grid operators is to design penalty signals that make consumers impose the least total cost on the grid. As already discussed, the cost depends not only on time, but on the consumers location on the grid as well. This can easily be incorporated by first adjusting the cost function for spatial differences, and then considering one location at a time. It was demonstrated in (Junker et al. (2018)) that the value of energy flexibility can be quantified as the magnitude of the savings obtained by utilising the flexibility, i.e. the so-called Flexibility Index (FI). When utilising energy flexibility, it is important to keep in mind that the grid operators and consumers have different goals. Grid operators want to minimise grid costs, whereas consumers want to minimise their expenses. To evaluate the value of flexibility for both grid operators and consumers the FIs must be computed for both parties.

It is straight forward to do this for the consumers, if we assume that u^i is the penalty signal received by the i^{th} consumer and $y_n^i(u^i)$ is the power consumption of the same consumer at time step n, then the accumulated penalty $\mathcal{P}_{ac}$ at time $T > n$, which translates into the total cost for the i^{th} consumer, is given by

$$\mathcal{P}_{ac} = \sum_{n=0}^{T} u_n^i y_n^i(u^i). \tag{1}$$

The relative value of the flexibility is given by comparing $\mathcal{P}_{ac}$ to the normal operation $\mathcal{P}_0$, where penalty is not taken into account:

$$FI_i = 1 - \frac{\mathcal{P}_{ac}}{\mathcal{P}_0}. \tag{2}$$

For the grid operators, the cost is not related to the penalty signal, but to the grid cost. Thus, assume that λ_n^i is the cost imposed on the grid by the i^{th} consumer, when consuming energy at time step n. If there is a total of I consumers, then the FI for the grid is given by

$$FI_G = \frac{\sum_{i=1}^{I}\sum_{n=0}^{T} \lambda_n^i y_n^i(u^i)}{\sum_{i=1}^{I}\sum_{n=0}^{T} \lambda_n^i y_n^i(0)}. \tag{3}$$

It is worth mentioning that in this paper, both measures will be taken into account when evaluating flexibility.

3. DESIGNING INDIVIDUAL PENALTY SIGNALS

In (Junker et al. (2018)), it was also shown that the FI heavily depends on the penalty signal, meaning that a system might be considered very flexible in some scenarios, while not being particularly flexible in others. This fact is exploited here in a novel way to tailor penalty signals for each system. The key is to design penalty signals with time domain characteristics similar to the cost signal and with the same energy. This ensures that the signal is modified in such a way that each system is able to react more to it, but the energy flexibility is still utilised to solve the real problems such as the grid or consumer costs etc.

Suppose, that the consumption of building i at time n is given by the baseline consumption, μ_n, plus the effect of the penalty signal, u^i, as

$$y_n^i(u^i) = \mu_n + \sum_{k=0}^{N-1} h_k^i u_{n-k}^i. \tag{4}$$

Then the Flexibility Function (FF) (also called step-response function in time series analysis - see e.g. (Madsen (2008))) can be expressed in terms of the impulse response coefficients, $\{h_n\}_0^{N-1}$ by,

$$F(n) = \sum_{k=0}^{n} h_k, \quad \forall n \in \{0, 1, ..., N-1\}, \tag{5}$$

where N is the length of the impulse response of the system under consideration. The frequency response function can be simply obtained through the Discrete-time Fourier Transformation (DFT) of the impulse response coefficients:

$$\mathcal{H}(\omega) = \sum_{k=0}^{N-1} h_k e^{-\frac{ik}{N}\omega}, \tag{6}$$

where ω is the angular frequency. In short notation, this can be written as $\mathcal{H} = \mathcal{F}(h)$. It is important to note that the frequency-domain representation is equivalent to the time-domain representation, and time-domain representation can be obtained via the Inverse Discrete-time Fourier Transformation (IDFT), $h = \mathcal{F}^{-1}(\mathcal{H})$ given by

$$h_n = \frac{1}{N} \sum_{k=0}^{N-1} \mathcal{H}\left(2\pi \frac{k}{N}\right) e^{\frac{2\pi ik}{N}n}. \tag{7}$$

Similarly, if we define $Y = \mathcal{F}(y)$ and $U = \mathcal{F}(u)$, then

$$Y(\omega) = \mathcal{H}(\omega)U(\omega). \tag{8}$$

Equivalently this can be written as,

$$Y(\omega) = |\mathcal{H}(\omega)||U(\omega)|e^{i\angle\mathcal{H}(\omega)\angle U(\omega)}. \tag{9}$$

From this representation it is clearly seen that $|Y(\omega)| = |\mathcal{H}(\omega)||U(\omega)|$. This implies that the amplitude of the output signal at frequency ω is the amplitude of the same frequency in the input signal, scaled by $|\mathcal{H}|$. Thus, if we wish to increase the amplitude of the output, the power of the input should be focused around frequencies where $|\mathcal{H}|$ is large. The second part of (9) shows that the phase change from input to output at frequency ω is given by $\angle\mathcal{H}(\omega)$, where in this paper it is assumed that the phase has been unwrapped (Smith (2007)). So if the output signal should not be too delayed compared to the input signal, then the energy of the input signal should be concentrated around places where $\angle\mathcal{H}(\omega)$ is close to zero. Hence for each energy flexible system under consideration (in this case different buildings, see Section 5 for details), we can combine the amplification and the phase change to make a scaling function as described below:

$$S^i(\omega) = \frac{|\mathcal{H}^i(\omega)|}{c + \angle\mathcal{H}^i(\omega)}, \tag{10}$$

where c is a constant that determines how much weight is put on the amplification and on the phase change. As c goes to infinity all the weight is put on the amplification, while having c close to $\min_\omega \angle\mathcal{H}^i(\omega)$ puts all weight on having a small phase change. Using this scaling function, a penalty signal for system i can be designed by multiplying it unto the DFT of the cost signal, $\Lambda = \mathcal{F}(\lambda)$:

$$U^i(\omega) = S^i(\omega)\Lambda^i(\omega),$$

which can then be transformed back into the time-domain as $u^{i\prime} = F^{-1}(U^i)$.

Finally, the mean and the energy of the penalty signal is adjusted to match the original signal, so that it is only the shape that differs:

$$u^i = \frac{u^{i\prime} - a}{b}, \tag{11}$$

where a and b are chosen so that the

mean: (12)

$$\frac{1}{T}\sum_{n=0}^{T-1} u_n^i = \frac{1}{T}\sum_{n=0}^{T-1} \lambda_n^i, \tag{13}$$

and energy: (14)

$$\frac{1}{T}\sum_{n=0}^{T-1} (u_n^i - \bar{\lambda}^i)^2 = \frac{1}{T}\sum_{n=0}^{T-1} (\lambda_n^i - \bar{\lambda}^i)^2, \tag{15}$$

remains constant. The steps used to design a penalty signal for system i based on the grid-cost signal λ^i are summarised in Algorithm 1:

Algorithm 1 How to design individual penalties.

(1) Compute $\mathcal{H}^i = \mathcal{F}(h^i)$,
(2) Compute $S^i = \frac{|\mathcal{H}^i(\omega)|}{c+\angle\mathcal{H}^i(\omega)}$,
(3) Compute $u^i = \mathcal{F}^{-1}\left(\mathcal{F}(\lambda^i)S^i\right)$,
(4) Find a and b so that $u^i = \frac{u^i - a}{b}$ has mean and energy equal to λ^i.

Notice how λ^i was already adjusted to the location of consumer i (indicated by the superscript). The location-based penalty was then tailored towards the flexibility of the consumer, making a penalty signal that is ideal for both the flexibility *and* location of the consumer.

4. ONLINE IMPLEMENTATION

In the previous section, it was assumed that a full cost signal can be split into different penalty signals at once, but in reality we want to design penalty signals online, without knowing the future grid costs. Here, we address this issue and a simple solution using a sliding window is proposed. Results of this online approach are compared to the offline solution and discussed in Section 5.

In the previous section, we designed penalty signals from time 0 to time T, by using the original cost signal in the

same time interval. This means that u_n^i depends on λ_k for all $0 \leq k \leq T$, even if $n < T$. This violates the condition of causality, and means that in reality such penalty signals can only be designed for historical data. If the proposed approach needs to be useful for control, then the relation between u^i and λ^i must be made causal. Notice, how this is already the case for u_T^i, so the last value of the designed penalty signal could be useful in practice.

We can build on this fact, by designing the penalty signals for an interval of R time steps, $(n-R+1, n)$, but only use the last value of the designed signal, to get a penalty for time step n. The interval can then be moved one time step to $(n-R+2, n+1)$, to compute a new penalty signal, from which again only the last value is used. Now each value of the designed penalty signal only depends on the present and the last $R-1$ time steps. Compared to the previous approach, we only get one new value at a time, and thus will have to iteratively go through all time steps. The steps involved in the procedure for causal design of individual penalties, starting from time step $n = 0$ are summarised below in Algorithm 2:

Algorithm 2 Causal design of individual penalties.

(1) Compute $\mathcal{H}^i = \mathcal{F}(h^i)$,
(2) Compute $S^i = \frac{|\mathcal{H}^i(\omega)|}{c + \angle \mathcal{H}^i(\omega)}$,
(3) Compute $v^i = \mathcal{F}^{-1}\left(\mathcal{F}(\lambda^i_{n-R+1\cdots n}) S^i\right)$,
(4) Find a and b so that $v^i = \frac{v^i - a}{b}$ has mean and energy equal to $\lambda^i_{n-R+1\cdots n}$,
(5) Assign $u_n^i = v_R^i$,
(6) Increase n to $n = n+1$,
(7) Repeat from step (3).

5. RESULTS AND DISCUSSION

The case-study conducted in this paper is performed for the same three conceptual buildings, with vastly different FCs, as described in (Junker et al. (2018)). The FFs of the buildings are shown in Figure 2. It is clearly seen, how Building 1 is slow to respond to a step increase in the penalty, but is able to sustain the response for a long time, while Building 3 responds very quickly, but only for a short amount of time. Building 2 is somewhat in the middle.

Furthermore, the data used for the comparison is identical to that used in (Junker et al. (2018)), where penalty signals are constructed based on wind and solar production in Denmark and consumption ramps in Norway. However, here the time frame is extended to include all data from 10/11−2015 to 17/09−2018. Moreover, the penalty signals are combined to form a cost signal that weighs each of the three signals equally, and for this study it is assumed to represent the cost that consumption imposes on the grid. A part of these signals can be seen in Figure 3, where the morning and afternoon ramps in the Norwegian grid are apparent along with the diurnal cycle for the Photovoltaic (PV) production and the very slow varying nature of the wind power production. These penalty signals will collectively be referred to as the natural penalty signals.

For the sake of simplicity, in this paper, it is assumed that the grid cost signal is equal for each of the buildings

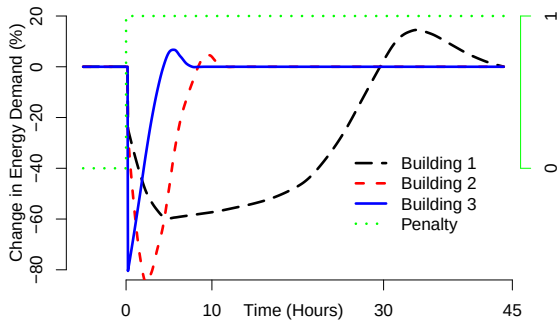

Fig. 2. The Flexibility function (FF) or step-response function for three different idealised buildings, with vastly different flexibility characteristics (FC).

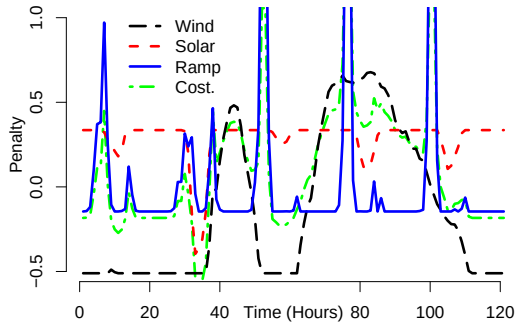

Fig. 3. Penalty signals based on wind production, solar production and consumption ramps are shown in black, red and blue respectively. The total grid cost signal is shown in green.

(i.e. $\lambda^i = \lambda^j$ for all i and j), so that only the combined consumption is of importance.

Initially the non-causal design introduced in Section 3 is considered, but before comparing it to the other method, the parameter c, must be tuned. The savings shown in Figure 4 are based on the grid costs and consumer costs for varying sizes of c. The dashed lines show the results for when only $|\mathcal{H}|$ is used, which corresponds to letting $c \to \infty$. On the y-axis the savings compared to having constant consumption are shown, which implies that larger values are better. It is clear that larger values of c lead to larger savings for both the grid and the consumers. Moreover, the savings seem to converge to that obtained for $c \to \infty$.

This observation implies that, when seen both from the perspective of consumers and grid operators, it is not useful to consider the delay at least for the simple models used here for the simulation. The delay is therefore disregarded, mathematically corresponding to letting $c \to \infty$ and practically obtained by replacing (10) and step (2), for both the offline and online algorithms, by the simpler expression

$$S^i(\omega) = |\mathcal{H}^i(\omega)|. \tag{16}$$

With this scaling function, the tailored penalty signals shown in Figure 5 are obtained. The penalty signal de-

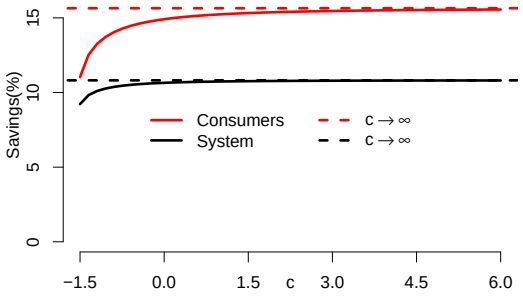

Fig. 4. Grid savings (equation (3)) and consumer savings (equation (1)), when using penalty signals designed according to algorithm 1, with varying sizes of c.

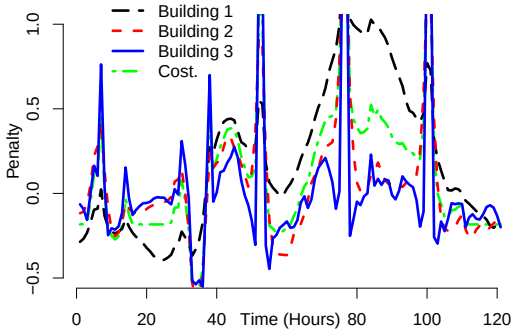

Fig. 5. Penalty signals, based on the cost signal shown in Figure 3, but tailored towards building 1, 2 and 3, using Algorithm 1.

signed for Building 1 is quite similar to the wind penalty, while that designed for Building 3 resembles the ramp penalty a lot. This fits with the findings reported in (Junker et al. (2018)), where it was shown that the largest savings are obtained when exposing Building 1 to the wind penalty, Building 2 the solar penalty and Building 3 to the ramp penalty.

Now that we have tailored penalty signals specifically to each of the buildings they should outperform the natural penalty signals from Figure 3, so we include these in the comparison. Table 1 shows the savings for both consumers and the grid for each combination of penalty signals. The cost when using the designed signals is the same as what was shown by the dashed line in Figure 4. Most importantly, we see that the designed individual penalties yield the largest savings for both consumers and the grid. This means that there is no conflict of interest between consumers and grid operators. Moreover, each consumer is receiving the penalties yielding him/her the largest savings. It is worth noticing how the savings are equal for consumers and the grid, when the original cost signal is used as the penalty signal, since in this case the consumers are faced with the exact same cost as the grid. For the natural penalty signals, consumers save more than from the original cost signal, but the grid saves less.

Table 1. Flexibility Index (FI) for each of the buildings and the grid, when exposed to either the cost signal, the original penalty signals or the designed penalty signals.

	Original	Natural	Designed	Causal
Consumers	8.3 %	11.6 %	15.6 %	13.9 %
Grid	8.3 %	7.5 %	10.8 %	9.3 %

Up-till now it is shown that the designed signals offer great promise, but it is worth mentioning that these are designed in a non-causal way, and thus it is not possible to implement them in practice. The performance of the causally designed signals for FI for varying bandwidths, i.e. R is shown in Figure 6. The maximum savings are found for $R = 2$ years, with a local maximum at $R = 1$ year, which is no coincidence. The DFT results in spectral leakage when the length of the transformed data does not coincide with the periods of the signals (Proakis and Manolakis (2007); Pintelon and Schoukens (2012)). That is why the spectral leakage is minimised when the period is an integer amount of years, since renewable electricity production follows a seasonal pattern, mainly due to varying weather conditions. A hamming window was used for the shown results, to reduce spectral leakage.

For the consumers, it is not of particular interest to avoid spectral leakage, since it is of less relevance to consumers whether the designed individual signals are similar to the original cost signal or not. On the contrary, for the grid, if the penalty signals are not similar to the cost signal, then the consumers are not trying to minimise their consumption at the time of high grid costs. Thus, it is of high importance to the grid that the penalty signals are similar to the cost signal, so that the flexibility is used to solve the grid problems. For small values of R the savings are very sensitive to changes in R, and so, it would make sense to stay away from this region.

Figure 6 also shows the FI found for the original cost, natural and non-causal designed signals, and as it is clearly seen the causally designed signals do not result in quite as large FIs as the non-causal signals. On the other hand, using the causally designed penalty signals still result in larger savings than when using either the original cost signal or the natural penalty signals. Hence, for an online application, the causally designed signals should be used.

The last column of Table 1 shows the FIs for the causally designed signals using a window of $R = 2$ years, where an improvement of 5.6 % and 1 % can be seen for the consumers and system respectively, as compared to using the original cost signal.

6. CONCLUSION

Penalty-based control design of smart grids not only offers a good possibility to exploit the energy flexibility offered by various sources in full capacity but also helps in accommodating more fluctuating renewable energy sources in the grid. Design of the penalty signals for such a control-loop is a challenging task. In this paper, we have proposed a novel yet very simple frequency domain method for tailoring the penalty signals towards consumers. This, in turn facilitates each grid problem being solved by the consumers with the most appropriate kind of energy flexibility. It was shown

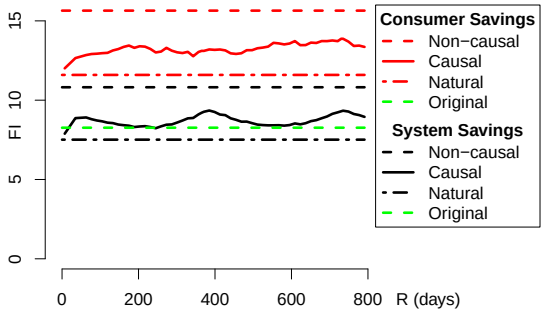

Fig. 6. Grid Savings (equation (3)) and consumer savings (equation (1)) for different penalty signals. For the causally designed penalties the bandwidth, R is varied.

that this tailoring of penalty signals towards the flexibility of consumers increases the savings from 8.3 % to 13.9 % for the consumers and 8.3 % to 9.3 % for the grid respectively. Finally, it was demonstrated how this simple approach can be combined with location-based penalties, so that the utilisation of energy flexibility can be maximised for grid specific problems. The other major advantage of the proposed approach is that it is computationally inexpensive, and can thus be used in real-time without any major modification.

REFERENCES

Coninck, R.D. and Helsen, L. (2016). Quantification of flexibility in buildings by cost curves – methodology and application. *Applied Energy*, 162, 653 – 665. doi: https://doi.org/10.1016/j.apenergy.2015.10.114.

Corradi, O., Ochsenfeld, H., Madsen, H., and Pinson, P. (2013). Controlling electricity consumption by forecasting its response to varying prices. *IEEE Transactions on Power Systems*, 28(1), 421–429. doi: 10.1109/TPWRS.2012.2197027.

Dominković, D., Dobravec, V., Jiang, Y., Nielsen, P., and Krajačić, G. (2018). Modelling smart energy systems in tropical regions. *Energy*, 155, 592 – 609. doi: https://doi.org/10.1016/j.energy.2018.05.007.

Dréau, J.L. and Heiselberg, P. (2016). Energy flexibility of residential buildings using short term heat storage in the thermal mass. *Energy*, 111, 991 – 1002. doi: https://doi.org/10.1016/j.energy.2016.05.076.

Fabietti, L., Qureshi, F.A., Gorecki, T.T., Salzmann, C., and Jones, C.N. (2018). Multi-time scale coordination of complementary resources for the provision of ancillary services. *Applied Energy*, 229, 1164 – 1180. doi: https://doi.org/10.1016/j.apenergy.2018.08.045.

Halvgaard, R., Poulsen, N.K., Madsen, H., and Jørgensen, J.B. (2012). Economic model predictive control for building climate control in a smart grid. *Innovative Smart Grid Technologies (ISGT)*, 30, 270–278. doi: 10.1109/ISGT.2012.6175631,.

Junker, R.G., Azar, A.G., Lopes, R.A., Lindberg, K.B., Reynders, G., Relan, R., and Madsen, H. (2018). Characterizing the energy flexibility of buildings and districts. *Applied Energy*, 225, 175 – 182. doi: https://doi.org/10.1016/j.apenergy.2018.05.037.

Kneiske, T.M. and Braun, M. (2017). Flexibility potentials of a combined use of heat storages and batteries in pv-chp hybrid systems. *Energy Procedia*, 135, 482–495. doi: 10.1016/j.egypro.2017.09.498.

Lindberg, K.B. (2017). *Impact of Zero Energy Buildings on the Power System*. NTNU. Doctoral Thesis, 2017-35.

Lund, H., Østergaard, P., Connolly, D., Skov, I., Mathiesen, B., Hvelplund, F., Thellufsen, J., and Sorknæs, P. (2016). Energy storage and smart energy systems. *International Journal of Sustainable Energy Planning and Management*, 11, 3–14. doi:10.5278/ijsepm.2016.11.2.

Madsen, H. (2008). *Time Series Analysis*.

Madsen, H., Nielsen, T.S., and Søgaard, H.T. (1996). Control of supply temperature. *Department of Mathematical Modelling, Technical University of Denmark, DK-2800 Lyngby, Denmark*.

Oldewurtel, F., Sturzenegger, D., Andersson, G., Morari, M., and Smith, R.S. (2013). Towards a standardized building assessment for demand response. In *52nd IEEE Conference on Decision and Control*, 7083–7088. doi: 10.1109/CDC.2013.6761012.

Pintelon, R. and Schoukens, J. (2012). *System identification: a frequency domain approach*. John Wiley & Sons.

Proakis, J. and Manolakis, D. (2007). *Digital Signal Processing*. Pearson Prentice Hall.

Reynders, G., Amaral Lopes, R., Marszal-Pomianowska, A., Aelenei, D., Martins, J., and Saelens, D. (2018). Energy flexible buildings: An evaluation of definitions and quantification methodologies applied to thermal storage. *Energy and Buildings*, 166, 372–390. doi: 10.1016/j.enbuild.2018.02.040. Cited By 4.

Smith, J. (2007). *Introduction to Digital Filters: With Audio Applications*. Music signal processing series. W3K.

Stinner, S., Huchtemann, K., and Müller, D. (2016). Quantifying the operational flexibility of building energy systems with thermal energy storages. *Applied Energy*, 181, 140 – 154. doi: https://doi.org/10.1016/j.apenergy.2016.08.055.

Tahersima, F., Madsen, P.P., and Andersen, P. (2013). An intuitive definition of demand flexibility in direct load control. In *2013 IEEE International Conference on Control Applications (CCA)*, 521–526. doi: 10.1109/CCA.2013.6662802.

Zemtsov, N., Hlava, J., Frantsuzova, G., Madsen, H., Junker, R.G., and Jørgensen, J.B. (2017). Economic MPC based on an LPV model for thermostatically controlled loads. *International Siberian Conference on Control and Communications (SIBCON)*. doi: 10.1109/SIBCON.2017.7998560.

Zhou, X., Dall'Anese, E., Chen, L., and Simonetto, A. (2017). An incentive-based online optimization framework for distribution grids. *IEEE Transactions on Automatic Control*, 63(7). doi:10.1109/TAC.2017.2760284.

Østergaard Jensen, S., Marszal-Pomianowska, A., Lollini, R., Pasut, W., Knotzer, A., Engelmann, P., Stafford, A., and Reynders, G. (2017). IEA EBC Annex 67 Energy Flexible Buildings. *Energy and Buildings*, 155, 25 – 34. doi:https://doi.org/10.1016/j.enbuild.2017.08.044.

PAPER D

Price-Based Modelling of Energy Flexibility applied to a Water Tower in the Scandinavian Electricity Market

Authors:
Rune Grønborg Junker, Carsten Skovmose Kallesøe, Jaume Palmer, Bianca Howard, Rui Amaral Lopes and Henrik Madsen.

Submitted to:
-

Stochastic Nonlinear Modelling and Application of Price-Based Energy Flexibility

Rune Grønborg Junker[a,*], Carsten Skovmose Kallesøe[b,c], Jaume Palmer[a], Bianca Howard[d], Rui Amaral Lopes[e,f], Henrik Madsen[a,g]

[a]*Technical University of Denmark*
[b]*University of Aalborg*
[c]*Grundfos*
[d]*Loughborough University*
[e]*Faculty of Sciences and Technology - NOVA University of Lisbon*
[f]*Center of Technology and Systems (CTS) - UNINOVA*
[g]*Norwegian University of Science and Technology*

Abstract

If CO_2-emissions are to be reduced, the shares of renewable energy sources will have to be significantly increased. However, energy flexibility is required to be able to cope with the increased shares of renewable energy. Utilising it necessitates mathematical models of the operational response of energy flexible consumers. In this paper we present an accurate and general dynamic model of energy flexibility based on stochastic differential equations. The intuitive interpretation of the parameters is explained, to show the generality of the proposed model. To validate the approach, the parameters are estimated for three water towers controlled by economic model predictive controllers. The model is then used to offer the energy flexibility on the current electricity market of Scandinavia, Nord Pool, using the so called "flexi orders". The energy flexibility is then used by controlling the demand of the water towers indirectly, through price signals designed based on the proposed model.

Keywords: Energy Flexibility, Demand Response, Flexibility Function, Stochastic Differential Equations, State Space Model

1. Introduction

Accompanying the ever increasing share of Renewable Energy Sources (RESs) is the challenge of controlling energy generation and matching it to the energy demand [1, 2]. Historically, demand has been the main source of uncertainty for energy grid operators [3], but now the challenge gets steeper with the uncertainty of RESs added to the equation. Furthermore, for electricity grids, the amount of synchronous generators is decreasing, limiting the available sources of control [4]. All in all, energy grids are faced with the challenge of increasing uncertainty and decreasing controllability. To counteract this, new ways of controlling either energy generation or demand have to be designed. On the generation side, it is possible to control RESs to some extent [5]. Unfortunately, while generation coming from energy sources such as wind and solar can be turned down, it can not be turned up, as it is limited by the given wind and radiation conditions. Thus, on the generation side, the only solution for providing electricity when sun and wind are insufficient is to produce it using other energy sources. Therefore, the controllability ought to be found on the demand side [6, 7].

Here, reducing demand has the same effect as increasing supply. Of course, the total amount of energy use is not expected to decrease, so reducing demand at one point in time translates into an increased demand during other periods. Furthermore, while it is easy to predict how much power a generator can supply [8], it is less straightforward to know how flexible energy demand can be. For instance, if the heating of a smart home is done in a flexible way, then the amount of flexibility varies depending on how it is being used [9]. If, for example, a home owner is having a party, then the range of allowed temperatures is probably smaller than if the owner was at work. This implies that the trouble resides not only in estimating how much flexibility is available, but also in agreeing on who is in charge of using it. The compensation required to persuade a home owner to have his heating being performed in a flexible way is highly dependent on the usage of the home [10]. Likewise, a system such as a wastewater treatment plant can provide a lot of energy flexibility most of the time, but during heavy rain it will be able to provide almost none [11], since it is more important to avoid waste water in the streets. For this reason, the owners of many energy flexible systems will not be willing to give up control to energy grid operators such as Distribution System Operators (DSOs) and Transmission System Operators (TSOs), since they can not trust the grid operators to know how to control the systems adequately. For this reason, most energy flexibility is expected to be made available through indirect price-based control [12–15]; in such cases, instead of controlling the energy flexibility directly, grid operators or aggregators will send varying prices to the energy flexible systems that they then react to as they please. It is still expected that energy flexible systems will be automatically controlled [16], but in the end the owner has full autonomy. This approach comes with its own challenges, such as what to do when no one wants to be

*Corresponding Author
Email address: rung@dtu.dk
Postal Address: Anker Engelunds vej 1, Building 101A, 2800 Kongens Lyngby, Denmark

flexible and the uncertainty of the response to changing prices. The challenge is to understand energy flexibility. This have been investigated using a bottom-up approach in [3, 17, 18]. However, while this gives insights into the physical capabilities of particular appliances, it does not address the fundamental challenge, namely to estimate the expected response for a given sequence of prices. This requires a top-down approach, where energy flexibility is estimated using system identification. In [19] this topic was explored, where the relation between prices and change in demand was assumed to be linear and time-invariant. This allows for easy interpretation of the energy flexibility through the step-response, termed the *Flexibility Function*.

However, the linearity assumption limits the possibility for applications significantly, and so, in this paper, a nonlinear, and more realistic, model of energy flexibility is developed, preserving the intuitive flexibility characteristics noted in [19]. The goal is the same; to characterise energy flexibility, but the method and resulting model are completely different, taking an idea and turning it into a useful tool.

The paper starts by presenting the developed model in Section 2, where the justification and interpretation of all parts are included as well. Next, a case study is presented in Section 3, consisting of three economically controlled water towers 3.1 located within the Scandinavian power market 3.2. In Section 4 the parameters of the developed model are estimated for the water towers 4.1 and subsequently the energy flexibility is bid into the day-ahead market of Nord Pool 4.2. Finally, the findings are summarised in Section 5 and perspectives for future work are discussed in Section 6.

2. Energy Flexibility Model

This section presents the complete model for characterising energy flexibility. Given the extent of this section, first the whole model structure is presented, and afterwards, each part is explained thoroughly.

The model is based on the variables presented in Table 1, where they have all been normalised to be between 0 and 1, to ease notation. The general formulation of the proposed model is given by (1)-(4):

$$\mathrm{d}X_t = \frac{1}{C}(D_t - B_t)\mathrm{d}t + X_t(1 - X_t)\sigma_X \mathrm{d}W_t, \tag{1}$$

$$\delta_t = l\left(f(X_t;\alpha) + g(u_t;\beta);k\right), \tag{2}$$

$$D_t = B_t + \delta_t \Delta\left(\mathbb{1}(\delta_t > 0)(1 - B_t) + \mathbb{1}(\delta_t < 0)B_t\right), \tag{3}$$

$$Y_t = D_t + \sigma_Y \epsilon_t \tag{4}$$

where W is a Wiener process [20**?**] and $\epsilon_k \sim \mathcal{N}(0, 1^2)$ *i.i.d.* $\forall k \in \mathbb{N}$. $\mathbb{1}$ is the indicator function, which is equal to 1 when the input is true and equal to 0 when the input is false e.g.:

$$\mathbb{1}(x > 0) = \begin{cases} 1 & x > 0, \\ 0 & \text{else.} \end{cases}$$

$C > 0$, $\Delta \in [0, 1]$, $k > 0$, $\alpha_i, \beta_i, \sigma_X > 0$ and $\sigma_Y > 0$ are parameters, that, together with the functions l, f and g characterise the energy flexibility of a price-controlled system. As summarised by Table 1, the model consists of 1 state, X, governed by the stochastic differential equation (1); B and u are inputs; Y represents the observations governed by equation (4); finally, two algebraic equations, (2) and (3), that link the value of the state and inputs to the output for each time step. An overview of the parameters and their interpretation can be seen in Table 2.

Table 1: Variables used for Flexibility Function.

Name	Quantity	Use	Unit
Y_t	Demand	Observation	Power
B_t	Baseline Demand	Input	Power
X_t	State of Charge	State	Energy
u_t	Energy Price	Input	Price

Table 2: Parameters of Flexibility Function and their interpretation.

Name	Interpretation	Unit
C	Amount of flexible energy	Energy
Δ	Proportion of flexible demand	Power
k	Energy flexibility eagerness	-
α	Demand-SoC relationship	-
β	Demand-Price relationship	-
σ_X	Process noise intensity	Power
σ_Y	Measurement noise	Power

2.1. The state equation

The interpretation of the state at time t, X_t, is the state of charge of the energy responsive system, where $X_t = 0$ means that it has no stored energy and thus can not reduce its energy consumption. Likewise, $X_t = 1$ means that it currently holds the maximum amount of energy possible, and thus can not increase its consumption. For a temperature-controlled building this could be translated into the temperature having reached the lowest or highest allowed comfort levels respectively. Even more straight forward, as shown in this paper, X_t could be proportional to the amount of water in a water tower, with $X_t = 0$ meaning that it is empty and $X_t = 1$ that it is full. The underlying assumption of the model is that, at a certain point in time, the energy demand of a price-responsive energy system is described by the price and state of charge at that time. Thus, (1)-(4) are simply predicting future values of the state of charge and the demand.

Assume that constant average prices would lead to a demand of B_t at time t, then this can be considered the baseline demand. If energy efficiency is unaffected by the energy consumption, then the state of charge increases whenever demand surpasses the baseline demand and decreases whenever the demand is lower than the baseline. This is described by the first term of (1), where the parameter C determines how fast the change in state of charge happens. As already mentioned it will be ensured that $0 < X_t, Y_t, B_t, u_t < 1$ $\forall t$, and since changing X_t from 0 to 1, in T time units, requires that $\int_0^T Y_t - B_t \mathrm{d}t = C$, the total amount of flexible energy is equal to C. Naturally, any

energy consuming system will have an upper bound on how much power it can consume at any given time, which is usually obtained by turning on everything at maximum capacity. Similarly there is a natural minimum consumption, which is usually when everything is turned off, or at least when all flexible components are turned off. For convenience Y_t can be assumed to be normalised such that $Y_t = 1$ means that the maximum demand is observed at time t and, similarly, the minimum when $Y_t = 0$. Now, the second term describes the process noise, which can stem from unexpected behaviour of the system, model deficiencies and errors in the assumed baseline demand; where, the latter is expected to be the main contributor in the system noise. These inaccuracies of the estimated baseline demand stem from the fact that it is not possible to know exactly what the baseline is. Notice that the exact same problem is experienced for today's energy systems, where the task of predicting demand is exactly the same as predicting baseline demand in this case. The noise intensity is proportional to the parameter σ_X, which is estimated, but also to the term $X_t(1 - X_t)$. The latter term is there to reflect that it is not possible for the state of charge to leave the interval $[0, 1]$, and thus the noise has to go to zero when the system approaches the edges of the interval, so that it can not push the state of charge out of bounds. This is a realistic assumption, since it is expected that prolonged high prices will push the state of charge close to the minimum and similarly prolonged low prices will push it close to the maximum with high certainty. On the other hand, with medium-sized prices, the exact state of charge is expected to be somewhere close to the middle, but it is very difficult to know exactly what it is.

2.2. Linking Demand to State of Charge and Price

Moving on to (2), δ_t can be interpreted as the change in demand from the baseline, due to energy flexibility. It is assumed that this is given by the state of charge, X_t, and energy price, u_t. In general, this can be expected to be a complicated and nonlinear relationship. However, the main expression can be split into two parts: one describing the effect of the state of charge, which is modelled by f; and another function, g, modelling the effect of the energy price. The reasoning behind this additive splitting lies in the fact that the variables, X_t and u_t, can reasonably be assumed to be uncoupled and affect δ_t independently; meaning that if, for instance, an energy system is controlled under a constant price, it should still be able to behave flexibly based only on its state of charge.

For the case of l, it is natural to model it in terms of a scaled logistic function:

$$l(x; k) = 2\text{logistic}(xk) - 1 = \frac{2}{1 + \exp(-kx)} - 1.$$

This way it is continuous and monotonously increasing while mapping all inputs to the interval $(0, 1)$. Then, $\delta_t = -1$ indicates that demand at time t is being limited as much as possible while $\delta_t = 1$ indicates that the demand is increased as much as possible. Also, $l(0; k) = 0$, so that $f(X_t)+g(u_t) = 0$ means that at time t demand is expected to equal the baseline. For f and g, it is also natural to require that they are continuous and monotonously decreasing, such that a higher state of charge or energy price will always lead to a lower expected demand and vice versa for lower state of charge or price. To ensure that X_t stays between 0 and 1 for all t, it is required that $f(1) + g(u) \leq 0\ \forall u \in [0, 1]$ and likewise $f(0) + g(u) \geq 0\ \forall u \in [0, 1]$. Recall that $g(u)$ is largest for $u = 0$ and smallest for $u = 1$; then, the boundary conditions are guaranteed by letting $f(1) = -g(0)$ and $f(0) = -g(1)$. This means that the desire to decrease demand due to having the largest possible state of charge is exactly equal to the desire to increase it due to the lowest possible price, and vice versa for lowest possible state of charge and largest possible price. Furthermore, since the parameter k controls how aggressively the price and state of charge are translated into changes in demand, the numerical magnitude of f and g is irrelevant, so without loss of generality it can be assumed that $f(1) = g(1) = -1$ and $f(0) = g(0) = 1$. Now the modelling task has been reduced to finding suitable functions that decreases continuously and monotonously from 1 to -1 for inputs between 0 and 1. Since the parameters have to be estimated the computational feasibility should also be taken into account. For g this is not a problem, since it is only a function of the input, but f is a function of the state, which severely limits the computationally feasible solutions.

By utilising that g is only a function of u it is modelled by a linear combination of I-splines [21]:

$$g(u; \beta) = -2\sum_{k=1}^{N_g} \beta_k I_k(u) + 1,\ \sum_{k=1}^{N_g} \beta_k = 1,\ \forall k = 1, 2, ..., N_g : \beta_k \geq 0,$$

where I are I-splines. In general, the I-splines are defined in terms of integrated normalised B-splines:

$$I_j(u; k, t) = \int_0^u M_j(x; k, t)dx,\ M_j(y|k, t) = \frac{B_j(y; k, t)}{\int_{-\infty}^{\infty} B_j(x; k, t)dx}$$

where $B_j(\cdot; k, t)$ is the j'th B-spline of a collection of k'th order B-splines with knots at t. Notice, that, since the B-splines have compact support, the I-splines equal exactly 0 for small inputs and exactly 1 for large inputs:

$$\exists a, b \in \mathbb{R}^2 : \forall x < a : I_j(x; k, t) = 0 \wedge \forall y > b : I_j(y; k, t) = 1.$$

The strength of this procedure comes from the fact that u_t is an input; thus, given that the variable is known, $I_k(u)$ can be computed for all $k \in 1, 2, ..., N_g$ before estimating the parameters. This reduces the task of estimating g to restricted linear regression, which can be done efficiently while estimating the rest of the parameters. Notice that the I-splines are chosen since they are monotonously increasing, and can be formulated such that $I_k : (0, 1) \to [0, 1]$. This, combined with the restrictions of β, ensures that g is monotonously decreasing and maps values to $[-1, 1]$, as required. The accuracy of the spline-based estimates depends on the location of their knots. Close to the knots accuracy is high, meaning that the data will be fitted closely. This is a virtue when there is enough data, but a disadvantage when there is too little, since the result will be overfitted. Thus, the knots should be placed far apart in data-sparse areas and close in data-rich areas. This can be done by locating them according to the quantiles in the data [21], and so, in this study

they are placed at the $(20\%, 40\%, 60\%, 80\%)$ quantiles of the price signal.

For f, the same method is not feasible, since the estimated values of the state, X, depend on the values of the parameter estimates, and thus the value of the splines would have to be re-estimated for each iteration of the parameter estimation. This has been obtained by parameterising f as

$$f(x,\alpha) = -\left\{2x - 1 + \alpha_1\left[1 - (2x-1)^2\right]\right\} \times \left(\alpha_2 + \alpha_3(2x-1)^2 + \alpha_4(2x-1)^6\right), \quad (5)$$

$$-1 \le \alpha_1 \le 1, 0 \le \alpha_2 \le 1, -1 \le \alpha_3 \le 1, -1 \le \alpha_4 \le 1, \sum_{k=2}^{4} \alpha_k = 1.$$

Notice that f is still monotonous. Additionally, if $x = 0$ or $x = 1$, then $(2x-1)^2 = (2x-1)^6 = 1$, thus the restriction of having $\sum_{k=2}^{4} \alpha_k$ in (5) ensures that $[\cdot] = 1$ if $x = 0$ or $x = 1$. Similarly, $\{\cdot\} = 1$ for $x = -1$ and $\{\cdot\} = -1$ for $x = 1$; thus, $f(0,\alpha) = 1$ and $f(1,\alpha) = -1$. Furthermore, for $\alpha_1 = 0$ and $x = 0.5$, $\{\cdot\} = 0$; while $\alpha_1 > 0$ makes f intersect with 0 for $x > 0.5$. Similarly, for $\alpha_1 < 0$, the intersection will take place for smaller values of x. In general, α_1 controls how skewed the relation towards the state of charge is. In addition, notice how, since $0 \le X_t \le 1$, and $\alpha_2 > 0$, then the main $(\cdot)$ is always between 0 and 1; thus, f is monotonously decreasing.

All exponents in expression (5) have been chosen to be positive so the parameterisation is symmetric around $x = 0.5$. It is important to notice how, an increase of α_3 and/or α_4 would make α_2 decrease. Thus, $(\cdot)$ gets small when x is close to 0.5. This results in a sub-linear price relationship. Likewise, having small values of α_3 and α_4 will result in having super-linear price relationships. The former would imply that the system cares little about the state of charge unless it is close to being empty or full; on the other hand, the latter suggests that the system mainly cares about whether the state of charge is above or below steady state, but not how much.

2.3. Demand and Observation Equation

Equation (3) represents the expected demand after a modification of the Baseline demand. Here Δ is a parameter between 0 and 1, describing what proportion of the overall demand that is flexible. If $\Delta = 1$ then all of it is flexible and $\delta_t = -1$ results in an expected demand of 0 while $\delta_t = 1$ results in an expected demand of 1 at time t. If $\Delta = 0$ then none of the demand is flexible and the expected demand is always equal to the baseline. If $\delta_t > 0$ then the third term is zero, and the deviation from the baseline is given by the second term. Notice how the change is proportional to $(1 - B_t)$, that is, the difference between the maximum demand and the baseline demand. This reflects how much demand that could potentially be switched on. If e.g. the baseline is close to 1, then the demand can only be increased a little, since it is not possible to increase demand more than having everything switched on at maximum capacity. The opposite is true when $\delta < 0$. In this case the change is proportional to B_t, reflecting that the potential maximum negative adjustment of demand is by switching off all demand. If again the baseline is close to 1, then it makes sense that there is potential to turn down the demand a lot.

(4) is the observation equation, describing that the observed demand will differ from the expected demand, due to both measurement errors and unexpected behaviour from the energy flexible system.

3. Case Study

To test the approach, a simulation of water supply networks delivering water to 3 smaller cites, is developed. Each of the local supply networks are composed of an elevated reservoir that introduces storage capacity in the network, and an Economic Model Predictive Control (E-MPC) that operates the pumping station supplying the local network. The E-MPC takes varying electricity costs when optimising the operation of the pumping stations, thereby creating a link to the electricity price optimisation considered in this paper.

3.1. Simulation model and local controller

The simulation model is developed using the pipe layout and reservoir size information from the water utility in Bjerringbro, Denmark. A small city with around 8000 inhabitants and one large industry (Grundfos). The structure of the system is shown in Figure 1.

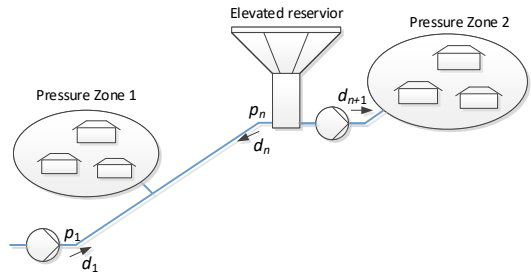

Figure 1: Sketch of the water supply network used as model of local energy consumers.

The consumption profiles for the two pressure zones are measured over a 2 month period in Bjerringbro and the obtained time series are used as input to a simulation of the network. The pipe networks in the pressure zones are obtained by simplifying the network layout of Bjerringbro by only considering what are expected to be the main water ways. The networks are simulated by solving the pipe pressures and flows for steady state conditions, meaning that the only energy storing element is the elevated reservoir.

The control of the pumping station 1 in Figure 1 is the concern of this paper. The local control is done using E-MPC minimising the operational cost still taking network constraints in the form of reservoir constraints and water quality constraints into account as described in [22].

To simulate the case where several utilities are controlled by the same energy price, two additional networks are included

in the simulation. These networks are derived by perturbation of main parameters in the Bjerringbro network model, that is, reservoir size and pipe resistances. Beside that, the consumer load profiles are differentiated between the networks by shifting the time series from Bjerringbro one and two weeks respectively for the two additional systems.

3.2. Flexi orders on Nord Pool

Currently, only a few possibilities for bidding flexibility into the power market exist. On the Scandinavian power market Nord Pool, the so called "flexi orders" are the most appropriate product for utilising energy flexibility on the day-ahead market. Flexi orders are submitted by indicating three things 1) a time interval, $[a, b]$ 2) an amount of hours, n 3) an amount of energy P. The flexi order is then accepted by finding the cheapest n hours within the time interval $[a, b]$. For each of these hours P energy is bought at the corresponding spot prices. This means that by using flexi orders one can buy electricity for the cheapest price within some interval at the cost of not deciding exactly what hours it will be [23].

Depending on how flexible the energy flexible system is, the length of the time intervals and amount of hours within them where electricity is needed can be adjusted. The most flexible case would be to have the time interval equal all 24 hours of the given day, and only purchase electricity in 1 hour. If the energy flexibility can handle this, then all demand can be bought during the cheapest hour of each day. Probably, for most systems it is more appropriate to split each day into several time intervals and request energy in some amount of the hours in these intervals. The longer the time intervals and the fewer hours of requested energy, the lower the price that the systems can expect to receive. Also, it is possible to buy some of the energy in a non-flexible way using regular hour-bids, and some of it using flexi orders. This can be used to cover non-flexible parts of the energy demand.

In this paper, the flexi orders are used by assuming that the total demand should equal the estimated baseline demand. In this way a proportion, κ_1, of the expected baseline demand is bought in each hour using conventional and non-flexible hour-bids. The remaining energy is bought using two flexi orders, each with an interval of 24 hours. For one of them energy is requested in 16 hours and for the second it is requested for 8 hours. In this way κ_2 and $1-\kappa_1-\kappa_2$ of the whole energy demand is bought. This means that if μ is the average hourly demand, then for the 8 most expensive hours, $\kappa_1 B_t$ is bought in hour t, this can be considered the inflexible part of the demand. For the 8 hours closest to the median price, $\kappa_1 B_t + \left(\kappa_2 \frac{24}{16}\right)\mu$ is bought and for the 8 cheapest hours $\kappa_1 B_t + \left(\kappa_2 \frac{24}{16} + (1-\kappa_1-\kappa_2)\frac{24}{8}\right)\mu$. This means that the pumps of the water towers are running to some extend at all times, but mostly in the cheap hours. Notice that even when the flexi orders are accepted such that the water towers can not deliver the sufficient amount of energy flexibility, it is not very expensive to use the balance market to make up for it. Optimising κ_1 and κ_2 is out of this papers scope, since it would require more data to avoid overfitting. Thus, simple values of $\kappa_1 = 0.6$ and $\kappa_2 = 0.3$ are used. This results in 40% of the electricity being bought using flexi orders, with $25\% + \frac{75}{2}\% = 62.5\%$ of this demand being bought in the 8 cheapest hours and the rest in the 8 intermediate hours.

Once the spot market has been settled, all participants know how much energy that they have bought for each hour, and the model can be used to design a price signal, which gives an expected demand equal or close to the amount of energy bought for each hour. This price signal is then sent to the water tower, and the local controller acts upon it. However, the real demand from the water towers is bound to deviate from the expected value, and thus there will be a difference between how much energy was bought and how much was consumed. This difference is paid for on the balance market, according to the regulation price [24]. The overall cost of running the water towers is then the cost of the energy bought on the spot market and the balance market:

$$\text{Cost} = \sum_{k=1}^{24} \lambda_k^{\text{Spot}} p_k + \sum_{k=1}^{24} \lambda_k^{\text{Regulation}} (Y_k - p_k). \tag{6}$$

Here, Cost is the cost of electricity consumption during one day, in which the spot and regulation price in hour k was λ_k^{Spot} and $\lambda_k^{\text{Regulation}}$ respectively, and where p_k energy was bought in hour k while the real demand in hour k was Y_k.

3.3. Estimating Parameters

Here the parameters of the energy flexibility model described in Section 2 will be estimated for the electricity consumption of the water pumps of the water tower. Before this can be done a number of issues have to be dealt with. First of all an objective function to be minimised is formulated in Section 3.3.1. Next, the baseline demand (i.e. B_t) is estimated in Section 3.3.2. Then, Section 3.3.3 deals with the challenge that the local water tower controllers anticipates future prices. Afterwards, a price signal for identifying the model parameters is designed in Section 3.3.4. Lastly, an optimisation method is chosen and described in Section 3.3.5

3.3.1. Objective Function

In this paper the model will be used to predict demand between 12 and 36 hours into the future. For this reason it has to provide accurate predictions on this time scale. While the classic maximum likelihood estimate is based on the one-step predictions, this often leads to parameter estimates which are poor for predictions much longer than the one-step predictions. The reason for this is that the maximum likelihood estimate is based on minimising the weighted squared residuals. The residuals are made up of bias and variance, in the sense that it can be assumed that each residual follows some distribution with a mean value μ and variance σ^2, that is $e \sim \mathcal{N}(\mu, \sigma^2)$. By definition of variance the expected value of the squared residual is then

$$\mathbb{E}(e^2) = \mathbb{V}(e) + \mathbb{E}(e)^2 = \sigma^2 + \mu^2, \tag{7}$$

where $\mathbb{E}$ and $\mathbb{V}$ denote the expectation and variance operators respectively. Here it is observed how the residuals consist of a variance or diffusion term, σ^2, and a bias or drift term μ^2.

In general, drift scales linearly with time while diffusion scales with the square root of time. Thus if e_n is a residual based on an n-step prediction, then

$$\mathbb{E}(e_n^2) \propto n\sigma^2 + n^2\mu^2. \tag{8}$$

From this expression it is clear that if (7) is used for parameter estimation, then the estimate will be equally focused on minimising σ and μ. But if the model is used for n-step prediction, then the performance is actually given by (8), in which it is n times more important to minimise μ than σ. Notice that usually it is assumed that $\mu = 0$, in which case the only thing that matters is to reduce σ. However, in practice it is almost never the case.

For this reason the estimation procedure used in this paper is the one described in [25]. Here the usual likelihood function based on one-step predictions is modified to instead consider predictions made from time 0, so that it consists of one n-step prediction for all $1 \leq n \leq N$, where N is the total amount of observations. The trade-off compared to using one-step predictions is that the residuals can no longer be assumed to be independent.

Thus, for the Stochastic Differential Equation (SDE)-based state space model formulation used in this paper

$$\mathrm{d}X_t = f(X_t, U_t; \theta)\mathrm{d}t + \sigma_X(X_t)\mathrm{d}W_t, \tag{9}$$

$$Y_k = X_{t_k} + \sigma_Y \epsilon_k, \tag{10}$$

the objective function is minimised for the parameter estimation is

$$F(\theta|\boldsymbol{\mathcal{Y}}_N, \boldsymbol{\mathcal{U}}_N) = \tag{11}$$

$$\sum_{k=1}^{N} \left(\underbrace{\frac{(Y_k - \hat{y}_{k|0})^2}{2\sigma_{k|0}^2}}_{\text{Weighted least squares}} + \underbrace{\log\left(\sqrt{2\pi\sigma_{k|0}^2}\right)}_{\text{Uncertainty penalty}} \right) - \underbrace{\log(p(Y_0|\theta))}_{\text{Initialisation}},$$

where θ contains the parameters of the model, as described in Table 2, $\boldsymbol{\mathcal{Y}}_N = \{Y_1, Y_2, ..., Y_N\}$ is the collection of the first N observations (energy demand), and likewise $\boldsymbol{\mathcal{U}}_N = \{B_1, B_2, ..., B_N, u_1, u_2, ..., u_N\}$ is the collection of the first N inputs (Baseline demand and energy price). $\hat{y}_{k|0}$ and $\sigma_{k|0}^2$ are the value and variance of the k-step prediction made at time 0, and are given by

$$\hat{y}_{k|0} = \mathbb{E}(X_{t_k}),\ \sigma_{k|0}^2 = \mathbb{V}(X_t) + \sigma_Y^2,$$

where the differential equations (12) and (13) describe how the mean and variance should be propagated:

$$\frac{\mathrm{d}\mathbb{E}(X_t)}{\mathrm{d}t} = f\Big(\mathbb{E}(X_t), u_t\Big), \tag{12}$$

$$\frac{\mathrm{d}\mathbb{V}(X_t)}{\mathrm{d}t} = A\Big(\mathbb{E}(X_t), u_t\Big)\mathbb{V}(X_t) + \mathbb{V}(X_t)A\Big(\mathbb{E}(X_t), u_t\Big)^\top + \sigma_X(X_t)\sigma_X(X_t)^\top, \tag{13}$$

where

$$A\left(\mathbb{E}(X_t), u_t\right) = \left.\frac{\mathrm{d}f(x, u_t)}{\mathrm{d}x}\right|_{x=\mathbb{E}(X_t)}.$$

3.3.2. Estimating Baseline Demand

The business as usual operation of the water tower, is to have a constant price, so that its only objective is to minimise energy consumption. As described by (3), the predicted demand when applying energy flexibility is given as a modification of the baseline demand. Thus, an estimate of the baseline demand is required for the methodology to function. Since this is a simulation study it would be possible to know exactly what the baseline demand is, by simply using the demand of the business as usual operation. However, as this is not possible in practice, it was chosen to test the methodology in a more realistic case, in which the baseline demand is not known with exact accuracy. The baseline was still estimated by simulating the system using a constant price, but instead of using the exact demand at all times as baseline demand, the average demand for each hour of the day was computed, for work days and for weekends. This results in two profiles of 24 values each. These provide reasonably accurate estimates of the baseline, since water consumption is well described by daily variation.

For retailers purchasing electricity on behalf of their consumers, their business as usual operation is to purchase electricity according to the predicted demand without trying to modify it. Since the estimated baseline demand is the best guess of the demand when energy flexibility is not applied, the retailer would simply purchase the estimated baseline demand.

3.3.3. Anticipating the Effect of Future Prices

The next issue is to deal with the fact that the E-MPC used to control the water towers uses forecasts of the price, to make its decisions. A realistic assumption for the use case presented in Section 3.2, is that the forecasts are 100% accurate between 12 and 36 hours ahead. The controller uses 24 hour forecasts, so it was chosen to provide it with the exact future prices during the parameter estimation process, since it should not effect the control actions significantly. Notice that if this were to be a poor decision it would only effect the results in a negative way, and thus this is not representing the methodology in an over-optimistic way.

For the parameter estimation it should be taken into consideration that the E-MPC sees future prices. For a particular time step, this can be boiled down to the E-MPC comparing the current price with the future prices. Prices in the near future are more important than further ahead in time, since it is easier for the E-MPC to move demand short periods than long periods. To account for this, a modified price signal, comparing the price at each time step to the future values was constructed as

$$u_t' = \Phi(u_t, \mu_t, \sigma_t^2),$$

where Φ is the cumulative distribution function of the normal distribution. That is, Φ gives the probability of a normally distributed random variable being smaller than the input:

$$\Phi(x, \mu, \sigma^2) = \mathbb{P}(X < x), \text{ where } X \sim \mathcal{N}(\mu, \sigma^2).$$

μ_t and σ_t^2 are weighted mean and sample variance of the price

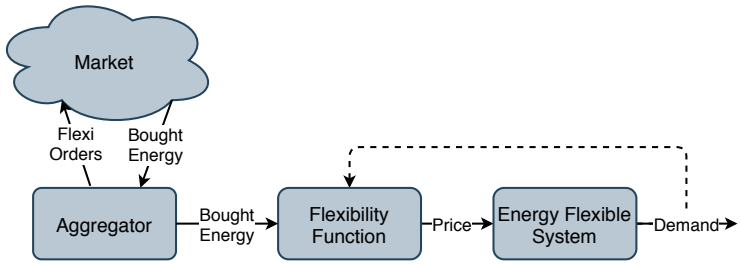

Figure 2: Information flow for using flexibility function to design price signals according to energy bought on the market

for the next $M = 24$ hours:

$$\mu_t = \frac{1}{\sum_{k=1}^{M} w_k} \sum_{k=1}^{M} w_k u_{t+k}, \quad \sigma^2 = \frac{1}{\sum_{k=1}^{M} w_k} \sum_{k=1}^{M} w_k (u_{t+k} - \mu_t)^2.$$

The weight is computed by exponential decay such that the first values receive the largest weight:

$$w_n = \gamma^{n-1},$$

where $0 < \gamma \leq 1$ decides how fast the exponential decay happens. This is a hyper parameter that should be tuned for the specific problem. In this case the value was found as the one given the largest negative correlation between price and demand, which in this case was $\gamma = 0.902$.

3.3.4. Price signal for system identification

Of course, a price signal has to be sent to the water tower, and this price signal has to be constructed. This should be done such that it excites the relevant frequencies for the system at hand. Since the water towerstakes several hours to fill or empty, it is expected that most dynamics are on a time scale of more then several hours. Thus the price signal should consist mainly of low-frequencies. In this study a uniform white noise signal is filtered through a low pass butterworth filter of degree 5 with a cut-off frequency of $\frac{1}{10h}$, meaning that most content with frequencies higher than $\frac{1}{10h}$ is removed from the white noise signal. Furthermore, if prices are designed based on the model it is expected that they often will include step-changes to drive the demand up or down as much as possible, so random step periods where the price was put equal to either the maximum or minimum price were randomly added to the signal.

3.3.5. Optimisation method

Notice that all terms in (11) are differentiable when applied to the formulation (1)-(4), except for the indicator functions, $\mathbb{1}(x > 0)$ and $\mathbb{1}(x < 0)$. Thus, these are replaced with the differentiable approximation

$$\frac{1}{1 + \exp(-\lambda x)} \approx \mathbb{1}(x > 0), \qquad \frac{1}{1 + \exp(\lambda x)} \approx \mathbb{1}(x < 0),$$

for large $\lambda > 0$.

This results in a differentiable objective function, and thus the software TMB [26] can be used to provide efficient evaluation of both the objective function and its gradient. These were used to minimise the function using the method of moving asymptotes [27]. By using the gradient the optimisation time is significantly reduced compared to usual methods that do not rely on the gradient.

3.4. Designing Price Signals for Control

Once energy has been bought, a price signal to make the consumption of the water towersfollow the amount bought, has to be designed, as explained by Figure 2. In this figure the aggregator first bids into the market using flexi orders and then receives the amount of energy bought for each hour. This is sent to the energy flexibility model, which is then used to find prices that makes the expected demand follow the amount of bought energy.

However, this is an inverse problem where it is easy to compute the expected demand given the price signal, but difficult to compute a price signal given the demand. Consider the expected demand at time t, D_t, from (3). This is a function of the baseline, B, and the price signal, u. The squared difference between the expected demand and a reference demand, D^{ref} can be minimised according to the price signal:

$$\underset{u}{\operatorname{argmin}} \sum_{k=1}^{M} \left(D_{t_k}(B, u) - D_{t_k}^{\text{ref}} \right)^2.$$

Doing so yields a price signal resulting in an expected demand as close as possible to the reference demand.

4. Results

In this section the parameters of the model defined by (1)-(4) are estimated and discussed in Section 4.1. Afterwards, in Section 4.2, the results of bidding energy flexibility into the spot market and simulating the operation of the water towerscorrespondingly are presented.

4.1. Parameter Estimates

Using the price signal designed in Section 3.3.4 modified according to Section 3.3.3, and the baseline demand estimated as in 3.3.2, the parameters are estimated by minimising (11), obtaining the values shown in Table 3. The time unit used here is 1 min, and the parameters should be interpreted according to this. It is noted that the estimate of C is 212, which means that

Table 3: Parameter estimates and 95%-confidence intervals for the energy flexibility model based on the electricity consumption of the pumps controlling the water towers.

Parameter	Estimate	CI
C	212	$[120, 303]$
Δ	1	-
k	2.1	$[1.8, 2.4]$
α_1	-0.07	$[-0.22, 0.21]$
α_2	0.88	$[0.42, 1.00]$
α_3	-0.88	$[-1.00, 0.04]$
α_4	1.00	-
β_1	0.55	$[0.47, 0.64]$
β_2	0.80	$[0.04, 0.12]$
β_3	0.25	$[0.19, 0.30]$
β_4	0.12	$[0.09, 0.14]$
β_5	0.01	$[0.0095, 0.0014]$
σ_X	0.087	$[0.050, 0.151]$
σ_Y	0.092	$[0.082, 0.103]$

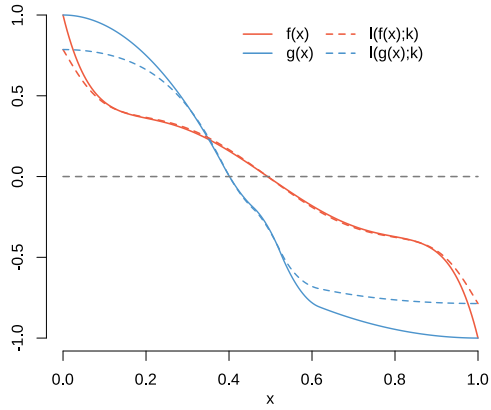

Figure 3: Functional relationships between the state of charge/energy price and energy demand.

it is estimated that all the water towers could could be filled in $\frac{212}{60} = 3.5$ hours without any demand. Perhaps more relevant, it is estimated to take $\frac{3.5}{0.41} = 8.6$ hours to fill it if the demand equals the average normalised demand of 0.41. Δ is estimated to equal 1, which is not surprising considering that the water towersonly has one energy consuming component, namely the pump which is being controlled according to the price. For α and β Figure 3 shows the functions f and g as solid lines, which gives the effect of the estimated state of charge and energy price respectively. For f, we observe that $f(0.5) \approx 0$, which means that the natural state of charge is 0.5, meaning that the water towers are usually filled around 50%, if there are no price incentives to do otherwise. For levels between 0.15 and 0.85 the effect is modest. For levels lower than 0.15 it quickly approaches 1, to make sure that there is always water available. Similarly for when the state of charge is above 0.85 it quickly converges to -1. This indicates that the controller does not care much about the exact level of the water, as long as it is between 0.15 and 0.85. For price, the relationship is not as symmetric, with 3 overall regions. When the price is between 0.2 and 0.55 there is a close to linear relation between between price and demand. For prices below 0.2, the effect is close to constant, slowly converging to 1. For prices above 0.55 the effect is very flat, with almost no effect of price. This indicates that the controller considers all prices above 0.55 to be expensive, but does not care about the exact value. Prices below 0.2 are considered cheap, and it will pump close to its maximal potential for all prices in this range. Between 0.2 and 0.55 it adjusts demand proportionally to the price.

The estimate of k is 2.1, which gives the responsiveness of the system. In Figure 3, the dashed lines show the change in demand purely caused by either state of charge or price. Larger values of k makes the effect go to -1 and 1 faster.

Figure 4 shows the predicted demand over the course of 3 days versus the measured demand. The estimated baseline demand is also shown. The difference between the baseline and the demand is due to the use of energy flexibility. The prediction corresponds well to the observations, especially for the first 24 hours. Considering that the model will not be used for predictions of more than 24 hours, this is satisfactory. The model explains most of the variation not explained by the baseline, reducing the root-mean-squared error of the baseline of 9.23 kWh to 3.99 kWh for the model.

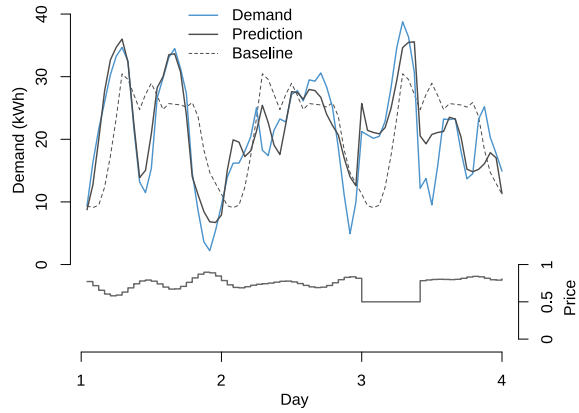

Figure 4: Predicted Demand compared to real demand.

4.2. Bidding Energy Flexibility into spot market

The energy flexibility of the water towers is sequentially bid into the spot market for 9 days using flexi orders as described in Section 4.2, and prices designed as described in Section 3.4 are sent to the water towers, which is then operated as explained in Section 3.1. A sample of the demand compared to the energy bought is shown in Figure 5. In this figure the prediction equals the bought energy, and it is seen that the actual demand follows quite well. The main deviations occur when the actual demand

Table 4: Costs of running three water tower, while being price-ignorant, using flexi orders and the potential when controlling the water towersdirectly according to spot prices.

Strategy	Costs $\left(\frac{\text{EUR}}{\text{year}}\right)$	Price $\left(\frac{\text{EUR}}{\text{MWh}}\right)$	Energy $\left(\frac{\text{MWh}}{\text{year}}\right)$
Baseline	44457	65.2	682
Flexible	42627 (-4.1%)	62.0 (-4.8%)	687 (+0.75 %)
Potential	42070 (-5.4%)	61.6 (-5.4%)	683 (+0.05%)

equals almost exactly zero or one, which is typically not anticipated by the model. In other cases the demand is similar to the prediction, and so the consumed energy fits well with what was bought, so that the usage of the balance market is very limited.

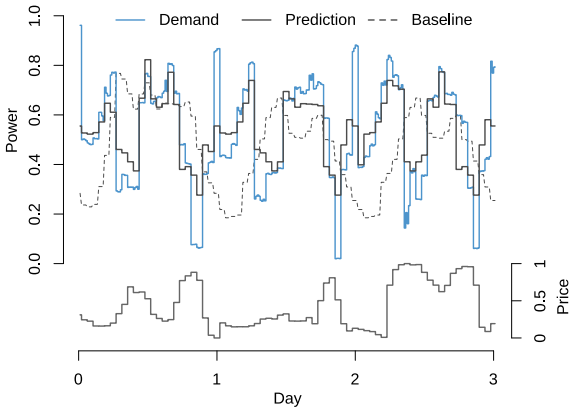

Figure 5: Energy flexible demand of the water towers when exposed to designed price signals compared to the amount of energy bought on day-ahead market.

The economic results can be seen in Table 4, where simulated results are compared. The baseline scenario is described in Section 3.3.2, where the energy demand of the water towers are not influenced. This is obtained by simply using a constant price, while purchasing electricity in the spot market according to the estimated baseline demand. The costs are computed according to (6). The energy flexibility yields expected savings of 4.1%, amounting to yearly savings of 1830 EUR for the three water towers combined. Comparatively, the average price that was paid per MWh was reduced by 4.8%, but the energy consumption was increased by 0.75%, reducing the capital savings.

To evaluate how successful the energy flexibility is being used, it should be compared to the largest possible savings. These are obtained by assuming that the water towers are able to perfectly predict their own demand and flexibility prior to the spot market being cleared. This corresponds to simply letting the controller use spot prices directly. In this way the costs are further reduced, arriving at total savings equal to 5.4%. Thus, the approach presented here managed to obtain 76% of the potential savings.

5. Conclusion

It was shown that energy consumption of a price-responsive system can be accurately predicted by price. This was done by modelling the relation through a combination of physical considerations and statistical methods. The method was tested with success for water towers controlled by economic model predictive controllers. Because of the physical considerations, the estimated relationship between price and consumption proved causal, in the sense that consumption can be controlled through price signals. Thus, this can be considered an accurate characterisation of energy flexibility. The model is general enough to be used for many other energy flexible systems.

The characterisation of the water towers was used to bid their energy flexibility into the Scandinavian spot market, using the currently available flexi orders. This amounted to operational savings of 4.1%, compared to potential savings of up to 5.4%. Notice that the exact strategy for bidding the energy flexibility into the market was not optimised, and thus it is expected that an even larger share of the potential could be obtained by doing so.

The water demand profiles were real data, and the water towers were simulated accurately. Since the energy flexibility was used on the day-ahead market, the model predictive controller can be supplied with future prices. This, combined with the fact that the assumed market products already exist means that the method could be employed in practice today.

6. Perspectives

The optimal way of using flexi orders was not pursued in this paper. This would have to be investigated to reach the full potential of the method. There are far too many possible combinations of flexi orders to test them all in a brute force manner, but it is expected that the physical interpretation of the flexibility parameters could be used to make heuristic procedures to find good combinations of flexi orders.

Because of the simplicity of operating in the day-ahead market this was chosen as the market in this paper. For future studies the method should be employed for the regulation market, since here the price variations are larger, and thus the potential savings are also larger. However, it is more difficult as well, since the prices are never known in advance, and thus it is difficult to supply the model predictive controller of the water towers with accurate price forecasts.

7. Acknowledgements

This work was mainly funded by Innovationsfonden through the CITIES project (nr. DSF1305-00027B) and Flexible Energy Denmark project (nr. 8090-00069B). The authors give their thanks to the water utility in Bjerringbro (Bjerringbro Fællesvandværk) for their support with data and information about their network.

References

[1] JM Morales, AJ Conejo, H Madsen, P Pinson, and Marco Zugno. *Integrating Renewables in Electricity Markets*. Springer, 2014.

[2] Napaporn Phuangpornpitak and Suvit Tia. Opportunities and challenges of integrating renewable energy in smart grid system. *Energy Procedia*, 34:282–290, 2013.

[3] Joakim Widén and Ewa Wäckelgård. A high-resolution stochastic model of domestic activity patterns and electricity demand. *Applied energy*, 87(6):1880–1892, 2010.

[4] NERC. Frequency response initiative report - the reliability role of frequency response. Technical report.

[5] Toshinobu Shintai, Yushi Miura, and Toshifumi Ise. Oscillation damping of a distributed generator using a virtual synchronous generator. *IEEE transactions on power delivery*, 29(2):668–676, 2014.

[6] Henrik Lund and Ebbe Münster. Integrated energy systems and local energy markets. *Energy Policy*, 34(10):1152–1160, 2006.

[7] Mark O'Malley, Benjamin Kroposki, Bryan Hannegan, Henrik Madsen, Mattias Andersson, William D'haeseleer, Mark F McGranaghan, Chris Dent, Goran Strbac, Suresh Baskaran, et al. Energy systems integration: Defining and describing the value proposition. *Contract*, 303:275–300, 2016.

[8] Allen J Wood, Bruce F Wollenberg, and Gerald B Sheblé. *Power generation, operation, and control*. John Wiley & Sons, 2013.

[9] Bijay Neupane, Torben Bach Pedersen, and Bo Thiesson. Towards flexibility detection in device-level energy consumption. In *International Workshop on Data Analytics for Renewable Energy Integration*, pages 1–16. Springer, 2014.

[10] Laura-Lucia Richter and Michael G. Pollitt. Which smart electricity service contracts will consumers accept? the demand for compensation in a platform market. *Energy Economics*, 72:436 – 450, 2018.

[11] Michael Schäfer, Inka Hobus, and Theo G Schmitt. Energetic flexibility on wastewater treatment plants. *Water Science and Technology*, 76(5):1225–1233, 2017.

[12] P Finn, C Fitzpatrick, David Connolly, M Leahy, and L Relihan. Facilitation of renewable electricity using price based appliance control in ireland's electricity market. *Energy*, 36(5):2952–2960, 2011.

[13] Frauke Oldewurtel, Andreas Ulbig, Alessandra Parisio, Göran Andersson, and Manfred Morari. Reducing peak electricity demand in building climate control using real-time pricing and model predictive control. In *49th IEEE conference on decision and control (CDC)*, pages 1927–1932. IEEE, 2010.

[14] Li Ping Qian, Ying Jun Angela Zhang, Jianwei Huang, and Yuan Wu. Demand response management via real-time electricity price control in smart grids. *IEEE Journal on Selected areas in Communications*, 31(7):1268–1280, 2013.

[15] Giulia De Zotti, S Ali Pourmousavi, Henrik Madsen, and Niels Kjølstad Poulsen. Ancillary services 4.0: A top-to-bottom control-based approach for solving ancillary services problems in smart grids. *Ieee Access*, 6:11694–11706, 2018.

[16] Giulia De Zotti, S Ali Pourmousavi, Henrik Madsen, Niels Kj, et al. Utilizing flexibility resources in the future power system operation: Alternative approaches. In *2018 IEEE International Energy Conference (ENERGYCON)*, pages 1–6. IEEE, 2018.

[17] Tobias Weiß, Anna Maria Fulterer, and Armin Knotzer. Energy flexibility of domestic thermal loads – a building typology approach of the residential building stock in austria. *Advances in Building Energy Research*, 13(1):122–137, 2018.

[18] Roel De Coninck and L. Helsen. Bottom-up quantification of the flexibility potential of buildings. 01 2013.

[19] Rune Grønborg Junker, Armin Ghasem Azar, Rui Amaral Lopes, Karen Byskov Lindberg, Glenn Reynders, Rishi Relan, and Henrik Madsen. Characterizing the energy flexibility of buildings and districts. *Applied Energy*, 225:175 – 182, 2018.

[20] Bernt Øksendal. Stochastic differential equations. In *Stochastic differential equations*, pages 65–84. Springer, 2003.

[21] Ronald A DeVore and George G Lorentz. *Constructive approximation*, volume 303. Springer Science & Business Media, 1993.

[22] Carsten Skovmose Kallesøe, Tom Nørgaard Jensen, and Jan Dimon Bendtsen. Plug-and-play model predictive control for water supply networks with storage. *IFAC 2017 World Congress, Toulouse, France*, 50:6582–6587, 2017.

[23] Flexi order. `https://www.nordpoolgroup.com/trading/Day-ahead-trading/Order-types/Flexi-order/`. Accessed: 2019-10-28.

[24] Henning Parbo. Regulation c2: The balancing market and balance settlement. Technical report, 2017.

[25] Rune Grønborg Junker, Rishi Relan, and Henrik Madsen. Physical-stochastic continuous-time identification of a forced duffing oscillator. *Submitted to ISA Transactions*, 2019.

[26] Kasper Kristensen, Anders Nielsen, Casper Berg, Hans Skaug, and Bradley Bell. Tmb: Automatic differentiation and laplace approximation. *Journal of Statistical Software, Articles*, 70(5):1–21, 2016.

[27] Krister Svanberg. The method of moving asymptotes—a new method for structural optimization. *International Journal for Numerical Methods in Engineering*, 24(2):359–373, 1987.

PAPER E

Implementing flexibility into energy planning models: soft-linking of a high-level energy planning model and a short-term operational model

Authors:
Dominik Franjo Dominković, Rune Grønborg Junker, Karen Byskov Lindberg and Henrik Madsen.

Published in:
Applied Energy.

Implementing flexibility into energy planning models: soft-linking of a high-level energy planning model and a short-term operational model

Dominik Franjo Dominković*[1]
[1]Department of Applied Mathematics and Computer Science
Technical University of Denmark (DTU), Asmussens Allé, 2800 Kgs. Lyngby, Denmark
e-mail: dodo@dtu.dk

Rune Grønborg Junker[1]
[1]Department of Applied Mathematics and Computer Science
Technical University of Denmark (DTU), Asmussens Allé, 2800 Kgs. Lyngby, Denmark
e-mail: rung@dtu.dk

Karen Byskov Lindberg[2,3]
[2] Department of Electric Power Engineering, Norwegian University of Science and Technology (NTNU), 7491Trondheim, Norway
[3] SINTEF Community, 0314 Oslo, Norway
e-mail: karen.lindberg@sintef.no

Henrik Madsen[1]
[1]Department of Applied Mathematics and Computer Science
Technical University of Denmark (DTU), Asmussens Allé, 2800 Kgs. Lyngby, Denmark
e-mail: hmad.dtu@gmail.com

Abstract

The operation of electric and heat grids alike is complicated due to the dynamic demand, with the increasing penetration of renewable energy sources adding to the problem. In order to improve the integration of variable renewable energy sources, the flexibility of the system needs to be improved. This paper proposed a novel characterization of the short-term energy flexibility, which was further utilized for the district heating capacity extension. The soft-linking of the models includes feedback, but the added computational complexity is kept at a minimum. Compared to the other literature in the field, due to the accurate characterization of the dynamics of the energy flexibility, flexibility is utilized much more frequently. The method was demonstrated for the case of the district heating of Zagreb. Results showed that both capital and operational savings can be achieved by adopting the proposed method. In the best performing scenario, which included the capacity extension planning, the socio-economic savings of the district heating system were 5.4%.

Keywords: Energy flexibility; energy planning; variable renewable energy; integrated energy systems; capacity extension planning; Demand response

Nomenclature

$C_{n,t}^{VO\&M}$	Variable operating and maintenance (O&M) cost of plant *n* in hour *t*	EUR/MWh$_{heat}$

$C_{n,t}^{fuel}$	The cost of fuel for plant *n* in hour *t*	EUR/MWh_{fuel}
C_t^{CO2}	The cost of CO2 emission in hour *t*	EUR/ton_{CO2}
K_n	The CO2 intensity of the plant *n*	ton_{CO2}/MWh_{heat}
$R_{n,t}^{ele}$	Revenues from electricity sales of plant *n* in hour *t*	EUR/MWh_{ele}
L_n	Electricity-to-heat generation ratio of plant *n*	MWh_{ele}/MWh_{heat}
$q_{n,t}$	Heat power of plant *n* in hour *t*	MW_{heat}
$C_{s,t}^{VO\&M}$	Variable operating and maintenance (O&M) cost of plant *s* in hour *t*	EUR/MWh_{heat}
$C_{s,t}^{fuel}$	The cost of fuel for plant *s* in hour *t*	EUR/MWh_{fuel}
C_t^{CO2}	The cost of CO2 emission in hour *t*	EUR/ton_{CO2}
K_s	The CO2 intensity of the plant *s*	ton_{CO2}/MWh_{heat}
$R_{n,t}^{ele}$	Revenues from electricity sales of plant *s* in hour *t*	EUR/MWh_{ele}
L_s	Electricity-to-heat generation ratio of plant *s*	MWh_{ele}/MWh_{heat}
$q_{s,t}$	Heat power of the plant *s* in hour *t*	MW_{heat}
C_n^{cap}	Annualized capacity cost of plant *n*	EUR/MW
$C_n^{FO\&M}$	Fixed O&M cost of plant *n*	EUR/MW
q_n^{cap}	The capacity of plant *n*	MW
C_s^{cap}	Annualized capacity cost of plant s	EUR/MW
$C_s^{FO\&M}$	Fixed O&M cost of plant *s*	EUR/MW
q_s^{cap}	The capacity of plant *s*	MW
E_t^{north}	District heating energy demand in hour *t* in the district heating north	MWh_{heat}
E_t^{south}	District heating energy demand in hour *t* in the district heating south	MWh_{heat}
s_t^{ch}	Heat charge of heat accumulator in hour *t*	MWh_{heat}
s_t^{dis}	Heat discharge of heat accumulator in hour *t*	MWh_{heat}
s_t^{level}	Stored energy in heat accumulator in hour *t*	MWh_{heat}
C	Heat capacity of energy flexible part of district heating water	MWh_{heat}/K
Δ	Energy flexible capacity of heat generation	MW_{heat}/MW_{heat}
Φ	Flexibility saturation rate	1/K
μ	Nominal temperature	K
k	Flexibility desire	1/K
B_t	Baseline heat demand at time *t*	MW_{heat}
Y_t	Flexible heat demand at time *t*	MW_{heat}
X_t	Temperature of district heating water at time *t*	K
u_t	Penalty for heat demand at time *t*	EUR/ MWh_{heat}
N	The set of plants operating in the district heating north	
S	The set of plants operating in the district heating south	
T	The set of hours of one year (8760 assumed in this paper)	
H	One hour (used for relating the energy generated (MWh) by using a certain power (MW) of the plant during the period of one hour)	

Introduction

Energy systems in many countries across the globe have started transitioning towards sustainable energy supply. Worldwide, the share of renewable energy sources in total energy generation was 25% in 2017 [1]. Hydropower is dominating the renewable energy capacity installed, having a share of 58% of the total installed renewable energy capacity [2]. However, the largest increase in the last decade occurred in the installed capacity of photovoltaics (PV) and wind turbines, both being variable renewable energy generators. Between 2010 and 2017, the installed capacity of wind turbines increased from 0.1 TW to 0.51 TW, while installed PV capacity increased from 0.015 TW to 0.39 TW (an increase of more than 20 times) [2]. Future

increase in renewable energy generation capacity is expected to be heavily dominated by variable renewable energy sources [1]. Some countries have already achieved large shares of variable renewable energy generation in total power demand. Denmark is one example, managing to meet more than 40% of total electricity demand by wind generation already in 2015 [3]. Moreover, power demand will significantly increase in the future. According to the International Energy Agency, electricity demand will increase by 40% by 2040 under the business-as-usual scenario [1].

Variable renewable energy sources can be successfully integrated into future energy systems if sufficient flexibility exists in the energy system. There are four main flexibility sources in an energy system: import and export of energy over the system boundaries, energy storage, power-to-heat and power-to-gas-to-power technologies, as well as different demand-response mechanisms [4]. The latter flexibility source is the focus of this research paper.

Looking into final energy consumption by sectors in the European Union (EU), 38% of the consumption occurs in the building sector [5]. Contrary to the power sector, the inertia of the heating and cooling systems allows for a temporary mismatch between demand and supply, without causing severe consequences. Taking into account the latter possibility, and successfully implementing controls for the activation of heat generators based on different signals, it is possible to implement demand-response mechanisms in the systems that supply thermal energy to buildings. District heating can make up a large proportion of the building energy consumption, as it is the case in Scandinavia, Eastern and South-eastern Europe and other regions.

There are two main options in district heating systems to increase the flexibility without imposing additional capital investments. Those are to use the thermal mass of buildings or heat capacity of water flowing through a heat distribution grid [6]. This paper focused on developing methods for flexibly utilizing the heat capacity of water flowing though the heat distribution grid.

Although some papers, such as [7], focused on representing flexibility on the building side, there is a lack of papers assessing the potential for utilizing the flexibility of the district heating grid and building's thermal mass for integrated energy planning. One paper has focused on the electrification of the heat supply for an Irish case study [8]. The authors have concluded that by utilizing the inertia of building systems, heating costs could be reduced to the cost of the cheapest alternative technology (gas boilers); however, district heating systems were not considered [8]. Another group of authors have developed an add-on for linear system-level optimization model (Balmorel) that could take building flexibility into account [9]. However, they have used a static thermal heat transfer model of the buildings, resulting in an under-representation of the peak loads that occur after demand-side management events take place. Implementing more detailed building dynamics into holistic energy planning models, either linear optimization ones or simulation ones, can be done via soft-linking or hard-linking of models. Moreover, soft-linking can include feedback between the two models. Soft-linking of a detailed dynamical building simulation model and holistic system-level linear optimization model has been carried out in [10]. It was found that the flexible heat load accounted for 5.5%-7.7% of the total district heating demand [10]. However, soft-linking of the models has not implemented a feedback loop. Due to the latter, a building simulation part of the model calculates the flexibility potential for simulated conditions defined prior to the revelation of the real weather conditions, potentially resulting in inaccuracies of building flexibility representation [10]. Furthermore, the computational complexity of the latter approach does not allow for the implementation of controls in a real-time [10].

Furthermore, a research paper on the utilization of heat capacity of water inside distribution grids has pointed out that the corresponding storage capacity is much smaller compared to the thermal mass of buildings as energy storage [6]. The latter paper has also pointed out that the storage capacity per 1 ^{o}C is

approximately 1000 times larger for the case of the thermal mass of buildings than the storage capacity of water located in the district heating distribution grid. Usually, the temperature of the water inside the distribution grid can vary much more than the thermal mass of buildings; however, the resulting difference in the storage potential is still 100 times. Another research paper has carried out a simulation using the heat capacity of water flowing in the distribution district heating grid [11]. The control strategy consisted of varying the supply temperature on a typical winter day. A typical loading phase started around 2 AM and lasted for 3.5 hours, in order to reduce the morning peak load [11]. The result showed that up to 15% of daily peak demand can be moved, increasing the distribution losses by about 0.3% [11]. A review paper on flexibility in district heating has mentioned the possibility of storing the energy by temporarily raising or lowering the temperature of water in the thermal network [12]. However, the authors have raised the concern, although without any results or references provided, that more frequent cycling could result in changing thermal stresses, possibly developing pipe cracks that could lead to pipe failures [12].

Although theoretically the thermal mass of buildings has much larger storage potential than the water in district heating systems, there are two challenges related to controlling the thermal building mass of buildings. The first problem arises from the estimation of the flexibility of many different building archetypes that can be found in a city. The existing literature showed that detecting typical archetypes and finding proper heat transfer and ventilation models on city-scales is complicated both for households [10] and for commercial buildings [13]. The second problem concerns the controlling of all the different buildings in a district heating system. Usually, the central district heating operators do not control temperature set-points of buildings and changing this could be challenging. On the other hand, differential pressure and supply temperatures in district heating distribution grids are usually controlled by the central operators. Thus, the flexible operation of the distribution grid itself is much easier from the implementation point of view. Likewise, economies of scale make the water in the district heating systems much more attractive than the building mass, since just a few controllers are needed to utilize the district heating water as opposed to a controller for every single household needed to utilize the building mass.

Thus, in order to improve the current state-of-the-art in research on district heating flexibility representation in holistic level energy models, and to develop a control approach that could be used in a real-time, soft-linking of energy flexibility and simulation-based energy planning is proposed in this paper. Moreover, the soft-linked models included the feedback from the operational model (flexibility function) to the District heating system model (Figure 2). This paper presents a continuation of the work carried out in [14], in which energy flexibility was characterized dynamically. The latter research was improved and expanded in this research paper. Furthermore, compared to the approach used in [6], which uses a very small part of a district heating grid for storing heat in heat capacity of water, and [11], which uses a fixed control strategy for starting and stopping the increased load in district heating distribution grid at predefined hours, we utilize the district heating grid for storage much more frequently, but with lesser amplitudes (temperature changes of ± 3.5 ^{o}C).

This paper improves the current state-of-the-art with the following three novelties:

1) Dynamic characterization of energy flexibility based on differential equations is proposed and used to represent the energy flexibility of district heating systems.
2) An energy system model that focuses on district heating systems is soft-linked with the energy flexibility of the district heating systems, with the objective of minimizing operational and/or total system costs of the district heating system.
3) The energy flexibility in district heating systems is utilized by using the heat capacity of the water in the district heating distribution system itself as storage. In this way, there is no need for complicated, data-intensive and time-consuming representations of different building archetypes for a whole city.

In the following section, the district heating model and the model predictive control are presented, as well as the linking between them. The Methods section consists of three different subsections. The first two subsections are related to the explanation of each of the two soft-linked models. The third subsection presents the developed method for the soft-linking of the models. The Methods section is followed by the Case Study section, in which the district heating system of the city of Zagreb is described. Results and Discussion sections present economic savings achieved by the model coupling, discuss the reasons for the encountered behaviour and point to the possible future research pathways. Moreover, the Results section shows the impact of implementing flexibility on both operational, as well as capacity extension planning. The main qualitative and quantitative findings can be found in the Conclusion section.

Methods

The energy model of the district heating system

A linear optimization district heating model was developed specifically for this research question in order to make it straightforward to soft-link it with the flexibility function. The hourly time resolution was used and the model was created in Python using Gurobi. Python is freeware while a Gurobi license can be obtained for free for academic purposes. The district heating model was based on the hourly heat energy demand, and energy equations were used instead of temperature and/or flow values in order to keep the problem linear. Keeping the problem linear is useful for capacity extension problems when many different investment possibilities exist. The grid layout was not explicitly modelled; it was rather taken into account via heat losses, which were obtained from the district heating operator.

The technologies predefined in the model were gas combined heat and power (CHP) plants, gas boilers, electric boilers, electric heat pumps and a heat accumulator (TES). The model allows for capacity expansion planning, or for operational optimization if the capacities of the plants are bounded in the model. The interaction between heat and power markets is modelled for CHPs, heat pumps and electric boilers. Revenues from electricity sales on day-ahead power market were modelled as income in the district heating system, while the total carbon emission, fuel and operating and maintenance (O&M) costs were all modelled as expenditures of the district heating system. Electricity needed for driving electric boilers and electric heat pumps was priced according to the hourly prices achieved on the day-ahead power market, on top of the fixed distribution and transmission fees.

The objective function consists of the total district heating socio-economic costs which included fuel costs (including electricity costs), fixed and variable O&M costs, annualized investment and carbon costs, while electricity sales from CHPs were considered as revenue of the system (1). By treating electricity revenues as an income in the district heating system, all the fuel and emission costs were also assigned to the district heating system, avoiding potential uncertainties regarding the assignment of costs to the power and district heating sectors separately.

$$
\begin{aligned}
minimize \sum_{n\in N}\sum_{s\in S}\sum_{t\in T}\Big[&\left(C_{n,t}^{VO\&M} + C_{n,t}^{fuel} + C_t^{CO2}\,K_n - R_{n,t}^{ele}L_n\right) q_{n,t}H \\
&+ \left(C_{s,t}^{VO\&M} + C_{s,t}^{fuel} + C_t^{CO2}\,K_s - R_{n,t}^{ele}L_s\right)q_{s,t}H\Big] + \left(C_n^{cap} + C_n^{FO\&M}\right)q_n^{cap} \\
&+ \left(C_s^{cap} + C_s^{FO\&M}\right)q_s^{cap}.
\end{aligned}
\qquad (1)
$$

The model can handle geographically distributed district heating systems. In this case, equations are represented for two separated district heating systems. Variables in the model were heat generation power in each of the district heating systems for each hour, TES charging, discharging and a level of heat stored in TES. For the initial run of the district heating system model, a perfect forecast was assumed and all the hourly heat demand values were known in advance.

Different equality and inequality constraints were used in the model. All the generation from plants within a certain district heating system needed to match the heat demand in each hour (2) and (3).

$$\sum_{n \in N} q_{n,t} H = E_t^{north}, \quad (\forall\, t \in T), \tag{2}$$

$$\sum_{s \in S} q_{s,t} H = E_t^{south} + s_t^{ch} - s_t^{dis}, \quad (\forall\, t \in T, \forall\, s \in S), \tag{3}$$

where $H = 1\ hour$.

The capacity of each plant needed to be larger than or equal to the generation values for each hour throughout the year (4) and (5).

$$0 \leq q_{n,t} \leq q_n^{cap}, \quad (\forall n \in N, \forall t \in T), \tag{4}$$

$$0 \leq q_{s,t} \leq q_s^{cap}, \quad (\forall s \in S, \forall t \in T). \tag{5}$$

Storage level in each hour needed to be equal to the storage level of the previous hour plus storage charge minus storage discharge, as described in (6).

$$s_t^{level} = s_{t-1}^{level} + s_t^{ch} - s_t^{dis}, \quad (\forall\, t \in T) \tag{6}$$

All the heat generation variables and storage charge and discharge were related to the corresponding efficiencies, which due to simplicity were not presented in the equations above.

The district heating linear optimization model was soft-linked with the flexibility function, which description can be found in the following subchapter.

Description of flexibility representation

The description of energy flexibility used here relies on the assumption that the temperature of all water in the district heating network increases whenever the heat generated by the heat plants exceeds the heating requirements of consumers, and vice versa when it is surpassed by the demand. This is modelled by the simple ordinary differential equation (ODE):

$$\frac{dX_t}{dt} = \frac{1}{C}(Y_t - B_t). \tag{7}$$

Here X_t is the water temperature at time t scaled between 0 and 1, so that $X_t = 0/1$ means that the water temperature is at the lowest/highest acceptable level at time t. Y_t is the heat generation, while B_t is the initial heat demand (before accounting for demand response). Thus, C is the total energy required to change the temperature from the lowest acceptable level to the highest acceptable level. The expected energy demand, Y_t, is modelled by the equations

$$\delta_t = 2logit\left(\Phi(\mu - X_t) - k\,u_t(\mathbb{1}(u_t \leq 0)g(1 - X_t) + \mathbb{1}(u_t > 0)g(X_t)) - 1,\right. \quad (8)$$

$$Y_t = B_t + \Delta\big(\delta_t(1 - B_t)\mathbb{1}(\delta_t > 0) + \delta_t B_t \mathbb{1}(\delta_t \leq 0)\big) \quad (9)$$

where logit is the logistic function $logit(x) = \frac{1}{(1+exp(-x))}$, that maps real values to the interval (0,1) and $\mathbb{1}$ is the indicator function for which $\mathbb{1}(x > 0) = \begin{cases} 1, & if\ x > 0 \\ 0, & if\ x \leq 0 \end{cases}$. Equation (8) describes the change in consumption due to flexibility, where $\delta_t = -1$ means that the consumption is reduced as much as possible, and $\delta_t = 1$ means that it is increased as much as possible. This change is governed by two terms, the first describing the desire to be close to normal operation, defined as having $X_t = \mu$. When this is not the case, $\Phi(\mu - X_t)$ will change the consumption in order to make X_t approach μ. The rate at which this happens is decided by the size of Φ>0. The second term describes how price influences the consumption. Most of the time, this is approximately given by ku_t, where u_t is the price of energy (district heating in this case) normalized between – 1 and 1 and k>0 is the parameter describing how important price is for the flexibility. However, when the state of charge is close to 0 or 1, it cannot be decreased/increased any further, and the appetite for being flexible diminishes gradually, as the state of charge approaches the boundaries. This is described by g, which is a function for which $g(0) = 0$ and $g(1) = 1$. An example of this is $g(x) = x$, in this case, the system is twice as sensitive to low prices $(u < 0)$ when the state of charge is e.g. 0.8 compared to 0.4. Usually, it is more realistic to assume that the system is equally sensitive to the price as long as the state of charge is not close to the boundaries. In this paper $g(x) = 1 - exp(-\lambda x)$, which for large values of λ quickly approaches 1 as x increases.

Finally, the expected generation Y_t, normalized between 0 and 1, is given by (9) as the baseline demand, B_t, modified according to δ_t. Since the consumption is non-negative, and cannot surpass the maximum consumption, the potential increase is scaled by the difference between the baseline consumption and maximum consumption, $1 - B_t$. Similarly, potential decreases are scaled by B_t. It is also reasonable to expect that there is a limited flexible capacity. This is given by Δ, where for example $\Delta = 0.6$ means that, if flexibility is available consumption can be decreased by 60% or 60% of unused capacity can be switched on.

Each of the parameters controls a particular part of the flexibility, which is illustrated for different parameter values. For the examples shown here, the parameter values shown in the description of Figure 1 are used unless otherwise stated. Figure 1a) shows the change in demand for block increases in price with varying amplitudes. Unlike linear flexibility functions, the amplitude of the response is not linearly related to the amplitude of the price. In fact, the amplitude of the response for a step increase of 1 is only slightly larger than an increase of 0.5, but the larger increases in price sustain the large response for longer, until the flexibility is exhausted, after which the response quickly drops off. For the smaller increases in price, the response is smaller and quickly decreases, but since this means that the flexibility is not exhausted, the response is sustained to a small extent for a long time. Nevertheless, a larger change in price means that a larger part of the energy flexibility is used. This can be observed when the price drops down to the initial value, where the increase in demand reflects the state of charge. The case with the largest price also has the

largest amplitude in the rebound, since in this case the flexibility has almost been depleted, while there is more left in the other cases. Similarly, Figure 1b) shows the change in demand for a fixed block increase of price and varying values of Δ, the maximum change in demand. It can be seen how the initial change in demand is proportional to Δ. However, as the total amount of available flexibility is independent of Δ, this flexibility is simply spent faster for larger values of Δ. The rebound is the same, where larger values of Δ allows for faster recharge of the state of charge. In Figure 1c) the energy capacity, C, is varied. In this case, the initial change in demand is equal for all cases, but as the flexibility is depleted faster for smaller values of C, the demand returns to the baseline faster in these cases. Similarly, it takes more time to recharge the flexibility for larger values of C. Finally, Figure 1d) shows the effect of changing the propensity for utilizing flexibility, by varying Φ. This parameter controls how inclined the system is to have a state of charge close to $\mu = 0.5$ in this case. Consequently, the initial change in demand is equal for all cases, but as the state of charge decreases, those cases where Φ is larger returns to the baseline demand faster. Similarly, larger values of Φ results in a more pronounced rebound effect, since the state of charge, X_t, is brought back to μ faster.

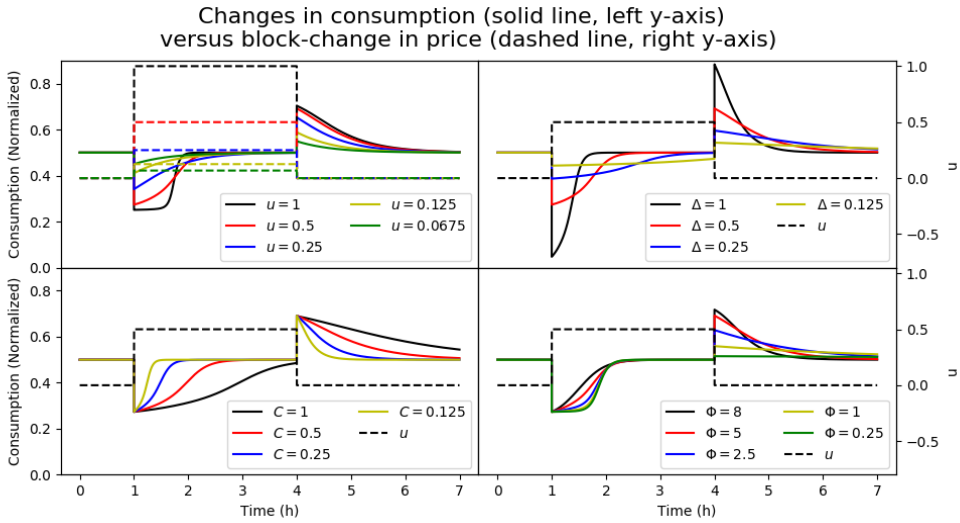

Figure 1. Expected consumption for a block increase in price. The default parameters are as follows $\Delta = 0.5, C = 0.4, \Phi = 5, \lambda_2 = 10, k = 3, \mu = 0.5$.

Soft-linking of the models

Schematic representation of the district heating planning and operational models can be seen in Figure 2. Initially, the district heating model was run in order to detect the hourly shadow prices in the district heating system, i.e. the price of generating one more unit of district heat. The shadow prices were then used as an input to the flexibility function, which output was new hourly district heat demand (*Flexible Demand* in Figure

2). The initial district heating planning model was then updated with new heat demand time series. The second run of the district heating model was the one that generated the final results.

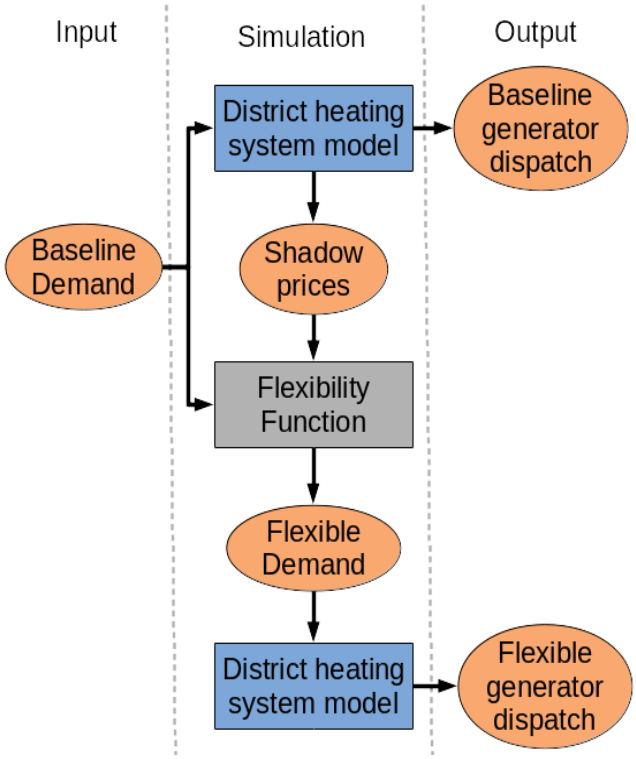

Figure 2. Flow-chart of the soft-linked models.

One should note here that $q_{n,t}$ from (2) and $q_{s,t}$ from (3) are equal to B_t in the original run but equal to Y_t (7) in the second run of the *District heating system model*. Besides the shadow price of the district heating system, those variables were used to interlink the models.

Case study

District heating system used in the case study

A district heating system located in the city of Zagreb, Croatia was chosen for a case study. Zagreb has 800,000 inhabitants. The district heating system consists of two separated grids, one located in the north-west, and the other in the south-east. Supply plants are locally called EL-TO Zagreb (north-west) and TE-TO Zagreb (south-east). Both of those locations consist of several different heat and/or heat and power generators. Approximately 28% of households are connected to one of the district heating systems [15]. All the currently operating district heating plants are driven by natural gas. The complete overview of the plants and their technical parameters can be seen in Table 1.

Table 1. Technical parameters of the heat generation plants used in this study [16,17].

Type of the plant	Nº units	El. capacity MW	Heat capacity MW	Total efficiency	El. efficiency	Lifetime
District heating north						
Back pressure cogeneration plant*	2	0	71 + 162	85%	-	25
Combined cycle cogeneration plant	2	2 x 25	2 x 10.25	85%	50%	25
Gas boiler	2	0	2 x 116	94%	0%	30
District heating south						
Back pressure cogeneration plant	1	120	200	85%	30%	25
Gas boiler	2	0	2 x 116; 2 x 58	94%	0%	30
Combined cycle cogeneration plant	2	202 + 110	2 x 80	85%	50%-51%	25
Thermal storage	1	0	150	98%	0%	40
District heating north and district heating south						
electric boiler		0	116+135**	98%	0%	20
heat pump		0	116+135**	320%	0%	25

**Although it is a back pressure cogeneration plant, the DH operator reported that it is malfunctioning and thus, only operating in the heat generation mode*

*** Capacities installed in the Ele_DH scenario. No capacity installed in the Basic scenario. In the Cap_Ext scenario, the installed capacities of electric boilers and heat pumps were a result of the optimization. If needed, consult* Table 4 *for the description of the scenarios.*

Economic parameters of the heat generation plants used in this paper can be seen in Table 2.

Table 2. Economic parameters of plants used in the case study [18].

Type of the plant	Nº units	Investment cost (EUR/MW)	Annualized investment cost (EUR/(MWyear))	Fixed cost (EUR/ (MWyear))	Variable cost (EUR/MWh)	Discount rate
District heating north						
Back pressure cogeneration plant	2	720,000	61,784	30,000	4.5	7%
Combined cycle cogeneration plant	2	1,350,000	115,844	30,000	4.5	7%
Gas boiler	2	100,000	8,059	2,000	0.9-1.1	7%
District heating south						
Back pressure cogeneration plant	1	650,000	55,777	30,000	4.5	7%
Gas boiler	4	100,000	8,059	2,000	1.0-1.2	7%
Combined cycle cogeneration plant	2	1,350,000	115,844	30,000	4.5	7%
Thermal storage	1	3,000	225	8.6	0.1	7%
Electric heat generators						
electric boiler		75,000	7,079	1,100	0.8	7%

heat pump		700,000	60,067	2,000	2	7%

In Table 3 the annual heat generation and demand for the district heating networks are shown and it can be noted that generation and demand have been steady in the last three years. Zagreb District heating operator provided the info presented in Table 3, as well as the hourly pattern of heat generation [19]. The hourly pattern of heat generation was not allowed to be publicly shared and that is the reason why it is not presented here. Yearly pattern and total heat generation for the year 2017 has been used in the case study carried out in this paper. Furthermore, the Zagreb District heating operator provided the information that the total volume of water in the distribution grid equals to 48 800 m^3.

Table 3. Yearly historic district heating consumption (the difference between the two columns represent grid losses).

year	Total (north and south) gross district heating generation (TWh)	Total (north and south) final district heat demand (TWh)
2012	1.95	1.70
2013	1.93	1.69
2014	1.68	1.41
2015	1.79	1.48
2016	1.79	1.50
2017	1.79	1.48

Although Croatia started its power day-ahead market in February 2016, called Cropex, and its data has been used for the hourly day-ahead electricity prices [20]. The latter also means that the methods presented in this paper are transferable to any country that has developed day-ahead power markets. The average electricity price on Cropex day-ahead power market for the year 2017 was 52.04 EUR/MWh (with a standard deviation of 24.05 EUR/MWh).

As gas prices for non-household consumers were very volatile between different years in the period 2013-2018, an average between those years for non-household consumers for the case of Croatia was used in the case study, which equalled to 34 EUR/MWh of gas [21]. The carbon price was assumed to be 50 €/t. Opposite to the business-economic approach, the socio-economic approach used in this paper does not include business taxes in the model, as those are only internal transfers within the society [22]. However, negative externalities such as climate change effects should be internalized in the socio-economic approach and thus, the CO2 emission price was adopted in the model.

In the time of writing of this paper, transmission and distribution tariffs for non-household consumers were complex, and several different tariffs existed in Croatia. However, the difference between different tariffs was not large, so the average price of 20 €/MWh of consumed electricity was used for the transmission tariff and a price of 20 €/MWh was also used for the distribution tariff (totalling at 40 €/MWh of electricity consumed). The latter numbers were added on top of the day-ahead electricity price for electric boilers and electric heat pumps, in scenarios where those two technologies were installed.

Flexibility parameters

Since the district heating networks are not currently operating with price-responsive control it is not possible to estimate the parameters from data. However, qualified guesses can be made, based on the physical

properties of the district heating network. First of all, the total amount of water is approximately 48800 m^3, amounting to the heat capacity of 56.8 MWh/K. In this paper, it is assumed that a change of +/- 3.5K in the temperature of the district heating water can be handled by the local heat exchangers receiving the district heating water. The parameter C is scaled by the maximum demand, 1057 MWh. This means that the total range of allowed temperatures is 7 K, which is obtained by having $C = 7 \cdot 56.8/1057 \approx 0.4$. It is expected that all of the heat generators can be flexible, in which case $\Delta = 1$. The parameter Φ was set to 4, a medium sized value, as it is preferable to have the temperature of the district heating water close to the business as usual temperature, but at the same time t,he exact temperature is not important. Similarly, there are no fatal consequences of having the temperature leave the temperature interval, and so $\lambda = 50$, which is a large value that allows the temperature to get very close to the boundaries before the price is ignored to keep the temperature within the boundaries. The price responsiveness is controlled by k, where large values makes the system more responsive to price changes. It was chosen to have $k = 5$, so that the largest possible effect of price is 5, when the price is -1 or 1 which should be compared to $\Phi = 4$, which means that the largest possible effect of the state of charge is $\Phi\mu = 4 \cdot 0.5 = 2$, when the state of charge is 0 or 1. The largest Having the largest effect of price 2.5 times larger than the effect induced by the state of charge, means that prices are expected to be 2.5 times more important than efficiency losses, which seems reasonable. Of course, without data to support the parameter estimates, they are nothing but qualified guesses, and thus a sensitivity analysis was carried out to analyze the effect of the parameter estimates on the objective value of the energy planning model. For λ, values between 10 and 100 were tested with effects below 0.05%, while values between 1 and 10 were tested for both k and Φ with effects of at most 0.25% and 0.01%, respectively.

Description of scenarios

Three different scenarios were carried out in the paper, as described in Table 4. The *Electrified District Heating (Ele_DH)* scenario represented a move to transition the heat sector towards electrification, in order to reduce CO2 emissions and help integrating more variable renewable energy sources in the power sector. For this specific case study, the electric boilers and the heat pumps replaced gas plants older than the year 2000.

The *Capacity Extension (Cap_Ext)* scenario was created to present the possibility of utilizing the flexibility function when carrying out a capacity extension planning. A potential district heating grid extension was not modelled, as there are currently no plans for doing that in the region. The latter possibility could be added to the model if there would be available input on the heat demand density of the potentially newly connected districts. The Zagreb district heating operator assumes that newly built buildings within the area of the current district heating grid will be connected to it and that this new demand will cover a reduced demand originating from the improved energy efficiency of buildings, keeping the overall district heating demand flat. The *Cap_Ext* scenario showed the potential for reducing the needed capacity when expanding the district heating system in comparison to the original expansion plan.

In the *Cap_Ext* scenario, out of the original plants operating in the DH system, only newly built boilers and CHP units were left. More specifically, DH north had installed two CHP generators with a heat capacity of 10.25 MW each and one gas boiler of 116 MW. DH south had two CHP plants with a heat generation capacity of 80 MW each, as well as the heat accumulator. The model allowed new investments in electric boilers, heat pumps, gas boilers, CHP units and the extension of the heat accumulator capacity. It is worth noting that the

initial capacity of plants in this scenario was insufficient, so the model had to invest in the additional capacity of heat generation technologies.

The original expansion plan corresponded to the first run of the district heating optimization model, while the second run of the district heating optimization model (after the flexibility function implementation) corresponded to the updated expansion plan (if needed, consult the scheme presented in Figure 2 for the sake of clarity).

Table 4. Description of scenarios used in the paper.

Basic	Electrified District Heating (Ele_DH)	Capacity extension (Cap_Ext)
All the heating plants data and inputs were adopted as described in the *District heating system used in the case study* subsection (Table 1). Represents the current case.	*Basic* scenario without two back pressure units in the DH north, and without four gas boilers in the DH south. Instead, a heat pump and an electric boiler with a capacity of 116 MW_h each were installed in the DH north, and a heat pump and an electric boiler with a capacity of 135 MW_h each were installed in the DH south.	Two gas CHP plants with a heat capacity of 10.25 MW each and a gas boiler with a capacity of 116 MW were installed in the DH north. Two gas CHP plants with a heat capacity of 80 MW each and a heat accumulator with a capacity of 750 MWh were installed in the DH south. Possible new investments in the model: electric boilers, heat pumps, gas boilers, CHP units and the extension of the heat accumulator capacity.

In all the runs of all the scenarios, the same amount of heat was needed in each hour.

Results

The results section starts with the overview of the installed capacities, followed by the presentation of differences between different scenarios in terms of generated energy from specific sources. The results section further continues with the presentation of the overall economic results of different scenarios and finally, it ends up with a detailed representation of operational changes during the chosen two days. The representation of the detailed operational changes explicitly shows the influence of the operational model on the energy planning model.

The resulting capacities of heat generation plants can be found in Table 5. As described earlier, in *Ele_DH* scenario, two back pressure units that were operating only as gas boilers were replaced with an electric boiler and a heat pump in the DH north. In DH south, four gas-driven heat boilers were replaced by a heat pump and an electric boiler with a capacity of 135 MW each.

Electric boilers, heat pumps, gas boilers, combined cycle CHPs and TES capacities were unconstrained in the *Cap_Ext* scenario. For the case of DH north, the model decided to invest also in the extension of CHP units from the starting capacity of 20.5 MW (lower constraint) to 156.15 MW, as well as in gas boilers from the starting capacity of 116 MW (lower boundary) to 170.5 MW. Electric boilers and heat pumps did not have a lower boundary and the resulting capacities were 47.7 MW and 53.7 MW, respectively. For the case of DH south, the model decided to invest in the extension of gas boilers, from zero starting capacity (lower boundary) to 146.3 MW, as well as in the heat accumulator (TES) extension, from the starting capacity of 750 MWh to 4023 MWh. The resulting capacity showed that the capacity of CHPs was not expanded beyond the initial capacity of 160 MW. The resulting capacities of electric boilers and heat pumps were 76.1 MW and

93.6 MW, respectively. Comparing the results of the latter scenario in the original run and a run with flexibility included (last two rows in Table 5), one can notice that by using the flexibility function, needed extension capacities of gas boilers and electric boilers dropped in the case of DH north. In the case of DH south, the needed capacity of TES storage reduced by 2.5%.

Table 5. Resulting (heating) capacities of different model runs (MW).

	District heating north					District heating south					
	Back pressure CHP (MW)*	Combined cycle CHP (MW)	Gas boiler (MW)	electric boiler (MW)	heat pump (MW)	Back pressure CHP (MW)	Gas boiler (MW)	Combined cycle CHP (MW)	electric boiler (MW)	heat pump (MW)	Heat accumulator (MWh)
Basic	71 + 162	2 x 10.25	2 x 116	0	0	200	58 x 2; 116 x 2	2 x 80	0	0	750
Ele_DH	0	2 x 10.25	2 x 116	116	116	200	0	2 x 80	135	135	750
Cap_Ext	0	10.25 + 145.9	170.5	47.7	53.7	0	146.3	2 x 80	76.1	93.6	4023
Cap_Ext with flexibility	0	10.25 + 145.9	169	46.4	53.7	0	146.3	2 x 80	76	93.6	3923

**Although it is a back pressure cogeneration plant, the DH operator reported that it is malfunctioning and thus, only operating in the heat generation mode*

An example of changes in plant operation in DH north in the Ele_DH scenario, with and without flexibility, can be seen in Figure 3. One can notice that the gas boilers with flexibility reduced the operation time under the high capacity and shifted that generation to the periods of lower operation capacity. On the other hand, heat pumps increased their operation at the maximum rated capacity, from 1811 hours to 2904 hours. CHPs also slightly increased their operation under the maximum rated capacity, from 4885 to 4943 hours.

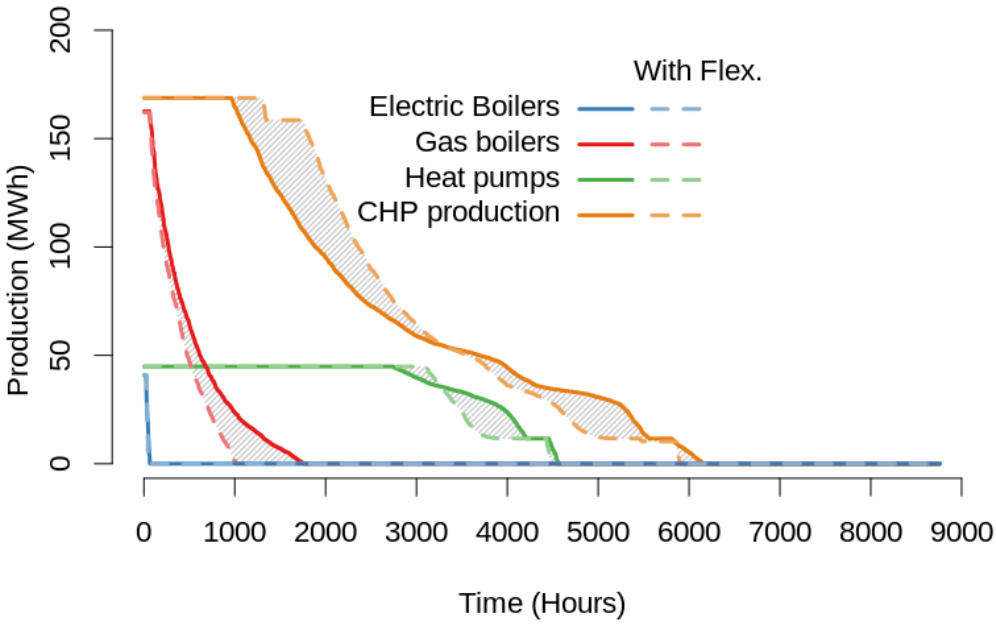

Figure 3. Load duration curves of different plant operations in Electrified district heating scenario, with and without flexibility.

Heat generation from different plants in different scenarios can be seen in Table 6. In the *Basic* scenario, flexibility utilization increased the operation of CHP plants and reduced the operation of gas boilers, reducing the overall socio-economic costs of the DH system.

In the *Ele_DH* scenario, the utilization of the flexibility increased the use of the CHPs, electric boilers and the heat pumps, while it decreased the use of the gas boilers. Reduced operation of the gas boilers was especially emphasized, as they generated 16.7% less heat in the case with the flexibility.

In the Cap_Ext scenario, the operation of CHP units increased significantly, while the use of gas and electric boilers was reduced correspondingly. Moreover, the operation of heat pumps also reduced in this case.

Summarizing the heat generation results as seen in Table 6, one can note that utilizing the flexibility, the CHP generation increased in all the scenarios, between 0.3% and 3.2%. On the other hand, gas boilers operation reduced in all the scenarios following the implementation of the flexibility. Finally, heat pumps and electric boilers increased their generation in the Ele_DH scenario, while they decreased their generation in the Cap_Ext scenario. The reason for the latter behaviour is that the Cap_Ext scenario had much larger capacities of CHPs than in the Ele_DH scenario, and this additional CHP capacity took over some of the generation of electric boilers and heat pumps.

Table 6. Heat generation from different plants in different scenarios

	Total CHP production (GWh)	Total gas boilers production (GWh)	Total electric boilers production (GWh)	Total heat pump production (GWh)
Basic	881	905	0	0
Basic with flexibility	893	893	0	0
Difference	1.3%	-1.3%		
Ele_DH	696	136	8.3	946
Ele_DH with flexibility	699	113	8.4	966
Difference	0.3%	-16.7%	1.2%	2.2%
Cap_Ext	963	236	3	584
Cap_Ext with flexibility	994	212	3	576
Difference	3.2%	-9.8%	-4.6%	-1.3%

Economic results of different scenarios are presented in Table 7. One can note that DH north achieved significantly larger savings compare to the DH south, which was the case in all the scenarios. In the basic scenario, the socio-economic savings were relatively low. This scenario was dominated by gas boilers and gas CHPs, without any heat generation plants driven by electricity. The latter shows that in gas dominated district heating system, steady intra-year gas prices reduce the possibility to utilize price arbitrage.

In the Ele_DH scenario, savings were more significant, especially in the case of the DH north. Total socio-economic costs reduced by 2.8% in the DH north. For the case of DH south, the total socio-economic costs of the DH system reduced by 0.6%.

The largest savings occurred in the capacity extension planning scenario, i.e. the Cap_Ext scenario. The objective value of the DH south improved only marginally; however, in the DH north, the savings amounted to the significant 15.5%. The most dominant factor in the improved performance of the DH north was the larger income achieved from electricity sales, i.e. revenues from selling electricity increased by 7.5%.

Table 7. Economic results from different scenarios (million euros).

		DH North					DH South				
	Objective Value Total	Objective Value	Capital Costs	Operational costs	Revenue from electricity sales	Operational costs with electricity sales income*	Objective Value	Capital Costs	Operational costs	Revenues from electricity sales	Operational costs with electricity sales income*
Basic	96.9	48.1	18.6	49.1	19.7	29.5	48.9	32.7	109.6	93.4	16.2
Basic with flexibility	96.6	48.0	18.6	49.2	19.8	29.4	48.6	32.7	110.0	94.1	15.9
Difference	-0.4%	-0.2%	0.0%	0.1%	0.7%	-0.3%	-0.5%	0.0%	0.4%	0.7%	1.6%
Ele_DH	78.5	31.9	12.0	36.4	16.6	19.9	46.6	38.9	88.5	80.8	7.7

Ele_DH with flexibility	77.4	31.0	12.0	35.6	16.6	19.0	46.3	38.9	88.6	81.2	7.4
Difference	-1.5%	-2.8%	0.0%	-2.2%	0.6%	-4.5%	-0.6%	0.0%	0.1%	0.5%	3.7%
Cap_Ext	57.5	19.7	23.8	74.5	78.7	-4.1	37.8	27.0	87.5	76.7	10.8
Cap_Ext with flexibility	54.4	16.7	23.8	77.4	84.6	-7.2	37.8	27.0	87.5	76.7	10.8
Difference	-5.4%	-15.5%	0.0%	3.9%	7.5%	-73.4%	-0.2%	-0.1%	-0.1%	0.0%	0.5%

*In the objective function of the optimization, the goal was to minimize the total costs of the district heating system, which included revenues from selling electricity as an income (the objective function is represented in (*1*)).

In the ***Cap_Ext*** scenario, the economic results showed that the needed extension capacity can be reduced if the flexibility function is utilized before the decision on the capacity extension is made. The change in capacities, as seen in the last two columns in Table 5, resulted in absolute savings of EUR 0.55 million. The adoption of the flexibility resulted in a reduced need for 1 MW of gas boilers, marginally reduced capacity of electric boilers, marginally increased capacity of heat pumps, and reduced capacity of heat accumulator for 181 MW. One should note that the latter cost saving is not directly observable in Table 7, as results presented in Table 7 include only annualized investment costs and not the total investment costs. The lowest overall cost of the energy system was achieved in the Cap_Ext scenario, which was expected as there was no excess capacity in the district heating system. The socio-economic cost of the district heating system in the Cap_Ext with flexibility scenario was 30% lower than the Ele_DH with flexibility scenario.

It is worth explaining here that the negative values for the *Operational costs with electricity sales income* that occurred in the DH north in the Cap_Ext were the consequence of electricity income being larger than the operational costs of the district heating system.

In Figure 4 and Figure 5 the heat production before and after applying the flexibility function is shown for the Southern and Northern grid respectively. The discharge of the heat accumulators is shown such that negative values correspond to filling the storage. The shadow price associated with marginal changes in consumption and the electricity price is shown as well. For DH South the most noticeable change is during the morning of 11-Jan where the electricity prices are very high and the peak demand is shaved so that the electric boiler is not needed, and the heat pumps are used less. Apart from this, the flexibility is mostly being used to change when the heat storage is being charged, so that this happens mostly when the marginal cost is low.

Generally, CHP's were the cheapest source of heat due to high electricity prices in this period, while heat pumps and electric boilers were used for the peak load. An exception was during the night between 11-Jan and 12-Jan, when the electricity price was relatively low, resulting in the heat pumps being cheaper than the CHP's. For DH North the effect of the flexibility is again seen to shave the peaks where the electric boiler was used during the morning of 11-Jan. This was accomplished mainly by increasing the demand during the night hours, where demand was low, as seen during the night between 11-Jan and 12-Jan. It is also clear how the high electricity prices during this period make the gas boilers cheaper than the heat pumps during the day of 11-Jan, 09:00 12-Jan and 20:00 12-Jan.

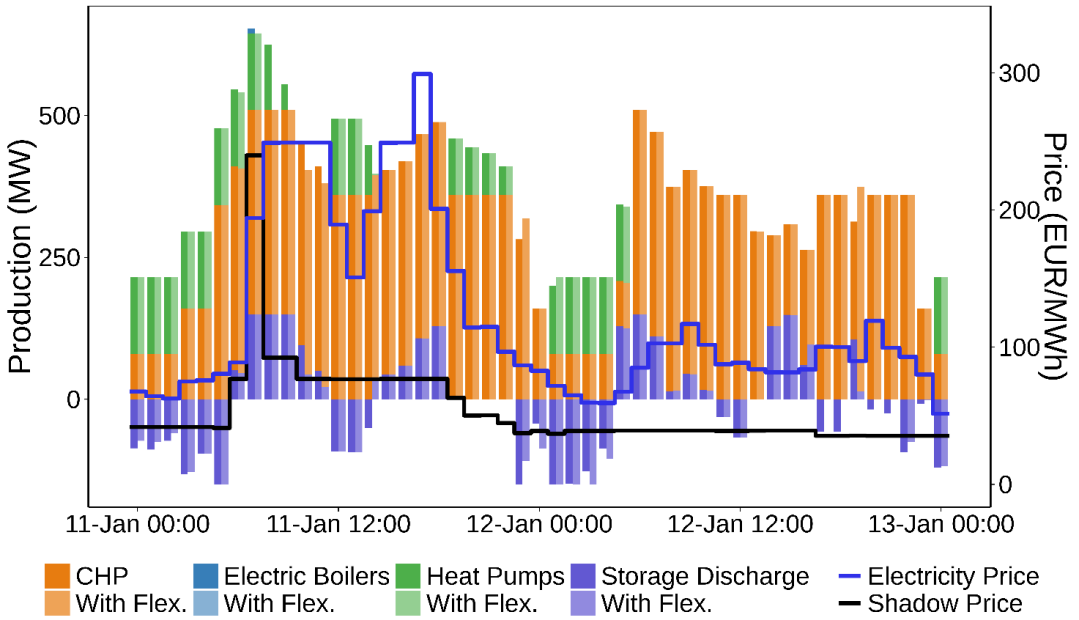

Figure 4. Heat generation of different plants in the DH south before and after application of the flexibility function for 48 hours of the year. Values correspond to the Ele_DH scenario.

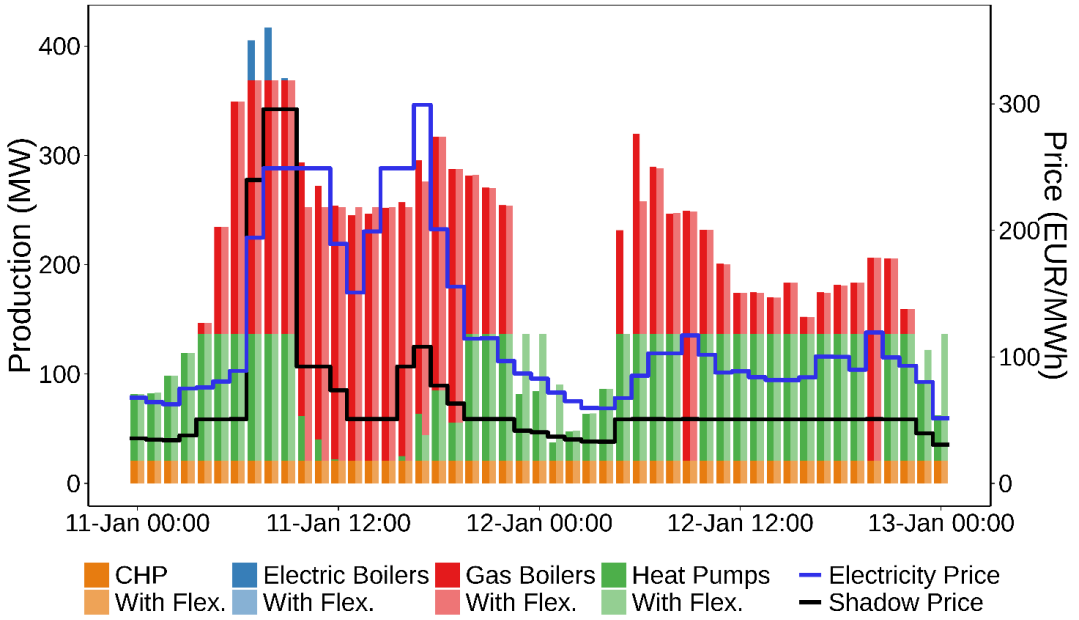

Figure 5. Heat generation of different plants in the DH north before and after application of the flexibility function for 48 hours of the year. Values correspond to the Ele_DH scenario.

In Figure 6, the accumulated savings for each of the district heating grids are shown. As already mentioned, the largest savings are obtained for DH North even though the overall demand is larger for DH South. As the heat demand is larger during the winter, in the heating season, it is no surprise that this is also where most of the total savings occur. Especially for DH South, there are almost no savings at all outside of the heating season, except for one event at the start of August. Except for that event, the savings due to the energy flexibility are steady, with a continuously varying slope that peaks during the coldest months; January, February and December.

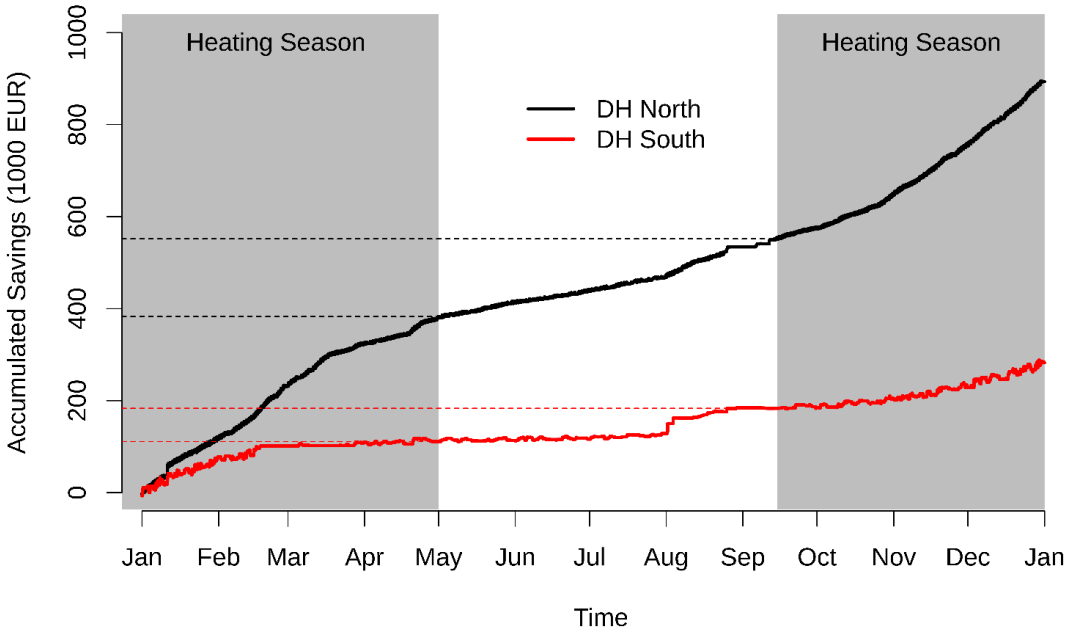

Figure 6. Accumulated savings in the Ele_DH scenario.

Discussion

The discussion section starts with a brief recap of the main economic results, followed by a discussion on the reasons for the achieved savings. It continues with a discussion on the influence of flexibility utilization on the optimal operation of heat accumulators. Furthermore, the section continues with the discussion on the operational constraints in the system, as well as a discussion on the possibility for an automatic parametrization of the flexibility function. Limitations of this study, comparison with the existing literature and possible future research directions are discussed at the end of the section.

In this paper, energy planning and operational models were soft coupled in order to assess the potential of utilizing water stored in district heating grids as flexible thermal energy storage. The case study carried out to analyze the methods of this paper confirmed the benefits of this approach. All three scenarios showed that significant socio-economic savings can be achieved by flexible operation of the heat generation in the

district heating systems. The total socio-economic savings ranged from 0.4 – 3.1 MEUR/year. In relative terms, economic savings were between 0.4% and 5.4%.

Most of the economic savings occurred from the combination of lower operating costs and/or higher revenues from electricity sales when the flexibility was utilized. The behaviour was different in the DH north and DH south in different scenarios. For the case of Cap_Ext scenario, increased revenues from electricity sales were by far the largest contributor towards reduced overall socio-economic costs in the DH North, while in the DH south, the largest contributor towards the overall socio-economic savings originated from reduced operating costs. The behaviour described here points to the conclusion that both reduction in operating costs, as well as an increase in revenues from better-performing electricity sales, contribute towards the overall economic improvement reached by utilization of the flexibility. This means that the biggest advantage of energy flexibility in district heating grids is that it supports the power grids.

It is also interesting to take a closer look at the behaviour of the heat accumulator. Following the implementation of flexibility, the utilization of the heat accumulator decreased by 12%, 12% and 19% in the three scenarios, respectively. Furthermore, the reduced installed capacity of the heat accumulator in the Cap_Ext scenario upon the implementation of the flexibility indicates competition between the different flexibility options. The final point that goes along the same line is that the operational savings in the DH South were always lower than in the DH North, which was especially emphasized in the Cap_Ext scenario. In the latter scenario, after the system optimized the initial size of the thermal accumulator, only slight savings were achieved by including flexibility. The competition between different flexibility sources was already tackled and discussed in the literature in a detailed way [23], which needs to be taken into account when discussing the potential of a single source of flexibility.

One should note that by adopting the coefficient C = 0.4 in this paper, we are varying temperatures only up to ±3.5 K from the original temperature values. In this way, neither a significant additional thermal stress on the piping nor a complicated control action demand on substations would be imposed. Current substations in district heating are already oversized, as they are designed for the critical conditions. Furthermore, the current controllers on the end-user side should already be able to adapt the flow to accommodate the slight temperature changes on the primary side of the system. Due to the latter, the approach used in this paper should be easy to implement.

Contrary to the approach used here, the parameters of the flexibility function should be estimated based on data, when possible. Indeed, if a district heating company would implement the control presented here, the data required for estimating the parameters would become available from their daily operation, and the parameters could adaptively be updated to reflect the flexibility [24]. Furthermore, with enough data available the representation could be improved, using appropriate machine learning techniques.

One of the strengths of the approach used in this paper is the easy implementation of the flexibility function with automatic estimation of the parameters. This implies that the same approach is valid for district heating systems with different characteristics. Also, following the digitalization of the district heating sector that has started gaining a stronger foothold, data-driven solutions will be easy to implement in many different district heating systems. Furthermore, this paper showed that the implemented soft-coupling of models with feedback can be used both for operation and capacity extension planning. In addition, the approach adopted in this study requires only slight temperature variations compared to the base operation, which could be implemented solely by central district heating operators, while the end-user substations should be able to adapt automatically to the changing conditions.

Limitations of the study include the potential reluctance of the centralized district heating operators to change the business-as-usual operation. Furthermore, district heating systems that have a direct exchange of heat, which can still be found in Eastern and Southeastern Europe, could have problems even adopting to the slight temperature variations. Moreover, the approach used in this case study is tailored for the district heating systems that have constant inertia, which means that flow velocities should be kept constant. The latter is usually only the case for winter operation of the district heating systems when flows are kept constant and temperatures are varying. Fortunately, this is exactly where most of the savings were obtained, so the inaccuracy related to non-constant flows should be very limited.

Comparing the results of this study with the literature, one can notice that our implementation of controls is novel compared to the other studies and no direct comparison can be obtained. In [11], the authors simulated a district heating system with the temperature control implemented such that the district heating network was preloaded (between 2 AM and 5:30 AM) in order to reduce the morning peak consumption that occurred at 6 AM in their simulated case [11]. Their temperature limiter was significantly alternated, from maximum supply temperature of 95 ^{o}C to maximum supply temperature of 115 ^{o}C. The authors achieved a peak load reduction of up to 15% [11]. In our case, the temperature variation in comparison to the original case was only ±3.5 ^{o}C and heat demand pattern was alternated very frequently based on the provided price signal.

In [6], a similar step function system was implemented; however, with preheating of the grid. The implementation of the increase in artificial penalty signal was fixed in the middle of the considered week. The authors concluded that the flexibility of the thermal mass of buildings is two orders of magnitude larger than the heat capacity of water located in the district heating grid [6]. However, having a completely different implementation of the penalty signal, and not calculating consequences on the economic performance of a district heating supplier makes it incompatible for comparison with the case study carried out in this paper.

Up to the knowledge of the authors, this is the first paper that focused on the implementation of the flexibility control, using economic performance as a penalty signal. The results of the paper showed that this set-up can be used both for operational planning, as well as for capacity extension planning. Moreover, penalty signals could easily be tailored in a way that it targets heat loss reduction or CO2 emissions reduction.

Furthermore, the approach taken in this research opens up several possible avenues for future research. One option is to adopt the same approach towards the representation of the flexibility of buildings. For this, the exact same model could be used; however, obtaining enough data for parametrization of the flexibility function of buildings could be challenging. Another problem that could arise with the demand-response utilization in buildings is the control of the substations and the individual thermostatic valves within the apartments, as those are usually not under the central control of district heating operators [12]. On the positive side, the potential thermal mass as storage of buildings is much larger than that of water in district heating pipes [6]. The second option is to apply the same approach to other energy markets, i.e. intra-day and balancing markets. The latter could be done with slight changes compared to the approach taken in this study, i.e. the one based on the day-ahead market operation. The third option could be to show that by tailoring the flexibility function in a different way, the soft-linked models could directly reduce peak demands in district heating systems over the year. The latter approach is different compared to the solution of this study that was minimizing the socio-economic costs of the system, which also included increased revenues from electricity sales.

Some further research possibilities would be to test the solution in different set-ups, such as low-temperature district heating grids, as well as district heating systems of varying sizes. Furthermore, the possibility to test the solution in a detailed dynamic simulation model would be beneficial. It would also be

of interest to adopt the coupled model to district heating systems that have more variable heat generation sources in its portfolio.

Conclusions

This paper presented soft coupling of the district heating system optimization model, which took the electricity system into account via day-ahead electricity prices, with the flexibility function that represented the heat demand response following a penalty signal. The penalty signal was obtained by computing the shadow price of consuming heat for each time step.

The method of this study proposed slightly varying supply temperature in the distribution grid compared to the baseline operation, i.e. ±3.5 K, in order to use the district heating distribution grid as storage. Results of the case study showed that significant socio-economic savings could be achieved. The savings ranged from 0.36 MEUR to 3.1 MEUR. The savings in relative terms ranged from 0.4% to 5.4%. Moreover, the scenario that included capacity extension possibility showed that the heat accumulator extension capacity could be reduced by 6%, still meeting all the district heating demand.

Furthermore, the influence of different parameters needed for the flexibility function on the heat demand behaviour was shown in order to make it easier to comprehend how the function would behave in other district heating systems. It was further debated that the parameter estimation in the district heating grids could be estimated in an automated way as operational data becomes available, thus improving the functionality. The latter is possible as the approach used in this paper can be implemented in a centralized way from district heating operators.

Acknowledgements

This work was funded by the CITIES project nr. DSF1305-00027B funded by the Danish Innovationsfonden, the Research Centre on Zero Emission Neighbourhoods in Smart Cities (FME ZEN) funded by the ZEN partners and the Research Council of Norway, and HEAT 4.0 project nr. 8090-00046B also funded by Danish Innovationsfonden. Their contribution and support are greatly appreciated. The authors were also funded by the Smart Cities Accelerator 2016 – 2020 project, funded by the EU programme Interreg-Øresund-Kattegat-Skagerrak and Flexible Energy Denmark project (nr. 8090-00069B) funded by Danish innovationsfonden.

Furthermore, we would like to acknowledge the support from the Croatian district heating operator HEP-Toplinarstvo, which provided us with the district heating data.

References

[1] International Energy Agency (IEA). World Energy Outlook 2018. 2018.

[2] International Renewable Energy Agency (IRENA). RENEWABLE CAPACITY STATISTICS 2018. 2018.

[3] Danish Energy Agency. Denmark's Energy and Climate Outlook. 2017.

[4] Dominković DF, Dobravec V, Jiang Y, Nielsen PS, Krajačić G. Modelling smart energy systems in tropical regions. Energy 2018;155:592–609. doi:10.1016/j.energy.2018.05.007.

[5] European Environment Agency. Final energy consumption by sector and fuel. Indic Assess 2017. https://www.eea.europa.eu/themes/data-and-maps/indicators/final-energy-consumption-by-sector-9/assessment-1.

[6] Vandermeulen A, Reynders G, van der Heijde B, Vanhoudt D, Salenbien R, Saelens D, et al. Sources of

energy flexibility in district heating networks: building thermal inertia versus thermal energy storage in the network pipes. Submitt to USIM 2018 - Urban Energy Simul 2018.

[7] Wang A, Li R, You S. Development of a data driven approach to explore the energy flexibility potential of building clusters. Appl Energy 2018;232:89–100. doi:10.1016/j.apenergy.2018.09.187.

[8] Heinen S, Turner W, Cradden L, McDermott F, O'Malley M. Electrification of residential space heating considering coincidental weather events and building thermal inertia: A system-wide planning analysis. Energy 2017;127:136–54. doi:10.1016/j.energy.2017.03.102.

[9] Hedegaard K. Wind power integration with heat pumps, heat storages, and electric vehicles - Energy systems analysis and modelling. 2013.

[10] Dominković DF, Gianniou P, Münster M, Heller A, Rode C. Utilizing thermal building mass for storage in district heating systems: Combined building level simulations and system level optimization. Energy 2018;153:949–66. doi:10.1016/j.energy.2018.04.093.

[11] Basciotti D, Judex F, Pol O, Schmidt R-R. Sensible heat storage in district heating networks: a novel control strategy using the network as storage. IRES - 6th Int Renew Energy Storage Conf Exhib 2011:4.

[12] Vandermeulen A, van der Heijde B, Helsen L. Controlling district heating and cooling networks to unlock flexibility: A review. Energy 2018;151:103–15. doi:10.1016/j.energy.2018.03.034.

[13] Salo S, Hast A, Jokisalo J, Kosonen R, Syri S, Hirvonen J. The Impact of Optimal Demand Response Control. Energies 2019;12(9). doi:https://doi.org/10.3390/en12091678.

[14] Junker RG, Azar AG, Lopes RA, Lindberg KB, Reynders G, Relan R, et al. Characterizing the energy flexibility of buildings and districts. Appl Energy 2018;225:175–82. doi:10.1016/j.apenergy.2018.05.037.

[15] Culig-toki D, Kraja G, Dora B, Vad B, Krklec R, Møller J. Comparative analysis of the district heating systems of two towns in Croatia and Denmark 2015;92:435–43. doi:10.1016/j.energy.2015.05.096.

[16] EL-TO Zagreb. HEP Toplinarstvo EL-TO 2018. http://www.hep.hr/proizvodnja/UserDocsImages/dokumenti/tehnicki_podaci_termoelektrane/EL-TO_Zagreb.pdf (accessed May 10, 2019).

[17] TE-TO Zagreb. HEP Toplinarstvo TE-TO 2018. http://www.hep.hr/proizvodnja/UserDocsImages/dokumenti/tehnicki_podaci_termoelektrane/TE-TO_Zagreb.pdf (accessed May 10, 2019).

[18] Energinet.dk; Danish Energy Agency. Technology Data for Energy Plants for Electricity and District heating generation. 2016.

[19] HEP Toplinarstvo d.o.o., Mipevačka 15a 10 000 Zagreb. http://www.hep.hr/toplinarstvo/ 2018.

[20] Cropex. Cropex - Croatian Power Exchange n.d. https://www.cropex.hr/en/ (accessed July 23, 2019).

[21] Eurostat. Eurostat - gas prices n.d. http://ec.europa.eu/eurostat/ (accessed April 5, 2019).

[22] Dominković DF, Bačeković I, Sveinbjörnsson D, Pedersen AS, Krajačić G. On the way towards smart energy supply in cities: The impact of interconnecting geographically distributed district heating grids on the energy system. Energy 2017;137:941–60. doi:10.1016/j.energy.2017.02.162.

[23] Dominković DF. Modelling Energy Supply of Future Smart Cities. Technical University of Denmark, Department of Energy Conversion and Storage, 2018. doi:https://doi.org/10.11581/dtu:00000038.

[24] Nielsen TS, Madsen H. Control of Supply Temperature in District Heating Systems. 7 Int Symp Dist Heat Simul 1997;14:613–20.